

Diss. ETH No. 17747

# Total Ozone Measurements at Arosa (Switzerland): Seasonal Variation and Precision of Dobson and Brewer Observations

A dissertation submitted to  
ETH ZURICH

for the degree of  
Doctor of Sciences

presented by  
BARBARA SCARNATO

MSc Physics, Universita' degli Studi di Milano. Italia

born 9 June 1977  
citizen of Italy

accepted on the recommendation of  
Prof. Dr. Johannes Staehelin, examiner  
Prof. Dr. Thomas Peter, co-examiner  
Dr. Julian Gröbner, co-examiner  
Dr. Rene Stübi, co-examiner

2008



*‘‘Live as if you were to die tomorrow.  
Learn as if you were to live forever.’’*

*Mohandas Karamchand Gandhi*



# Contents

<b>Abstract</b>	<b>ix</b>
<b>Prefazione</b>	<b>xi</b>
<b>1 Introduction</b>	<b>1</b>
<b>2 Scientific Background</b>	<b>5</b>
2.1 Earth's atmosphere . . . . .	5
2.2 Ozone and solar radiation . . . . .	8
2.3 Processes determining stratospheric ozone concentrations . . .	12
2.3.1 Stratospheric ozone life-cycle and gas phase destruction cycles . . . . .	12
2.3.2 Polar ozone: Antarctic and Arctic ozone hole . . . . .	20
2.3.3 Effect of volcanic eruptions . . . . .	27
2.4 Spatial and seasonal variation of stratospheric ozone . . . . .	27
2.5 Montreal protocol . . . . .	29
2.6 Trends of stratospheric ozone . . . . .	33
<b>3 Stratospheric ozone measurements</b>	<b>37</b>
3.1 Total ozone column . . . . .	37
3.2 Satellites . . . . .	42
3.3 Ozone profiles . . . . .	44

<b>4 Dobson and Brewer Temperature and Ozone Slant Path Effect</b>	<b>45</b>
4.1 Abstract . . . . .	45
4.2 Introduction . . . . .	46
4.3 UV-spectrophotometers . . . . .	48
4.3.1 Instrumental principle . . . . .	48
4.3.2 Retrieval algorithms . . . . .	49
4.4 Data and method . . . . .	54
4.4.1 Used measurements . . . . .	54
4.4.2 Spectral ozone measurements . . . . .	55
4.4.3 Temperature influence on total ozone measurements . .	55
4.4.4 Stray light effect . . . . .	59
4.5 Results and Discussion . . . . .	61
4.5.1 Total ozone multi annual time series . . . . .	61
4.5.2 Effective ozone temperature variation and its influence on total ozone measurements . . . . .	61
4.5.3 Ozone slant path effect and its influence on observations	70
4.5.4 Effect of temperature variability and stray light on sea- sonal cycle . . . . .	72
4.6 Conclusions . . . . .	76
4.7 Acknowledgments . . . . .	77
<b>5 Long Term Total Ozone Observations: transfer function</b>	<b>79</b>
5.1 Abstract . . . . .	79
5.2 Introduction . . . . .	80
5.3 Measurements and Methods . . . . .	82
5.3.1 Total ozone measurements at Arosa since 1988-2007 and inter-comparison results . . . . .	82
5.3.2 Multi-linear regression model used for transfer function	86

---

5.4	Results and Discussion . . . . .	87
5.4.1	Comparison of measurements of the same type of instrument . . . . .	87
5.4.2	Comparison of Dobson and Brewer observations . . . . .	91
5.4.3	Relative Long term stability of Dobson and Brewer series at Arosa . . . . .	96
5.4.4	Comparison of Arosa data with NIWA satellite measurements . . . . .	97
5.5	Discussion and Conclusions . . . . .	101
5.6	Acknowledgments . . . . .	103
5.7	Appendix . . . . .	104
<b>6</b>	<b>Final Remarks</b>	<b>107</b>
	<b>List of Figures</b>	<b>110</b>
	<b>List of Tables</b>	<b>114</b>
	<b>Bibliography</b>	<b>117</b>
	<b>Acknowledgements</b>	<b>124</b>
	<b>Curriculum Vitae</b>	<b>127</b>





# Abstract

Over roughly the last 30 years, the annually-averaged total column ozone has decreased by approximately 3% in the northern midlatitudes, largely in response to anthropogenic effects. In an attempt to document and quantify long term ozone trends, a network of ground based instruments has been operated since the mid 1970s under the auspices of the WMO. The network is comprised of two main instruments: Dobson and Brewer spectrophotometers. The observed rate of ozone depletion, while significant, is small enough that data quality control of ground based measurements is of the utmost importance if long term trends are to be accurately diagnosed. The Dobson spectrophotometer network is based on a Primary Dobson instrument which is regularly calibrated by the Langley plot method at the Mauna Loa observatory and maintained by ESRL-NOAA. The calibration scale is subsequently transferred to a traveling standard instrument, used to compare with regional standard Dobson instruments. The station instruments are calibrated by side-by-side comparisons against the regional standard instruments during Dobson inter-comparisons. A similar procedure has been organized for the newer Brewer instruments.

Another important facet of the quality control of a long term ozone time series is data homogenization. Occasionally, an instrument must be replaced. It then becomes imperative to ensure the consistency between the old and new measurements. The problem is further complicated by the presence of two different types of instruments: there is a general trend to replace the older Dobson with the newer Brewer instruments. Therefore, both intra- and inter-instrumental data homogenization is at times necessary. With this in mind, the WMO suggests the simultaneous operation of both types of instruments in order to study the difference between observations and improve data quality.

At Arosa, two Dobson and two Brewer instruments have been simultaneously operated since 1992 and a third Brewer instrument was added in 1998, thereby providing a unique dataset for an in depth examination of data quality.

In the present work, a first step is to calculate instrumental precision. At Arosa, one standard deviation of the total ozone measurements (performed within 10 minutes) for Dobson ((observed with the AD wavelength pair) and Brewer instruments is found to be  $\pm 0.5\%$  and  $\pm 0.2\%$ , respectively. As pertains to inter-instrumental differences, quasi-simultaneous measurements between the two spectrophotometers in the mid- and high-latitudes typically exhibit a seasonal bias of a couple percent. This bias can be at least partially attributed to the different sensitivities of the wavelengths used in the respective retrieval algorithms: different estimations of total column ozone during different seasons might be a consequence of the seasonal variability of, mainly, ozone effective temperature (a weighted convolution of air temperature and ozone profile) and ozone slant path (air mass multiplied by total ozone; OSP).

The temperature dependence of the ozone cross section has been calculated using three distinct ozone absorption cross section spectra with differing resolutions (*Bass and Paur*, 1985; *Malicet et al.*, 1995; *Burrows et al.*, 1999). It is found that *Bass and Paur* (1985) or *Malicet et al.* (1995) are the most suitable spectra for total ozone measurements by Dobson and Brewer spectrophotometers. Taking into account the temperature dependence of the ozone cross sections and the OSP effect, the seasonal bias can be reduced from 2% to less than 1%, which deems sufficient for the study of long term trends. Furthermore, it is found that the OSP effect is comparable in comparison with the temperature effect.

In order to sustain homogeneous ground based total ozone measurements, Dobson instruments should not be replaced by Brewer instruments without a careful examination that takes advantage of quasi-simultaneous measurements. To convert the measurement of a Brewer instrument, empirical transfer functions are used, incorporating the ozone effective temperature and ozone slant path as proxies. However, even after the application of the transfer functions, a drift between Arosa's Dobson and Brewer observations on the order of 3% during the early 1990s is observed and remains unexplained.

# Prefazione

Nel corso degli ultimi 30 anni, nell' emisfero nord a medie latitudini la media annuale della colonna totale di ozono é diminuita di circa del 3 %, in gran parte in risposta a effetti di origine antropica. Con il tentativo di documentare e quantificare le tendenze a lungo termine dell'ozono, una rete di strumenti basati sulle misure da terra opera dalla meta' dagli anni settanta sotto il controllo dell'organizzazione mondiale meteorologica (WMO). La rete di monitoraggio é composta principalmente da due strumenti: gli spettrofotometri Dobson e Brewer. La percentuale osservata di riduzione della fascia di ozono é abbastanza piccola (sebbene significativa), quindi il controllo della qualita' dei dati basato sulle misure da terra é della massima importanza, se le tendenze a lungo termine dell'ozono devono essere accuratamente diagnosticate. La rete di monitoraggio operante con gli spettrofotometri Dobson é basata su un Dobson primario (standard) mantenuto da ESRL-NOAA, che é regolarmente calibrato attraverso un metodo chiamato grafico di Langley all'osservatorio di Mauna Loa. La scala di calibrazione é successivamente trasferita a degli strumenti standard secondari che vengono usati per calibrare degli strumenti di riferimento regionali. Quest'ultimi successivamente vengono trasportati nei diversi siti per la calibrazione sul luogo degli strumenti Dobson. Una procedura analoga é stata realizzata per gli spettrofotometri Brewer.

Un altro importante aspetto per il controllo di qualita' delle serie temporali storiche dell'ozono é l'omogeneizzazione dei dati rispetto agli strumenti in uso nei relativi periodi. Occasionalmente, uno strumento deve essere sostituito e diventa importante garantire la coerenza tra le vecchie e le nuove misure. Il problema é ulteriormente complicato dalla presenza di due diversi tipi di strumenti: c'e' una tendenza generale a sostituire il vecchio Dobson con il nuovo Brewer. Pertanto, é necessaria l'omogeneizzazione delle serie temporali

sia provenienti dallo stesso tipo di strumento che differente. Con questo in mente, la WMO suggerisce il funzionamento simultaneo di entrambi gli strumenti per studiare le differenze tra le misure e migliorare, di conseguenza, la qualità dei dati. Ad Arosa, due Dobson e due Brewer operano simultaneamente dal 1992 ed un terzo Brewer è stato aggiunto nel 1998, fornendo in tal modo un unico set di dati utile per un approfondito esame della qualità delle misure.

Un primo passo è quello di calcolare la precisione strumentale. Ad Arosa, la deviazione standard delle misure della colonna di ozono è rispettivamente  $\pm 0.5\%$  per Dobson (per osservazioni con lunghezze d'onda AD) e  $\pm 0.22\%$  per i Brewer. Per quanto riguarda le differenze inter-strumentali, a medie e alte latitudini, misure quasi simultanee tra i due spettrofotometri tipicamente mostrano differenze stagionali nell'ordine di un paio di percento. Questo bias è almeno in parte attribuito alle diverse sensibilità delle lunghezze d'onda utilizzate nei rispettivi algoritmi. Diverse stime della colonna totale di ozono durante le diverse stagioni potrebbero quindi essere una conseguenza della variabilità dell'effettiva temperatura dell'ozono (ponderata convoluzione del profilo della temperatura dell'aria e dell'ozono) e della dipendenza dalla massa d'aria d'ozono (massa d'aria moltiplicata per la colonna totale di ozono; OSP). La dipendenza della sezione trasversale di assorbimento (cross section) dell'ozono dalla temperatura è stata calcolata utilizzando tre distinti spettri di assorbimento di ozono con diverse risoluzioni (*Bass and Paur, 1985; Malicet et al., 1995; Burrows et al., 1999*). Da questo studio risulta che (*Bass and Paur, 1985*) e (*Malicet et al., 1995*) sono gli spettri ottimali per la misura della colonna di ozono effettuata con gli strumenti Dobson a Brewer. Tenendo conto della dipendenza del coefficiente di assorbimento dell'ozono alla temperatura e della dipendenza dalla massa d'aria di ozono (OSP), le differenze stagionali possono essere ridotte da 2% a meno di 1%, la seconda cifra risulta essere sufficiente per lo studio delle tendenze a lungo termine dell'ozono. Inoltre, si è riscontrato che l'effetto dell'OSP è dello stesso ordine di grandezza rispetto all'effetto della temperatura.

Al fine di ottenere delle misure della colonna di ozono omogenee gli strumenti Dobson non dovrebbero essere sostituiti da i Brewer senza un attento

esame, che si avvale di misure quasi-simultanee per un estensivo periodo. Per trasformare le misure effettuate dagli strumenti Brewer in scala Dobson, sono state utilizzate delle funzioni di trasferimento empiriche, che incorporano la temperatura effettiva dell'ozono e la massa d'aria di ozono come variabili esplicatorie. Tuttavia, anche dopo l'applicazione delle funzioni di trasferimento, le serie temporali di ozono dei due strumenti mostrano una tendenza a divergere del 3% durante i primi anni del 1990.



# Chapter 1

## Introduction

The depletion of the global ozone layer has emerged as one of the major global scientific and environmental issues of the twentieth century. The discovery of the Antarctic ozone hole (*Farman et al.*, 1985) naturally raised the question of whether other latitudes might also display greater ozone depletion than expected. Within a few years after the ozone hole was discovered, statistically significant trends in ozone were found at northern mid-latitudes as well (*WMO*, 1989). By the 1990s, significant trends had been established for both the northern and southern mid-latitudes (e.g., *Stachelin et al.*, 1998a).

Enhanced ozone depletion in the Antarctic and Arctic regions is linked to heterogeneous chlorine chemistry that occurs on the surfaces of polar stratospheric cloud particles at cold temperatures. Observations also show that some of the same heterogeneous chemistry occurs on the surfaces of particles present in the mid-latitudes as well, and the abundance of these particles are enhanced following explosive volcanic eruptions (*Solomon*, 1999). The partitioning of chlorine between active forms that destroy ozone and inert reservoirs that sequester it is a central part of the framework for the understanding of the Antarctic ozone hole, the recent Arctic ozone losses in particularly cold years, and the observation of record mid-latitude ozone depletion after the major eruption of Mount Pinatubo in the early 1990s. Laboratory studies have also shown that heterogeneous process involving  $\text{N}_2\text{O}_5$  can deplete  $\text{O}_3$ .  $\text{N}_2\text{O}_5$  hydrolysis and chlorine activation on sulfuric acid aerosols enhances the possibility of heterogeneous chemistry can occur on the liquid sulfate layer, that is pervasive throughout the stratosphere (e.g., *Tolbert et al.*, 1988; *Mozurkewich*

and Calvert, 1988; Hofmann and Solomon, 1989). However, the completeness of present understanding of mechanisms leading to polar ozone depletion is today in discussion, because a recent study of Pope *et al.* (2007) reported, in polar conditions, a much lower ClO dimer (ClOOC1) photolysis rate than Burkholder *et al.* (1990), which is the recommended in the models. Using Pope *et al.* (2007), ClO dimer cycle would not be longer a major ozone loss cycle and the ozone hole formation would no longer be explained.

Human use of ozone depletion substances (i.e. chlorofluorocarbons) continues to decrease as consequence of Montreal Protocol provisions, therefore changes throughout the ozone layer are expected to gradually reverse during the twenty-first century (WMO, 2007). At mid latitudes, a variety of processes are important for stratospheric ozone trends (chemical depletion in gas phase (upper stratosphere), advection of ozone depleted polar air, changes in dynamics, heterogeneous reaction on sulphuric aerosols).

Detection of long-term changes in ozone are based on statistical models containing explanatory variables accounting for natural variability and anthropogenic changes in ozone. They well represent the ozone variability with a residual of the model between  $\pm 5$  DU, for  $60^{\circ}\text{S} - 60^{\circ}\text{N}$  latitudes in 1964-2006 period (WMO, 2007). Measurements of atmospheric ozone by different ground instruments and space-born systems result in the creation of diverse datasets. All of these are required to understand the spatial and temporal distribution patterns of ozone in the atmosphere resulting from natural processes and anthropogenic emissions. Estimation of ozone trends and the beginning of recovery of the ozone layer are high-priority research tasks, therefore good ground based data quality is mandatory for a reliable ozone trend detection and for validation of satellite measurements.

In order to be able to document small long term changes, a world wide network of ground based spectrophotometers has been operated, since the middle of the 1979s under the auspices of the World Meteorological Organization (WMO). Dobson and Brewer spectrophotometers are the standard instruments for ground based total ozone monitoring in the WMO's Global Atmospheric Watch (GAW) program (WMO, 2003). Currently, the number of both types of instruments are nearly equal; however, the capacity of the Brewer



---

network is continuously increasing due to installation of Brewers at newly established stations and the replacement of Dobsons by Brewers at existing stations.

This work has been motivated by the documented systematic significant differences between the seasonal variations of total ozone measurements at mid- and high-latitudes between the two types of spectrophotometers. Because of these seasonal differences, the instruments cannot be replaced by each other without creating a systematic break in measurements unless simultaneous measurements of few years are available to allow constructing reliable transfer functions between the two types of instruments. These differences can influence the estimation of ozone trends if combined data series are used after replacement of the Dobson instrument by the Brewer spectrophotometer.

The Arosa site boasts the longest continuous time series of total ozone in the world, starting in 1926 with Dobson spectrophotometers. Since 1988, Dobson and Brewer spectrophotometers have been simultaneously operated (presently, two Dobson and three Brewer instruments).

The first main subject of the thesis was an in depth physical study of the seasonal differences of Dobson and Brewer instruments using the Arosa datasets and laboratory studies of the temperature dependence of the ozone cross section. Subsequently, the focus was moved on long term analysis using a statistical methods. Moreover, the precision and stability of long term Dobson and Brewer total ozone time series at Arosa has been reviewed.

An outline of this thesis is the following. In Chapter 2, an overview of chemical and dynamical processes responsible for ozone variability is given. Chapter 3 is a synopsis of different ground based instruments and space-borne systems for ozone measurements. An analysis of relation between high quality quasi-simultaneous Dobson, Brewer ground based total ozone measurements at Arosa is presented in Chapter 4. Part of the seasonal bias between ground based measurements has been explained in terms of the stratospheric temperature dependence of the ozone cross sections and slant path effect. Focus on long term analysis of ground based and assimilated satellite total ozone datasets is in Chapter ??, where a transfer function for Brewer observations

scaled by Dobson has been proposed. The main findings of this thesis are summarized in Chapter 6, those are relevant to other mid- and high-latitude stations.

## Chapter 2

# Scientific Background

## 2.1 Earth's atmosphere

The Earth's atmosphere is a layer of gases surrounding the planet Earth and retained by the Earth's gravity. Dry atmosphere contains roughly (by molar content/volume) 78.08% molecular nitrogen ( $N_2$ ), 20.95% oxygen ( $O_2$ ), 0.93% argon Ar, 0.038% carbon dioxide ( $CO_2$ ), trace amounts of other gases, and a variable amount of water vapor (around 0.25%, average in all column not included in the dry atmosphere). The atmosphere protects life on Earth by absorbing ultraviolet solar radiation and reducing temperature extremes between day and night. The gases that account for the remaining 0.1% are all called trace gases. They include ozone ( $O_3$ :  $0\%-7 * 10^{-6}\%$ ), methane ( $CH_4$ : 0.0001745%), nitrous oxide ( $N_2O$ : 0.00005%), nitrous dioxides ( $NO_2$ :  $2*10^{-6}\%$ ), neon (Ne: 0.001818%), helium (He: 0.000524%), Chlorofluorocarbons, etc. There is no definite boundary between the atmosphere and outer space. It slowly becomes thinner and fades into space. Three quarters of the atmosphere's mass is within 11 km above mean sea level. The atmosphere has a vertical thermal structure as well as a vertical pressure structure. The atmosphere has been divided into layers according to the behavior of temperatures in their relationship to altitude, Figure 2.1.

The troposphere is the "region of mixing" nearest the surface, it extends up roughly 10 km of high depending upon location/weather conditions. Temperature decreases with altitude (average normal lapse rate  $6\text{ }^\circ\text{C/km}$ ). When

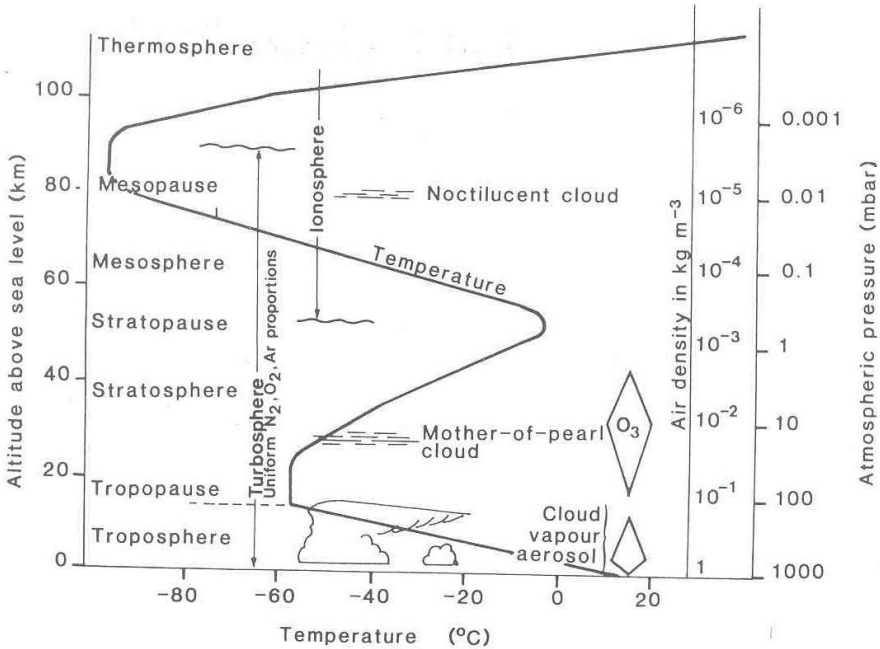


**Figure 2.1:** Earth's atmosphere layers and temperature profile.

temperature decreases more rapidly (e.g., cold front comes in over a warm front), the atmosphere becomes unstable against vertical mixing, leading to a relatively well mixed troposphere. The heat source is the absorption of light by the surface of the Earth, which yields vertical mixing of gases. In this region the winds increase with height up to the jet stream. The moisture concentration decreases with height up to the tropopause.

The tropopause is the boundary between troposphere (below) and stratosphere (above). It is situated about 10 km up. It's more like 8 km over the polar regions in winter (cold air tends to settle downward) and 18 km over the equatorial regions, due to greater convection there (heating caused by the direct radiation of the sun). In the mid-latitudes, the tropopause is lower in

winter and higher in summer, for the same reasons. At the tropopause, temperatures stop dropping with increasing altitude. The normal lapse rate no longer applies forming an “isothermal” belt. Temperatures at the tropopause are very cold: about  $-50\text{ }^{\circ}\text{C}$ . The tropopause, also separates the intensely mixed air of the troposphere from the much stratified air of the stratosphere.

The stratosphere extends from the tropopause up to about 50 km. It is characterized by a direct relationship between temperatures and altitude: temperature increases with altitude. Because of the temperature inversion, vertical mixing is strongly restricted, hence various layers are not mixed (= stratified, hence the name of the layer). The heat source is absorption of UVC+UVB (240-320 nm radiation) by the ozone layer.

The mesosphere is the layer above the stratopause, which is another isothermal belt above the stratosphere. It extends up from the stratopause to about 80 km. It is characterized by resumption of an inverse relationship between temperature and altitude. Temperature gets down to nearly  $-100\text{ }^{\circ}\text{C}$ . This is the coldest layer in the atmosphere. That low temperature is attained at the mesopause, which tops the mesosphere.

The thermosphere is the last thermally defined layer of the atmosphere. It is characterized by a direct relationship between temperature and altitude, temperatures get up to  $725 - 1,225\text{ }^{\circ}\text{C}$ . The lower thermosphere is called the ionosphere. The ionosphere extends from roughly 80 km to somewhere around 300 to 600 km out. It is the first protection of the Earth against the extremely short wave radiation (e.g., UV-B and UV-C) and, to a lesser extent, high energy particles from the sun and cosmic “rays”. These particles are ionized atoms, that is, atoms with missing electrons, including isolated protons and alpha-particles (two protons with two neutrons and no electrons). Cosmic “rays” are deadly to life on Earth. These rays and really high energy, fast-moving particles smash into the few molecules of the ionosphere with such force that they strip them of electrons, turning them into ions, or electrically-imbalanced atoms, too. The ions, with their electrical imbalances, are drawn by the earth's magnetic field and align themselves with that field's lines of force. This means that they are concentrated in great abundance where those magnetic field lines converge, at the north and south magnetic poles.

## 2.2 Ozone and solar radiation

Ozone ( $O_3$ ) is a triatomic molecule, consisting of three oxygen atoms. It is an allotrope of oxygen that is much less stable than the diatomic  $O_2$ . It was discovered in laboratory experiments in the mid-1800s by Schönbein, (e.g., *Mordecai*, 2001). Already a few years after its discovery Schönbein provided evidence, that ozone is present in ambient air which was confirmed by optical methods (*Strutt*, 1964). In the 1920's the British scientist, G.M.B. Dobson developed a spectrophotometer that for many decades remained the only accurate instrument to measure the atmospheric ozone column amount within reasonable measuring time. This instrument was installed in the 1920s at different locations, which led Dobson to describe the seasonal variation of the ozone column and its dependence on latitude. Dobson also discovered a strong influence of atmospheric dynamics on ozone (*Dobson*, 1973).

About 90% of the ozone in our atmosphere is contained in the stratosphere, the region from about 10 to 50 km above Earth's surface (ozone layer) and only approximately ten percent of the ozone resides in the troposphere. The maximum of ozone (in partial pressure) occurs at mid-latitudes at approximately 23 Km above mean sea level (see Figure 2.2) as first documented by *Götz et al.* (1934) using Dobson spectrophotometers operated at low solar elevation at Arosa. This result was based on Umkehr method, which was discovered by Götz during the expedition in Spitzbergen (Norway).

In the stratosphere near the peak of the ozone layer, there are up to 12,000 ozone molecules for every billion air molecules. In the troposphere near Earth's surface, ozone is even less abundant, with a typical range of 20 to 100 ozone molecules for each billion air molecules. The highest surface values are a result of ozone formed in air polluted by human activities (*WMO*, 2007). Ozone molecules are vitally important to life because they absorb the biologically harmful ultraviolet radiation from the Sun. Ultraviolet (UV) radiation is referred to as UV-A, UV-B and UV-C, based on the wavelength of the radiation. Most of the UV-A (315-400 nm) reaches the surface, but it is not as genetically damaging. UV-B radiation (280-315 nm) can cause sunburn and also genetic damage, resulting in health problems like skin cancer

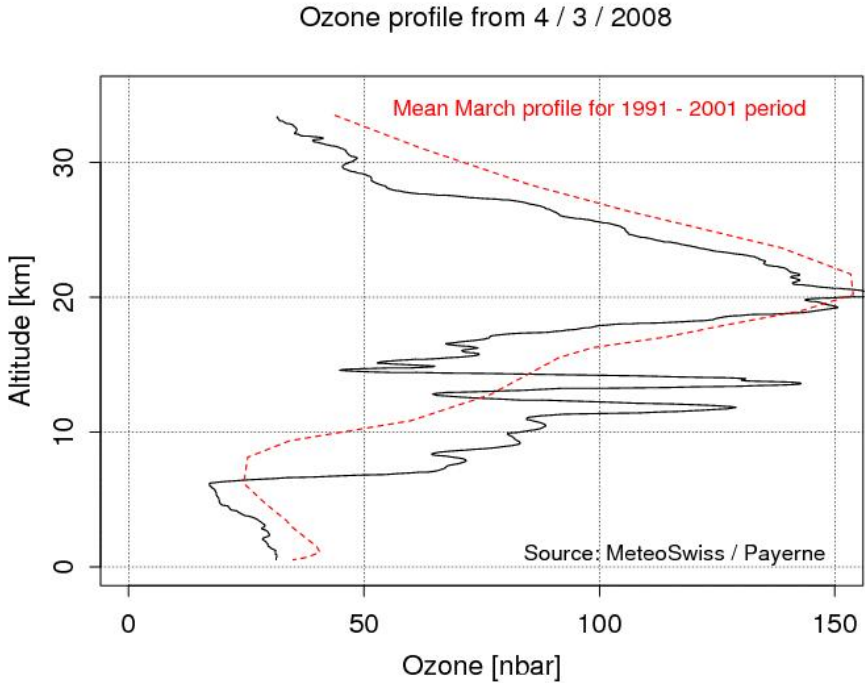


**Figure 2.2:** Ozone profile in partial pressure from balloon soundings launched in Payerne, Switzerland ( $46^{\circ}50'N$ ,  $6^{\circ}58'E$ , 454 m a.s.l.). Black line ozone profile from 04.03.2008 launch and red dashed line 10 years mean for the month of March. Most ozone resides in the stratospheric “ozone layer” above Earth’s surface (10-30 km). Increases in ozone occur near the surface as a result of pollution from human activities.

if exposure to is prolonged. Atmospheric ozone screens out most UV-B, but some reaches the surface. If the ozone layer decreases, more UV-B radiation reaches the surface, causing increased genetic damage to living beings at the Earth’s surface (plant life, cell organism and aquatic ecosystem). The UV-C (100-280 nm) is entirely screened out by ozone ( $O_3$ ) and molecular oxygen ( $O_2$ ) around 35 km altitude.

In contrast to the beneficial effect of stratospheric ozone, tropospheric ozone is a pollutant found in high concentrations in photooxidant smog. The high reactivity of ozone results in damage to the living tissue of plants and animals. Damage by heavy tropospheric ozone pollution is often manifested as eye and lung irritation. Tropospheric ozone is mainly produced during the daytime in polluted regions such as urban areas. Significant government efforts are underway to regulate the gases and emissions that lead to this harmful pollution.

Stratospheric and tropospheric ozone both absorb infrared radiation emitted by Earth's surface, effectively trapping heat in the atmosphere. Stratospheric ozone also significantly absorbs solar radiation. As a result, increases or decreases in stratospheric or tropospheric ozone cause radiative forcing and represent direct links of ozone to climate change. In recent decades, stratospheric ozone has decreased due to rising chlorine and bromine amounts in the atmosphere, while troposphere ozone in the industrial era has increased due to pollution from human activities. Stratospheric ozone depletion causes a negative radiative forcing, while increases in tropospheric ozone cause a positive radiative forcing. The radiative forcing due to tropospheric ozone increases is currently larger than that associated with stratospheric ozone depletion (see Figure 2.3).



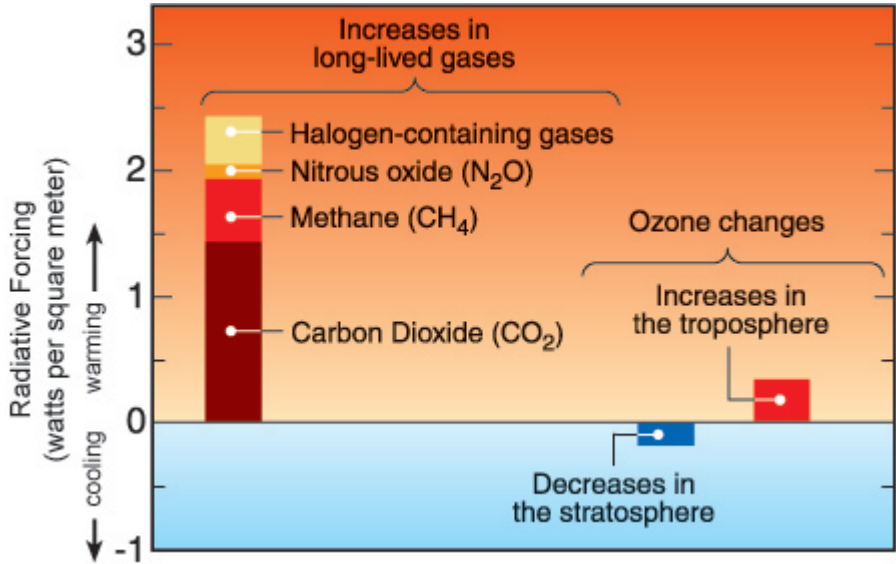


**Figure 2.3:** Radiative forcing of climate change from atmospheric gas changes. Human activities since the start of the Industrial Era (around 1750) have caused increases in the abundances of several long lived gases, changing the radiative balance of Earth’s atmosphere. These gases, known as “greenhouse gases”, result in radiative forcings, which can lead to climate change. Other international assessments have shown that the largest radiative forcings come from carbon dioxide, followed by methane, tropospheric ozone, the halogencontaining gases, and nitrous oxide. Ozone increases in the troposphere result from pollution associated with human activities. All these forcings are positive, which leads to a warming of Earth’s surface. In contrast, stratospheric ozone depletion represents a small negative forcing, which leads to cooling of Earth’s surface. In the coming decades, halogen gas abundances and stratospheric ozone depletion are expected to be reduced along with their associated radiative forcings. The link between these two forcing terms is an important aspect of the radiative forcing of climate change. Source: (WMO, 2007)

## 2.3 Processes determining stratospheric ozone concentrations

### 2.3.1 Stratospheric ozone life-cycle and gas phase destruction cycles

The ozone life-cycle reaction described by *Chapman* (1930) is summarized in Figure 2.4.

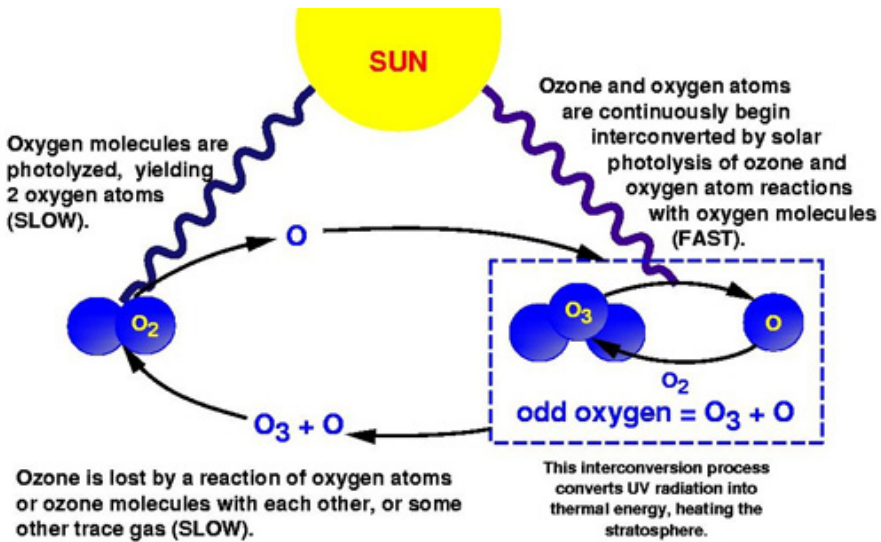
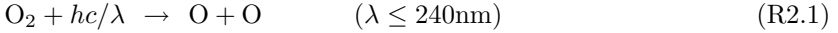


Figure 2.4: *Synthesis of the Chapman ozone life cycle reactions. Source: Newman et al. (2008).*

**Formation of ozone:** Short wave ultraviolet radiation (less than approximately 240 nm) photolysed an oxygen molecule (O<sub>2</sub>) into two oxygen atoms

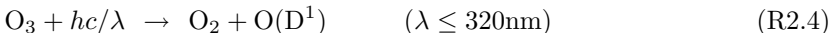
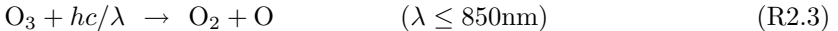


where  $hc/\lambda$  represents the photon,  $h$  the Planck's constant,  $c$  the speed of light, and  $\lambda$  the wavelength of the photon. The rate at which ozone is formed is slow, since the intensity of solar energy at wavelengths less than 240 nm is small (at 30 km solar flux  $\leq 10^{11}$  photons  $\text{cm}^{-2} \text{sec}^{-1}\text{nm}^{-1}$ ). Oxygen atoms react subsequently with other oxygen molecules to form 2 ozone molecules ( $\text{O}_3$ ), per one photolysed molecular oxygen ( $\text{O}_2$ )

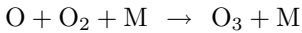


where M is another molecule (typically  $\text{N}_2$  or  $\text{O}_2$ ). It carries away the extra energy of this 3 body reaction. These reactions occur continuously wherever UV sunlight is present in the atmosphere. The greatest ozone production is found in the tropical stratosphere, where solar radiation is largest.

**Photochemical destruction:** Ozone absorbs UV radiation leading to the separation of the ozone molecule ( $\text{O}_3$ ) into an oxygen molecule ( $\text{O}_2$ ) and an oxygen atom (O). In this process UV radiation increases the kinetic energy of ozone yielding an increase in temperature.



Reaction R2.4 was not included in the original theory of Chapman, but it is here presented for the importance of modern theory. A recombination of the oxygen atom with another oxygen molecule leads ozone again (see right side of Figure 2.4), represented by



Ozone and oxygen atoms are quickly continuously inter-converted by solar photolysis and oxygen atoms reactions. Ozone is lost by reaction of oxygen atoms. Equivalent to this, is the reaction of two oxygen atoms, because odd oxygen (O and O<sub>3</sub>) are converted in each other. These slow process could not remove enough ozone to explain the values measured in the real atmosphere.



The Chapman chemical reactions lead to predicted ozone amounts that are twice as high as actual tropical observations and at high latitude predictions are too low (see Figure 2.5).

The deviations from stratospheric ozone concentrations from Chapman chemistry result from two processes. First, an equator to pole stratospheric circulation, known as Brewer and Dobson circulation, which transports ozone from the production region in the tropics to mid to high latitudes. Second, ozone production is fixed by intensity of solar UV radiation but loss reactions exist catalyzed by free radicals formed by photolysis, i.e. Chlorofluorocarbons (CFCs), carbontetraclorine (CCl<sub>4</sub>), methylchloroform (CH<sub>3</sub>CCl), methyl bromide (CH<sub>3</sub>Br).

When gases containing e.g. Chlorine and Bromine reach the stratosphere, they are becoming exposed to UV-radiation from the sun, (see Figure 2.6). They are converted to more reactive radicals. The most important radicals causing ozone depletions belong to the families of HO<sub>x</sub><sup>•</sup>, NO<sub>x</sub><sup>•</sup> and ClO<sub>x</sub><sup>•</sup> and BrO<sub>x</sub><sup>•</sup>, e.g. (*Crutzen*, 1970) and (*Molina and Rowland*, 1974).

*Crutzen* (1970) pointed out that emissions of nitrous oxide N<sub>2</sub>O, a stable, long-lived gas produced by soil bacteria, from the earth's surface could affect the

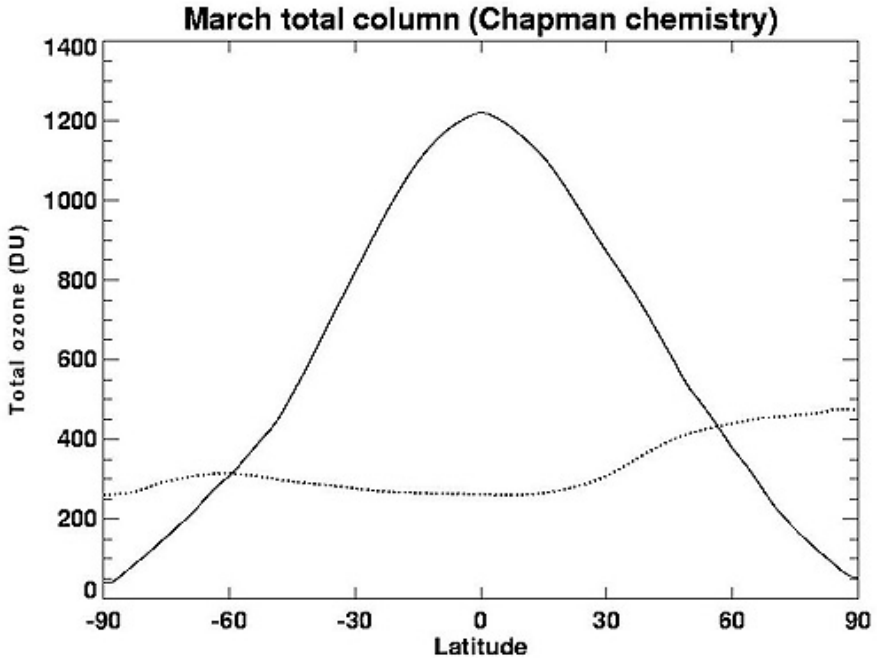


**Figure 2.5:** Total column ozone estimated using Chapman chemistry for March conditions (solid line) compared with ozone derived from satellite instrument measurements (dotted line). The measurements were made by the Total Ozone Mapping Spectrometer (TOMS) instrument. Source: Newman et al. (2008).

amount of nitric oxide NO in the stratosphere. Crutzen showed that nitrous oxide lives long enough to reach the stratosphere, where it is converted into NO. He noted that the increasing use of fertilizers might have led to an increase in nitrous oxide emissions over the natural background, which would in turn result in an increase in the amount of NO in the stratosphere. Thus, this type of human activity could have an impact on the stratospheric ozone layer. In the following year, Crutzen and (independently) Harold Johnston suggested that NO emissions from supersonic aircraft, which fly in the lower stratosphere, could also deplete the ozone layer.

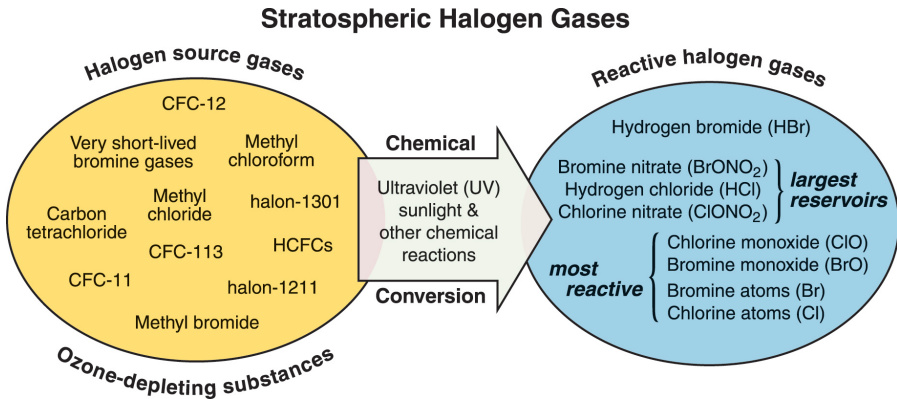


**Figure 2.6:** Conversion of halogen source gases. Halogen source gases (also known as ozone-depleting substances) are chemically converted to reactive halogen gases primarily in the stratosphere. The conversion requires ultraviolet sunlight and a few other chemical reactions. The short-lived gases undergo some conversion in the troposphere. The reactive halogen gases contain all the chlorine and bromine originally present in the source gases. The reactive gases separate into reservoir gases, which do not destroy ozone, and reactive gases, which participate in ozone destruction cycles. Source: WMO (2007).

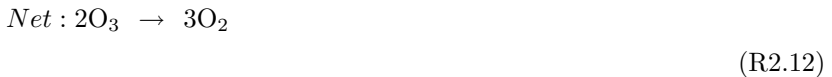


In 1928, Thomas Midgely produced a compound called CFC-12. Midgely developed CFC-12 as a replacement for highly toxic and flammable refrigerants such as ammonia. Midgely showed that CFC-12 was non-toxic, non-

flammable, and had thermal properties that made introduce an excellent refrigerant. In 1930, Dupont and General Motors began to introduce CFCs into the market under the trade name Freon. Since then, other CFCs have been synthesized and produced in large quantities. CFCs have been extensively used in refrigerators and as propellants in aerosol cans. CFCs are composed of fluorine, carbon, and chlorine. Vast amounts of chlorine are found on the Earth in other forms, particularly sea salt (NaCl). Fortunately, sea salt is water soluble, so this form of chlorine is essentially completely rained out before getting to the stratosphere. CFCs are not water soluble, and are essentially nonreactive in the troposphere. The stability of CFC molecules means that CFCs can only be destroyed by the extremely energetic UV radiation (i.e by photolysis) above most of the ozone layer.

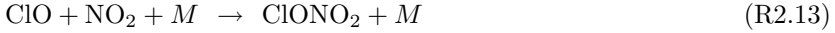
*Molina and Rowland* (1974, 1975) suggested that long-lived organic halogen compounds, such as CFCs, might behave in a similar fashion as Crutzen had proposed for nitrous oxide.

Cycle 1 (*Molina and Rowland*, 1974):



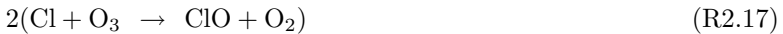
The net effect of this reaction is the formation of 3 oxygen molecules from two  $\text{O}_3$  molecules, while the ClO (chlorine monoxide) molecule is unaffected. Cycle 1 requires sunlight because atomic oxygen is formed only with ultraviolet sunlight. Cycle 1 is most important in the stratosphere at tropical and middle latitudes at high altitudes (35-50 Km), where ultraviolet sunlight is most intense. For typical stratospheric conditions at middle and low latitudes a single Cl atom can destroy hundreds of ozone molecules, before Cl reacts with another gas breaking the catalytic cycle (*WMO*, 2007).

Cl can also react with nitrogen dioxide to form the metastable compound chlorine nitrate



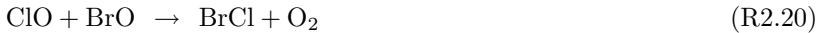
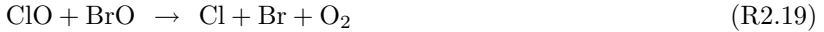
Significant destruction of ozone occurs in polar regions (see Chapter 2.3.2), where chlorine monoxide (ClO) abundances reach large values. In this case, the cycles initiated by the reaction of chlorine monoxide (ClO) with another ClO (*Molina and Molina, 1987*) or the reaction of ClO with Bromine monoxide (BrO) (*McElroy et al., 1992*) efficiently destroy ozone. The net reaction in both cases is the destruction of two ozone molecules forming three oxygen molecules. The reaction of ClO with BrO has two pathways to form the Cl and Br product gases. Sunlight is required to complete each cycle and to help form and maintain ClO abundances.

Cycle 2 (*Molina and Molina, 1987*):



Cycle 3 (*McElroy et al., 1992*):

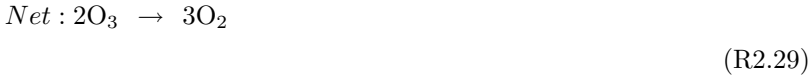




Cycles 2 and 3 require visible sunlight to complete the reaction cycles and to maintain ClO abundances. In the continuous darkness of winter in the polar stratospheres, reaction Cycles 2 and 3 cannot occur. It is only in late winter/early spring when sunlight returns to the polar regions that these cycles can occur. Therefore, the greatest destruction of ozone occurs in the partially to fully sunlit periods after midwinter in the polar stratospheres. The visible sunlight needed in Cycles 2 and 3 is not sufficient to form ozone because this process requires ultraviolet sunlight at wavelength smaller than 240 nm. In the stratosphere in the late winter/early spring period, ultraviolet sunlight is weak because sun angles are low. As a result, ozone is destroyed by Cycles 2 and 3 in the sunlight but is not produced in significant amounts.

Bromine (Br) is present in much smaller quantities than Chlorine (Cl), but it is much more destructive on a per-atom basis. There is a large natural source; man-made compounds contribute about 40% of the total. In Antarctica chlorine is more important than Bromine, but at middle latitudes their effects are comparable.

This implies, that reducing stratospheric chlorine concentrations will, as a side-effect, slow down the Bromine pathways as well. Another important mechanism combines Br with HOx radicals:



### 2.3.2 Polar ozone: Antarctic and Arctic ozone hole

Severe ozone depletion appears over Antarctica because atmospheric conditions increase the effectiveness of ozone depletion by reactive halogen gases. The formation of the Antarctic ozone hole requires abundant reactive halogen gases, temperatures low enough to form polar stratospheric clouds (PSCs), isolation of air from other stratospheric regions and sunlight, (e.g., *Solomon*, 1999). Halogen source gases emitted at Earth's surface are present in comparable abundances throughout the stratosphere in both hemispheres even though most of the emissions occur in the Northern Hemisphere. The concentrations are comparable because most source gases have no important natural removal processes in the lower atmosphere and because winds and warm-air convection redistribute and mix air efficiently throughout the troposphere. Halogen gases enter the stratosphere primarily from the tropical upper troposphere. Atmospheric air motions then transport them upward and toward the poles in both hemispheres (see Figure 2.7). During winter, the polar regions of both the Arctic and Antarctica are surrounded by a very strong jet stream blowing from east-to-west. This jet acts as a barrier to air moving from the mid-latitudes into the polar region, isolating the poles. Temperatures poleward of this jet are very cold, dropping to below  $-80$  °Celsius. Air in the polar stratospheric regions is relatively isolated from other stratospheric regions for long periods in the winter months.

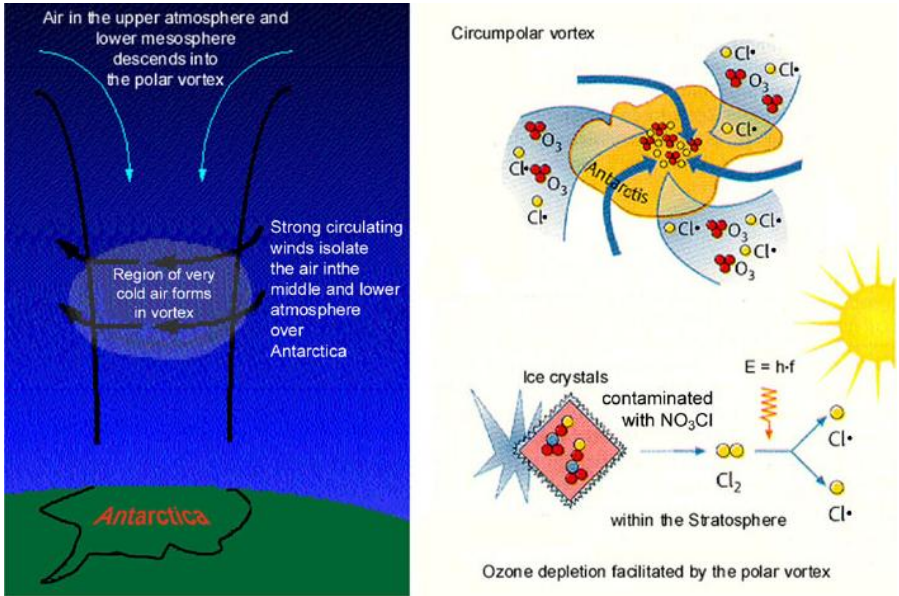


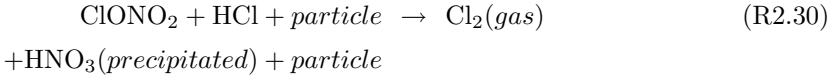
**Figure 2.7:** The ozone hole occurs during the Antarctic spring, from September to early December, as strong westerly winds start to circulate around the continent and create an atmospheric container. The overall cause of ozone depletion is the presence of chlorine-containing source gases (primarily CFCs and related halocarbons). In the presence of UV light, these gases dissociate, releasing chlorine atoms, which then go on to catalyze ozone destruction. The Cl-catalyzed ozone depletion can take place in the gas phase, but it is dramatically enhanced in the presence of polar stratospheric clouds (PSCs). These polar stratospheric clouds form during winter, in the extreme cold. Polar winters are dark, consisting of 3 months without solar radiation (sunlight). Not only lack of sunlight contributes to a decrease in temperature but also the “polar vortex” traps and chills air. Temperatures over around or below  $-80^{\circ}\text{C}$ . These low temperatures form cloud particles and are composed of either nitric acid (Type I PSC) or ice (Type II PSC). Both types provide surfaces for chemical reactions that lead to ozone destruction. Source: Newman et al. (2008)

The isolation is caused by the strong winds that encircle the poles, preventing substantial motion of air in or out of the polar stratospheres. The isolation is much more effective in the Antarctic than the Arctic. In the Antarctic winter, minimum temperatures are generally lower and less *variable* than in the Arctic winter (Figure 2.8). Antarctic temperatures also remain below the PSC formation temperature ( $-78$  °Celsius) for much longer periods during winter. This occurs, mainly, because there are significant meteorological differences between the hemispheres, resulting from the differences in the distributions of land, ocean, and mountains at middle and high latitudes.

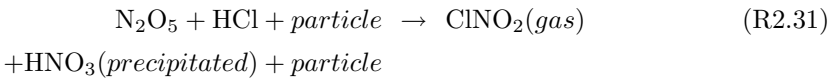
The amount of water vapor in the stratosphere is low.

This means that under normal conditions there are no clouds in the stratosphere. However, when the temperature drops below  $-78$  °C clouds that consist of a mixture of water and nitric acid start to form. These clouds are called PSCs of type I. On the surface of particles in the cloud, chemical reactions occur that transform passive and innocuous halogen compounds (e.g.  $\text{ClONO}_2$ ,  $\text{HCl}$  and  $\text{HBr}$ ) into so-called active chlorine and bromine species (e.g.  $\text{ClO}$  and  $\text{BrO}$ ) (compare Figure 2.6 and reactions R2.30 and R2.31). These active forms of chlorine and bromine cause rapid ozone loss in sunlit conditions through catalytic cycles where one molecule of  $\text{ClO}$  can destroy thousands of ozone molecules before it is passivated through the reaction with nitrogen dioxide ( $\text{NO}_2$ ). When temperatures drop below  $-85$  °C clouds that consist of pure water ice will form. These ice clouds are called PSCs of type II. Particles in both cloud types can grow so large that they no longer float in the air but fall out of the stratosphere. In doing so they bring nitric acid  $\text{HNO}_3$  with them. Nitric acid is a reservoir that liberates  $\text{NO}_2$  under sunlit conditions. If  $\text{NO}_2$  is physically removed from the stratosphere (a process called denitrification), active chlorine and bromine can destroy many more ozone molecules before they are passivated. The formation of ice clouds will lead to more severe ozone loss than that caused by PSC type I alone since halogen species are more effectively activated on the surfaces of the larger ice particles. PSCs are often found near mountain ranges in polar regions because the motion of air over the mountains can cause local cooling of stratospheric

air. Key heterogeneous reactions leading to reactivation of reservoir species are for example



*or*



Where more in detail, the reservoir species chlorine nitrate  $\text{ClONO}_2$  and dinitrogen pentoxide ( $\text{N}_2\text{O}_5$ ) react with hydrochloric acid (HCl) on the surface of a particle, releasing ( $\text{Cl}_2$ ) or ( $\text{ClNO}_2$ ) and producing nitric acid.  $\text{Cl}_2$  and  $\text{ClNO}_2$  are readily photolysed by UV light producing ozone destroying radicals (Cl and also ClO). The  $\text{HNO}_3$  however sticks to the cloud and will eventually precipitate out of the atmosphere, removing the nitrogen oxides that would otherwise prevent Cl from destroying  $\text{O}_3$  by forming the relatively inert  $\text{ClONO}_2$  again. Thus, forms of chlorine (HCl and  $\text{ClONO}_2$ ), that do not affect ozone, can react on the surfaces of these PSC's and produce chlorine radicals that can catalytically destroy ozone. Chlorine and Bromine catalytic destruction reactions are so fast that all of the ozone over Antarctica between 12 and 20 km is destroyed within a few weeks during the September (Antarctic spring) period (Figure 2.9). The cycle 2 described in Chapter 2.3.1 dominates the ozone-destruction process. Photolysis of chlorine peroxide, requires UV light which only becomes abundant in the lower stratosphere in the spring. Thus one has a long build up of ClO and  $\text{ClOOCl}$  during the winter, followed by massive ozone destruction in the spring. This mechanism is believed to be responsible for about 70% of the antarctic ozone loss. Cycle 3 in Chapter 2.3.1 is believed to be responsible for about 20% of the Antarctic ozone depletion (WMO, 2007). When temperatures increase by early spring, PSCs no longer form and the production of ClO ends. Without continued ClO production, ClO amounts decrease as other chemical reactions reform  $\text{ClONO}_2$

and HCl. As a result, the intense period of ozone depletion ends, when polar vortex break down and the polar air is mixed with mid-latitudes air. However, note that the reaction constants of some key chemical reactions are still under consideration. In a recent study of *Pope et al.* (2007), it has been found that the rate of photolysis of ClOOCl in the stratosphere is much lower than the currently recommended. For conditions representative of the polar vortex (solar zenith angle of  $86^\circ$ , 20 km altitude, and  $O_3$  and temperature profiles measured in March 2000) calculated photolysis rates are a factor of 6 lower than the current JPL/NASA recommendation. This large discrepancy calls into question the completeness of present atmospheric models of polar ozone depletion.

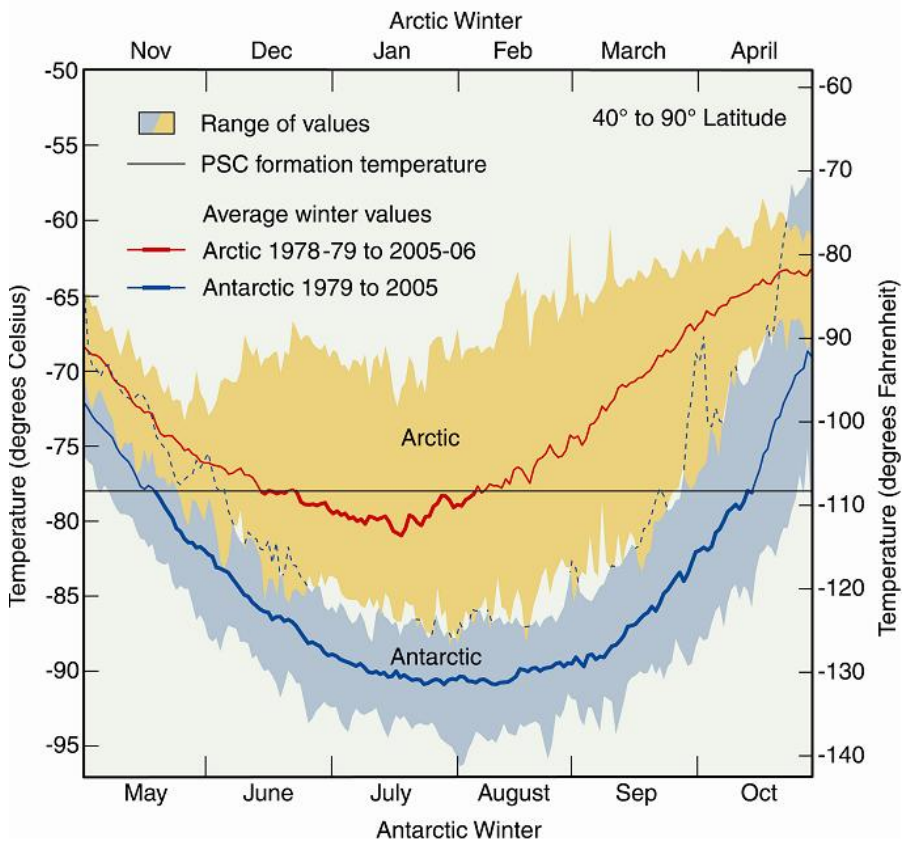


**Figure 2.8:** Stratospheric air temperatures in both polar regions reach minimum values in the lower stratosphere in the winter season. Average minimum values over Antarctica are as low as  $-90^{\circ}\text{C}$  in July and August in a typical year. Over the Arctic, average minimum values are near  $-80^{\circ}\text{C}$  in January and February. Source: (WMO, 2007)

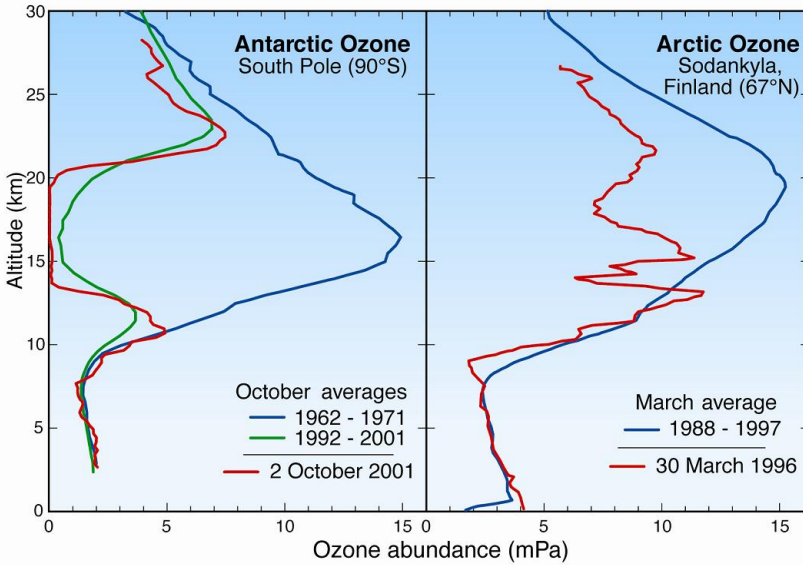


**Figure 2.9:** Arctic and Antarctic ozone distribution. The stratospheric ozone layer resides between about 10 and 50 kilometers above Earth's surface over the globe. Long-term observations of the ozone layer with balloon borne instruments allow the winter Antarctic and Arctic regions to be compared. In the Antarctic at the South Pole, halogen gases have destroyed ozone in the ozone layer beginning in the 1980s. Before that period, the ozone layer was clearly present, as shown here using average ozone values from balloon observations made between 1962 and 1971. In more recent years, as shown here for 2 October 2001, ozone is destroyed completely between 14 and 20 kilometers in the Antarctic in spring. Average October values in the ozone layer now are reduced by 90% from pre-1980 values. The Arctic ozone layer is still present in spring as shown by the average March profile obtained over Finland between 1988 and 1997. However, March Arctic ozone values in some years are often below normal average values as shown here for 30 March 1996. In such years, winter minimum temperatures are generally below PSC formation temperatures for long periods. Source: (WMO, 2007)



### 2.3.3 Effect of volcanic eruptions

Explosive volcanic eruptions can inject large amounts of sulfate aerosols into the stratosphere. The largest eruptions of the last 150 years, such as the June 1991 eruption of Mount Pinatubo in the Philippines, injected large amounts of material into the stratosphere. Volcanic sulfur dioxide is quickly transformed into sulfate aerosol. Sulfate aerosol provides a catalytic surface on which nitrogen and chlorine are converted from reservoir species to active forms that can destroy ozone. The chemical effect of an eruption is dependent on the chlorine content of the stratosphere. The chemical effect is also strongly dependent on temperature. The largest effect is in the winter lower stratosphere where cold temperatures allow the sulfate particles to grow and increase their surface area. Many observations have linked the 1991 Mt. Pinatubo eruption to a 20% increase in the ozone hole that following spring (*Solomon, 1993*). The effects of a large volcanic eruption on total global ozone are more modest (less than 3%) and last no longer than 2-3 years. However Volcanic Pinatubo signal has not been seen in the southern hemisphere.

## 2.4 Spatial and seasonal variation of stratospheric ozone

The abundance of stratospheric ozone, described in the previous section, is determined by a combination of chemical and dynamical processes. The importance of these processes changes with location (particularly altitude and latitude) and with time.

The total column ozone amounts near the equator are rather low (less than 300 DU, where 1 Dobson Unit (DU) is defined to be 0.01 mm thickness at standard temperature and pressure) over the course of the year.

Throughout the year, low total ozone amounts in the tropics combines with the direct overhead sun to create the very high amounts of UV erythemal exposure. The total column amount of ozone generally increases when moving

from the tropics to higher latitudes in both hemispheres. However the overall column amounts are greater in the northern hemisphere high latitudes than in the southern hemisphere high latitudes. In addition, while the highest amounts of column ozone over the Arctic occur in the northern spring (March-April), the opposite is true over the Antarctic, where the lowest amounts of column ozone occur in the southern spring (September-October).

The stratospheric circulation, known as the Brewer-Dobson circulation, transports high ozone amount from the tropics poleward and downward to the lower stratosphere at the high latitudes. It consists of a meridional circulation in each hemisphere, with air rising into the stratosphere in the tropics (where there is little seasonal variation in ozone), moving poleward, with descent and entrainment into the troposphere at high latitudes (*James, 1994*).

Ozone maximal concentrations are at higher altitude in the tropics, and at lower altitude in the extra-tropics, especially in the polar regions. This altitude variation of ozone results from the slow circulation that lifts the ozone-poor air out of the troposphere into the stratosphere. This air slowly rises in the tropics and ozone is produced by the overhead sun which photolyses oxygen molecules (as shown in the previous section). As this slow circulation bends towards the mid-latitudes, it carries the ozone-rich air from the tropical middle stratosphere to the mid-and-high latitudes lower stratosphere. The high ozone concentrations at high latitudes are due to the accumulation of ozone at lower altitudes. The time needed to lift an air parcel from the tropical tropopause near 16 km to 20 km is about 4-5 months (*Newman et al., 2008*). Even though ozone in the lower tropical stratosphere is produced at a very slow rate, the lifting circulation is so slow that ozone can build up to relatively high levels by the time, when it reaches 26 km.

Other processes also effect ozone variability on different time scales: the influence of the solar cycle on total column ozone varies over its 11-year cycle, the quasi-biennial oscillation (QBO) over an approximately 27-month cycle, and strong volcanic eruptions have an effect lasting a few years. Because of the man made emission of ozone depletion substance (ODS), the ozone layer decreased most strongly in the Antarctic region. Clear differences in ozone abundance between the two hemispheres were noted around the 2000. An-

nually averaged total ozone over the northern mid-latitudes was 3% lower than pre-1980 levels, with twice as much decline in winter than in summer. Over the southern mid-latitudes, by contrast, a long-term decrease of 6% had occurred, roughly constant through the year, (*WMO*, 2007). *WMO* (2003) concluded that computed models including observed changes in halocarbons, other source gases, and aerosols captured the long-term behavior in mid-latitudes reasonably well. Increasing evidence was found that the observed changes in atmospheric dynamics had a significant influence on ozone over northern mid-latitudes on decade time scales, (*WMO*, 2007).

The relative contributions of different processes will change with the time period considered and between the hemispheres. Chemical changes in mid-latitudes may result from changes in  $O_3$  loss processes occurring locally or those at polar latitudes, whose effects are subsequently transported to mid-latitudes. Both gas-phase and heterogeneous chemical processes are important in these processes. A major chemical driver for long-term lower stratospheric ozone changes is increases in stratospheric Chlorine and Bromine.

## 2.5 Montreal protocol

In 1985 the Vienna Convention established mechanisms for international cooperation in research of stratospheric ozone and to protect the ozone layer against destruction by ozone depleting chemicals (ODCs). In 1985 the Antarctic ozone hole was discovered (*Farman et al.*, 1985). On the basis of the Vienna Convention, the Montreal Protocol on Substances that Deplete the Ozone Layer was negotiated. The Protocol called the Parties to decrease the emission of CFCs, Halons and other man-made ODCs.

After a series of meetings and negotiations, the Montreal Protocol on Substances that Deplete the Ozone Layer was finally agreed upon on 16 September 1987 at Montreal. The Montreal Protocol was strengthened several times and stipulates that the production and consumption of compounds that deplete ozone in the stratosphere chlorofluorocarbons (CFCs), halons, carbon tetra-

chloride, and methyl chloroform are to be phased out by 2000 (2005 for methyl chloroform).

For each group of ODS, the treaty provides a timetable on which the production of those substances must be phased out and eventually eliminated.

The stated purpose of the treaty is that the signatory states:

”...Recognizing that world-wide emissions of certain substances can significantly deplete and otherwise modify the ozone layer in a manner that is likely to result in adverse effects on human health and the environment, ... Determined to protect the ozone layer by taking precautionary measures to control equitably total global emissions of substances that deplete it, with the ultimate objective of their elimination on the basis of developments in scientific knowledge ... Acknowledging that special provision is required to meet the needs of developing countries...”

The provisions of the Protocol include the requirement that the Parties to the Protocol base their future decisions on the current scientific, environmental, technical, and economic information that is assessed through panels drawn from the worldwide expert communities. To provide that input to the decision-making process, advances in understanding on these topics were assessed in 1989, 1991, 1994, 1998, 2002 and 2006 in a series of reports entitled *Scientific assessment of ozone depletion*, published by World Meteorological Organization (WMO) and the United Nations Environmental Program (UNEP).

Global ozone levels are now no longer declining as they were from the late 1970s until the mid-1990s, and some increases in ozone have been observed. These improvements in the ozone layer have occurred during a period when stratospheric halogen abundances reached their peak and started to decline. These declining halogen abundances clearly reflect the success of the Montreal Protocol and its Amendments and Adjustments in controlling the global production and consumption of ozone-depleting substances (ODSs) (see Figure 2.10).

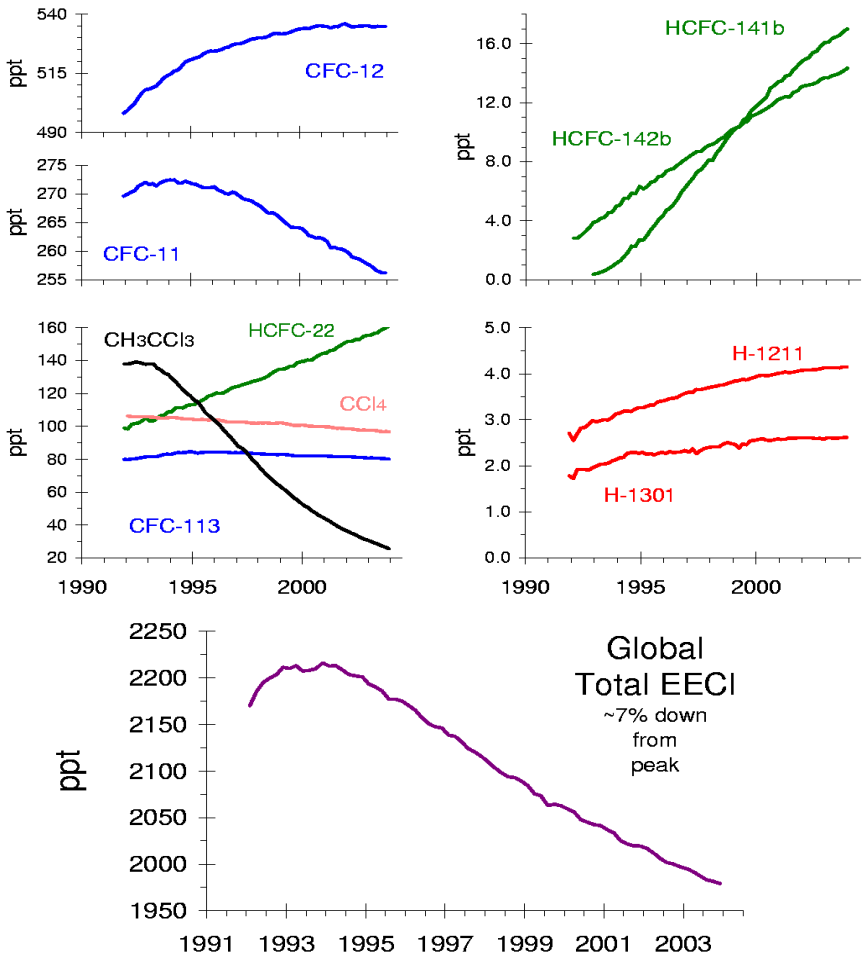


**Figure 2.10:** *Mixing ratio of anthropogenic Halocarbons. Since the Montreal Protocol came into effect, the atmospheric concentrations of the most important chlorofluorocarbons and related chlorinated hydrocarbons have either leveled off or decreased. The concentration of the HCFCs increased drastically and they will continue to increase in the coming decades until the 2040 year, at least partly because for many uses CFCs were substituted with HCFCs. Source: (WMO, 2007)*

Stratospheric ozone abundances are affected by a number of natural and anthropogenic factors in addition to the atmospheric abundance of ODSs, e.g., temperatures, transport, volcanoes, solar activity, and hydrogen and nitrogen oxides. Separating the effects of these factors is complex because of nonlinearities and feedbacks in the atmospheric processes affecting ozone. Figure 2.11 exhibits an idealized scheme of the temporal evolution of the ozone layer as expected from the effect of the Montreal Protocol. Three important stages can be identified:

- The slowing of ozone decline, identified as the occurrence of a statistically significant reduction in the rate of decline in ozone due to changing EESC (Equivalent Effective Stratospheric Chlorine).
- The onset of ozone increases (turnaround), identified as the occurrence of statistically significant increases in ozone above previous minimum values due to declining EESC and the full recovery of ozone from ODSs, identified as when ozone is no longer affected by ODSs.
- In the absence of changes in the sensitivity of ozone to ODSs, this is likely to occur when EESC returns to pre-1980 levels.

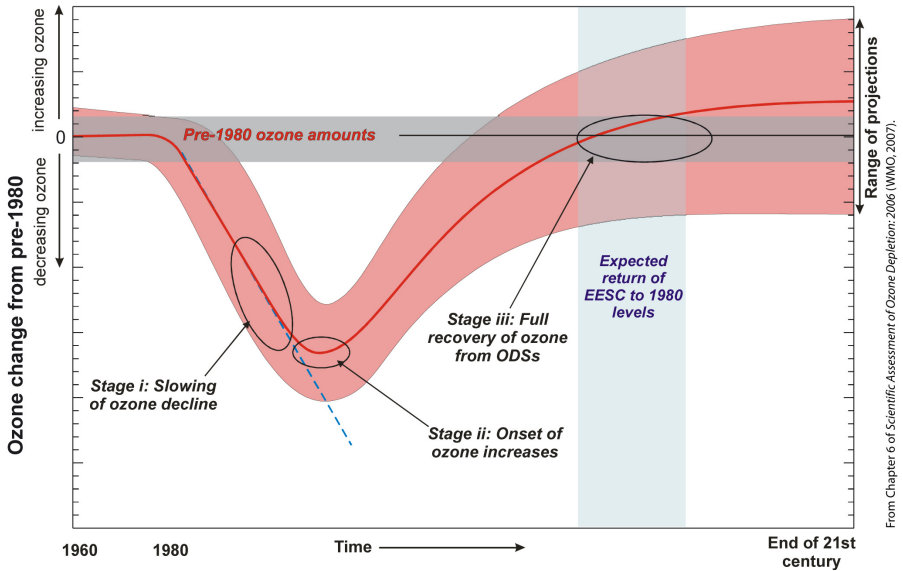


**Figure 2.11:** A schematic diagram of the temporal evolution of global ozone amounts beginning with pre-1980 values, which represent amounts before significant depletion due to anthropogenic ODS emissions, and stopping at the end of the 21st century. Observed and expected ozone amounts (solid red line) show depletion from pre-1980 values and the three stages of recovery from this depletion. The red-shaded region represents the range of observations and model results for both near-term and long-term ozone changes. The blue-shaded region represents the time period when declining global ODS concentrations are expected to reach 1980 values. The full recovery of ozone from ODSs may be delayed beyond the return of ODSs to 1980 levels by factors (e.g., a volcanic eruption close to that time) that could change the sensitivity of ozone to ODSs. Source: (WMO, 2007)

## 2.6 Trends of stratospheric ozone

Recent studies of long-term changes in ozone are focused on detection of the ODS-related signal in the available data. Typically this is done by including a term in statistical models that is proportional to the stratospheric burden of

ODSs, such as EESC or a similar function. The general purpose of statistical models is to characterize and quantify the relationship between predictor or explanatory variables and ozone. In ozone trends studies some of the explanatory variables describe natural variations in ozone, while others are included in the model to reflect possible anthropogenic changes in ozone.

Seasonal cycle, solar flux, and quasi biennial oscillation (QBO) indexes are commonly used as proxies for natural ozone variability (see Figure 2.12). Characteristics of volcanic aerosols, such as aerosol optical depth, are used in some models to account for effects of volcanic eruptions, particularly for the El Chichón and Mt. Pinatubo eruptions. The EESC is an index reflecting the amount of ozone-depleting chlorine and bromine in the stratosphere. The last plot in Figure 2.12 suggests that a change in total column ozone can be assumed to be generally proportional to the EESC, which provides evidence, that Montreal Protocol start to become effective. The slowing of ozone decline is identified as the occurrence of a statistically significant reduction in the rate of decline in ozone due to changing EESC.



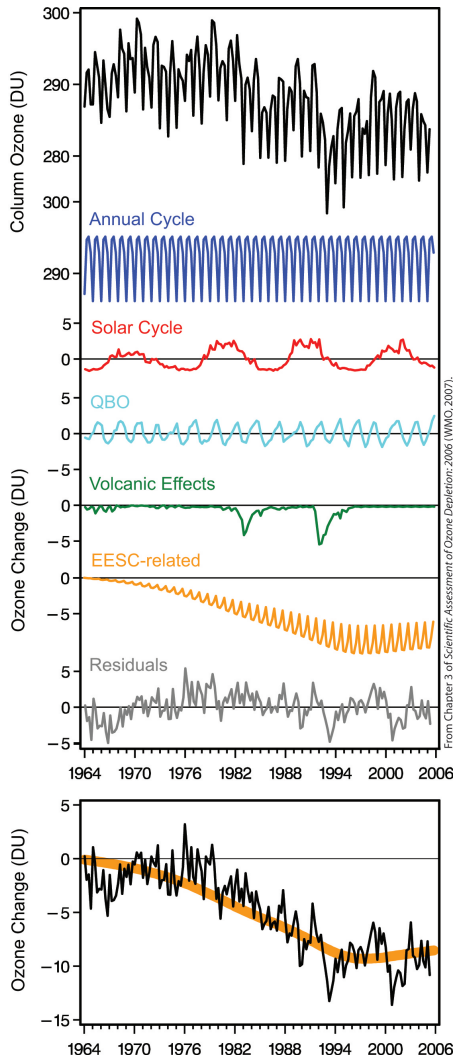


**Figure 2.12:** Top: Ozone variations for  $60^{\circ}S-60^{\circ}N$  estimated from ground based data and individual components that comprise ozone variations. Bottom: Deseasonalized, area weighted total ozone deviations estimated from ground based adjusted for solar, volcanic, and QBO effects, for  $60^{\circ}S-60^{\circ}N$ . The thick yellow line represents the EESC curve scaled to fit the data from 1964-2005. Source: (WMO, 2007).



## Chapter 3

# Stratospheric Ozone Measurements

Measurements of atmospheric ozone are required to understand the spatial and temporal distribution patterns of ozone in the atmosphere and, since the last decades, to document anthropogenic ozone changes. Ozone measurements are typically reported in one of four units:

- total column amount in Dobson Units (DU)
- mixing ratio in parts per million by volume (ppmv)
- number density (molecules per cubic centimeter)
- partial pressure in nanobars (nb)

Each of these ways of quantifying ozone provides a different perspective on the ozone distribution.

### 3.1 Total ozone column

The measurement of the total column of ozone is directly related to the amount of UV light reaching the surface 2.2. It is therefore a measure of UV

exposure received at the surface: the less total ozone in the column, the more UV light penetrates. The total column of ozone is expressed in the Dobson Unit (DU) which is a measure of the “thickness” of the ozone layer. One Dobson unit refers to a layer of ozone that would be 10  $\mu\text{m}$  thick under standard temperature and pressure. Approximately the global average of total ozone is 300 DU and therefore only approximately 3 millimeters thick. Dobson and Brewer spectrophotometers are the standard instruments for ground based total ozone monitoring in the World Meteorological Organization’s Global Atmospheric Watch (GAW) program (WMO, 2003).

The oldest type of ozone spectrophotometer is the Dobson instrument, originally designed in the 1920’s by *Dobson* (1931) suitable for routine observations (see Figure 3.1). The quality of total ozone data available from 17 Dobson sites prior to 1957 was assessed by (*Brönnimann et al.*, 2003b,a). About half of these pre-1957 datasets are reliable for analysis of total ozone variability; however, uncertainties in the absolute calibrations make most of these sets unsuitable for trend analysis (WMO, 2007).

The Brewer spectrophotometer was developed in the early 1980s (*Kerr et al.*, 1981) (see Figure 3.3). There are now about 200 instruments installed around the world. They are regularly calibrated against a traveling standard. The traveling standard itself is calibrated against the set of three Brewer instruments located in Toronto and known as the Brewer Reference Triad (*Fioletov et al.*, 2005).

Details of the instruments’ design and algorithms are presented in (*Scarnato et al.*, 200xa). Small systematic differences between Dobson and Brewer total ozone measurements have been reported (WMO, 2003), see Chapter 2.2.

Filter ozonometers are widely used in the former Soviet Union countries, and long-term reliable records are available from 1972. This instrument is less accurate than the Dobson and Brewer instruments, and the calibration is traceable to the Dobson reference.

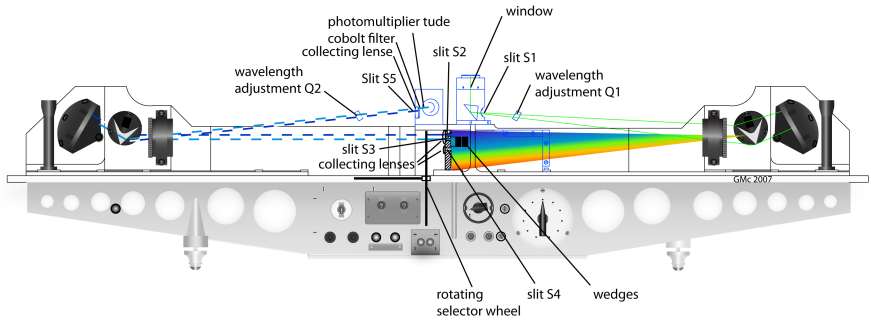


**Figure 3.1:** *Dobson instrument geometry and optics. The light pass through the window and dispersed form the quartz prism. Short wavelengths pass through slit S2 and long wavelength through slit S3. The ratio between the two intensities are determined by an R-dial located on the top of the Dobson spectrophotometer. The R-dial controls a filter wedge that gradually blocks out the 325 nm light. As the R-dial rotates from 0 to 300 degrees, the filter wedge increasingly blocks out more light. At 0 degrees the wedge does not block out any light. At 300 degrees, the wedge nearly blocks all of the light. The filter wedge gradually blocks more and more light until the intensity of the 325 nm and 305 nm light are equal. The R-dial is calibrated with the filter wedge, so that the original intensity of the 325nm light can be determined from the R-dial reading. By taking the R-dial reading when the intensities of the two wavelengths are equal, their ratio is determined. The left part of the system is to reduce stray light effect. Aerosols present in the atmosphere is assumed to scatter light at both wavelengths equally. Thus, aerosols should not have affect on the ratio of light intensities between 305 and 325 nm. Thanks to the courtesy of Glen Mc Conville for the plot.*

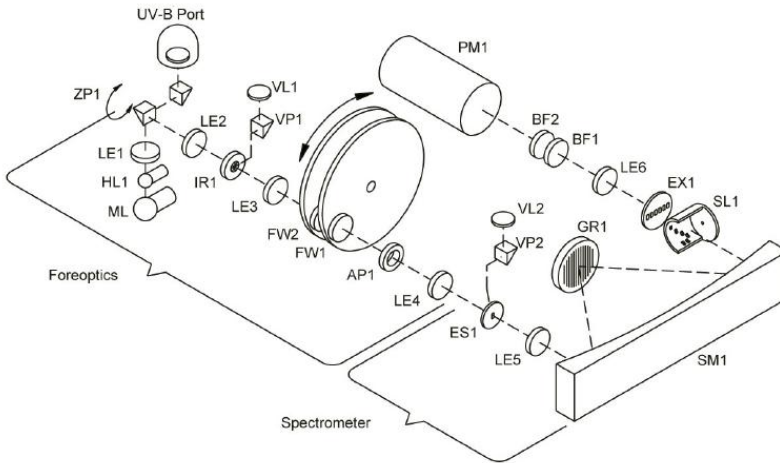


**Figure 3.2:** Brewer MKII optics. Foreoptics: The automated system drives stepper motors which control three elements in the foreoptics assembly - the Iris Diaphragm (IR1), Filterwheel (FW1), and Filterwheel (FW2). Incoming light is directed through the foreoptics by the director prism (ZP1), which may be rotated to select light from either the zenith sky, the direct sun, or one of the two calibration lamps. A mercury lamp provides a line source for wavelength calibration of the spectrometer, while a quartz halogen lamp provides a well regulated light source so that the relative spectral response of the spectrometer may be monitored. Elements in the foreoptics provide adjustment for field-of-view, neutral-density attenuation, ground-quartz diffusion, and selection of film polarizers. Spectrometer: Light enters the entrance slit and passes through a tilted lens (LE5) which corrects for the coma and astigmatic aberrations inherent in an Ebert system. The light is collimated by a spherical mirror (SM1) onto a diffraction grating (GR1) where it is dispersed. A second mirror reflection focuses the spectrum onto the focal plane of a slotted cylindrical slit mask (SL1) positioned at the exit of the spectrometer. After wavelength selection by the slit mask, the light passes through the exit slit plate (EX1). Six exit slits are located along the focal plane at the appropriate wavelength positions. One of the six exit slits (slit 0) is used for wavelength calibration against the 302-nm group of mercury lines; the other five are for intensity measurements and are nominally set at 306.3, 310.1, 313.5, 316.8, and 320.1 nm. Source: Brewer manual.

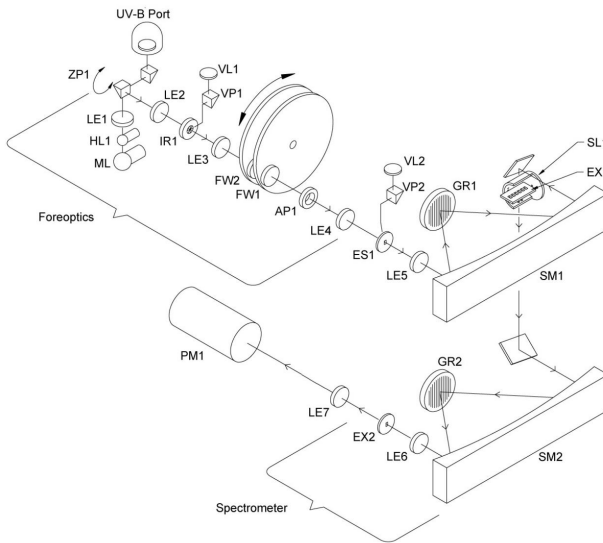


**Figure 3.3:** Brewer MKIII optics. *Foreoptics:* The same as in MkII. *Spectrometer:* Light enters the entrance slit and passes through a tilted lens (LE 5) which corrects for the coma and astigmatic aberrations inherent in an Ebert system. In the first spectrometer the light is collimated by a spherical mirror (SM 1) onto a diffraction grating (GR 1) where it is dispersed. A second mirror reflection focuses the spectrum onto the focal plane of a slotted cylindrical slit mask positioned at the entrance of the second spectrometer. Following wavelength selection by the slit mask, the light passes through the second spectrometer where it is recombined and directed onto the exit slit plane. Six exit slits are located along the focal plane at the appropriate wavelength positions. One of the six exit slits (slit 0) is used for wavelength calibration against the 302-nm group of mercury lines; the other five are for intensity measurements and are nominally set at 306.3, 310.1, 313.5, 316.8, and 320.1 nm. Source: Brewer manual.

## 3.2 Satellites

Ozone observations from satellites offer the opportunity to monitor the total ozone shield on near-global basis. The suitability for long term trend analysis of satellite  $O_3$  observations depends on sensor used, the orbit of the satellite defining the sequence and the coverage of the observations, and the lifetime of instruments.

Since the first satellite ozone measurements in 1960, basically three methods have been developed: backscattered solar ultraviolet, infrared emission, and occultation. Satellite measurements can provide a good global coverage. They can provide informations with a good accuracy of ozone amount and profile.

Total Ozone Mapping Spectrometers (TOMS) measure solar irradiance and radiance backscattered by Earth's atmosphere at six wavelengths extending from 310 to 380 nm. Because of the absorption of solar light by ozone in the Huggins band, total ozone measurements on satellites with Sun-synchronous orbits can provide daily map of total ozone except where Earth's atmosphere is shaded by polar night. The diffuser plate that reflects direct sunlight into the spectrometer is subject to degradation. The TOMS data were compared to the ground based total ozone observations in order to ensure the long term stability of its calibration.

Solar backscatter ultraviolet radiometers (SBUV) have been flown on a number of NASA and NOAA satellites over the last 20 years. SBUV instruments measure column ozone in a manner similar to TOMS. They also use the backscatter radiation at even shorter wavelengths (where the absorption by ozone is much stronger) to provide vertical ozone information, albeit with less precision. Because the instruments nadir viewing, data coverage is not as complete as that provided by TOMS instruments.

The TIROS-N Operational Vertical Sounders (TOVS) on NOAA polar-orbiting satellites measure  $O_3$  in the infrared ( $9.7 \mu\text{m}$ , high-resolution infrared sounder (HIRS)). These instruments are sensitive to lower stratospheric  $O_3$  and give near-global coverage even during polar night. Accurate total ozone determination is difficult because of the weak sensitivity of  $O_3$ .



The Global Ozone Monitoring Experiment (GOME) is an instrument on the second European Remote Sensing Satellite (ERS-2), which was launched in April 1995. Atmospheric ozone measurements are based on the principle of differential ozone absorption spectroscopy (DOAS) (*Burrows et al., 1999*). This instrument provides measurements of some other atmospheric trace components and ozone vertical profiles in addition to column ozone. Near-global maps of total ozone can be made from measurements taken over 3 days.

Occultation experiments is another class within the different types of methods to perform atmospheric constituent soundings. In essence, the method consists of measuring the atmospheric transmission of light as a function of time and wavelength while the host satellite is orbiting the planet (Earth). During the setting or rising of the light source with respect to the horizon the optical path crosses different atmospheric layers. After the measurement the data can, in principle, be used to obtain information on atmospheric constituent abundances: the wavelength variation of the transmittance delivers information on the different constituents (because of the characteristic spectral extinction signature of every constituent), while the time variation delivers spatial (altitudinal) information. The combined spectral/temporal variation of the measured signal can be processed to retrieve altitude profiles of gas number densities and aerosol extinction coefficients. At present, the occultation method has become a standard technique in atmospheric sounding. Among the extensive list of previously and presently operational experiments we can mention the Global Ozone Monitoring by Occultation of Stars (GOMOS) experiment (*Bertaux et al., 1991*), the Stratospheric Aerosol and Gas Experiment (SAGE) series (*Chu et al., 1989*), Atmospheric Trace Molecule Spectroscopy (ATMOS) (*Gunson and et al., 1996*), Polar Ozone and Aerosol Measurement (POAM) (*Lucke and et al., 1999*), etc.

NIWA data is one of the global data sets used by WMO, which integrates data from several US and EU satellites with a global set of ground stations.

This is an assimilated database that combines satellite-based ozone measurements from 4 Total Ozone Mapping Spectrometer (TOMS) instruments, 3 different retrievals from the Global Ozone Monitoring Experiment (GOME),

and data from 4 Solar Backscatter Ultraviolet (S-BUV) instruments (*Bodeker et al.*, 2005).

### 3.3 Ozone profiles

Profile measurements can be made by balloon borne instruments known as ozone sondes, laser instruments called lidar, and profiling satellite instruments. These measurements are usually reported in mixing ratio, number density, or partial pressure. Mixing ratio in ppmv reports the fractional concentration of ozone as the number of ozone molecules per million air molecules. Number density refers to the absolute concentration as the number of ozone molecules per cubic centimeter. Partial pressure refers to the fraction of the atmospheric pressure at a given altitude for which ozone is responsible.

## Chapter 4

# Temperature and Slant Path Effects in Dobson and Brewer Ozone Measurements

Scarnato B.<sup>1</sup>, Staehelin J.<sup>1</sup>, Gröbner J.<sup>2</sup>, Stuebi R.<sup>3</sup>, Schill H.<sup>3</sup>

<sup>1</sup>ETH, Zurich; Switzerland, <sup>2</sup>PMOD/WRC, Davos; Switzerland,

<sup>3</sup>MeteoSwiss, Aerological Station; Payerne Switzerland

Planned to be submitted to Journal of Geophysical Research

### 4.1 Abstract

There is a worldwide tendency to replace Dobson spectrophotometers in ground-based total ozone (TOZ) measurements by more advanced Brewer spectrophotometers. Ensuring the homogeneity of the data taken with these two distinct instrument types is of utmost importance if changes in TOZ of a few percent over long time periods are to be diagnosed accurately. Previous studies have identified a seasonal bias of few percent between mid-latitude Brewer and Dobson spectrophotometer measurements. At Arosa (Switzerland), two Dobson and three Brewer instruments have been co-located since 1998, producing a unique dataset of quasi-simultaneous observations invaluable for the study of systematic differences between these measurements. The

differences can be attributed at least partially to seasonal variability in atmospheric temperatures and ozone slant paths. The sensitivity to the temperature dependence of the ozone absorption cross section has been calculated using different reference spectra at high and low resolution, weighting of the slit functions for each operational Brewer and for the primary standard Dobson spectrophotometers. The Brewer retrieval algorithm shows stronger sensitivity on the reference spectra applied. Assuming the temperature dependence of the Bass and Paur (1985) ozone absorption spectra (current remote sensing standard) and the ozone slant path effect, the seasonal bias between Dobson and Brewer TOZ measurements is reduced from an amplitude of about 2% to 1%. Conversely, the use of the spectral data of *Burrows et al.* (1999) instead of *Bass and Paur* (1985) or *Malicet et al.* (1995) increases the differences between Dobson and Brewer TOZ observations at Arosa. This finding illustrates, that the accuracy of ground based spectrophotometric TOZ measurements is presently most strongly limited by the temperature dependence of the ozone cross section retrieved from different laboratory experiments. It is also critical for comparison of ground based and satellite TOZ measurements.

## 4.2 Introduction

The atmospheric ozone layer prevents harmful ultraviolet (UV) radiation from the sun from reaching the Earth's surface. Since the beginning of the 1970s, the depletion of the stratospheric ozone layer by anthropogenic activities has been a topic of scientific and public discussion (*Crutzen*, 1970; *Johnston*, 1971a,b; *Molina and Rowland*, 1974). The most dramatic effect is observed over Antarctica during southern hemispheric spring (*Farman et al.*, 1985; *Solomon*, 1988, 1999), but a significant decrease of the ozone shield is found also over mid-latitudes (e.g., *Staehelein et al.*, 2001; *WMO*, 2007). Halogens released from man-made chemicals such as chlorofluorocarbons (CFCs) and halons (containing bromine) lead to stratospheric ozone depletion (*WMO*, 2007).

After the International Geophysical Year (1958), and especially when the

impact of human activities on the ozone layer became clear, many Dobson instruments were installed to form a worldwide network. In the 1980s, an advanced instrument was built using state of the art technology, the Brewer spectrophotometer (*Kerr et al.*, 1981). Though the Dobson instrument has served its purpose well since the 1930s, the Brewer ozone spectrophotometer is today becoming more popular for studying ozone, sulphur dioxide, and UV radiation. Since the mid of 1970s a data quality assurance program has been introduced under the auspices of WMO, in which Dobson and Brewer spectrophotometers are regularly compared with standard instruments. Dobson and Brewer instruments are based on the same basic principle of measurement, but total ozone (TOZ) measurements exhibit characteristic differences in seasonal variation at mid-latitudes (*Kerr et al.*, 1988; *Köhler*, 1999; *Stahelin et al.*, 1998b; *Vanicek*, 2006). The WMO suggests the simultaneous operation of both instruments in order to study the difference between the observations and to improve the data quality (*WMO*, 2003). With this in mind, at Arosa two Dobson and two Brewers instruments have been simultaneously operated since 1988 and the third one has been added in 1998, producing a unique data base of quasi-simultaneous measurements. The primary goal of this paper is to study in detail the source of differences in TOZ measured by Dobson and Brewer instruments at Arosa. Section 4.3 includes a short overview about the measurement principle and the retrieval algorithms of Dobson and Brewer instruments. The applied data sets and the inter-comparison method are presented in Section 4.4. The effective ozone cross section temperature sensitivity has been calculated for different experimental spectra with different resolutions (*Bass and Paur*, 1985; *Malicet et al.*, 1995; *Burrows et al.*, 1999). With this knowledge, TOZ time series has been corrected for the ozone cross section temperature dependence and subsequently for the stray light problems, the results are presented in Section 4.5. Finally, conclusions are discussed in Section 4.6.

## 4.3 Dobson and Brewer measurement principle

### 4.3.1 Instrumental principle

The total ozone measurements by UV-spectrophotometers is based on the absorption differences of ozone at different wavelengths: the intensities of the solar light arriving at the Earth's surface is measured at different wavelengths (between 300 and 340 nm) and compared based on the known differences in laboratory-based O<sub>3</sub> absorption cross-sections (*Komhyr, 1980b; Komhyr and Evans, 1980*).

The solar light enters the spectrophotometers and is dispersed by a quartz prism in the Dobson and gratings in the Brewer instruments. Dobson spectrophotometers (*Dobson, 1931; Komhyr, 1980a*) are composed of two symmetric parts with two dispersive elements. The principal purpose of the first dispersive element of the instrument is the selection of the desired wavelength bands, while the principal purpose of the symmetrical second prism is the rejection of the stray light in those bands, improving the wavelength selection. For TOZ determination, the wavelength selection in the Dobson is done by two slits (S2 and S3). The radiation between 305 and 320 nm region passes through slit S2 and the longer wavelength band further to S3. An optical density attenuator (R-dial wedge) in front of S3 is used during a measurement cycle to attenuate the greater intensity of the longer wavelength band until it is registered by the null detection system as equal to the intensity of the shorter wavelength band. Ozone strongly absorbs solar light at short wavelengths and from the knowledge of its absorption spectrum (*Bass and Paur, 1985*) and the calibration of the instrument, the ozone content of the atmosphere is derived (*Komhyr et al., 1993*).

The automated Brewer instrument measures photons at selected wavelengths in the 290 to 325 nm range, to retrieve total ozone column and total column sulfur dioxide, which, because of its absorption in this wavelength band, is a significant interference at polluted sites with TOZ (*Kerr, 1985, 2002*). The

movement of holographic gratings (one in the single monochromator Brewer MKII instruments and two in the double Brewer MKIII instruments) ensures the wavelength selection, more efficiently than a prism as in the Dobson. The amount of stray light expected in a Brewer is defined by its stray light rejection value (R). R is defined as the ratio of the peak intensity to the background intensity measured while the UV dome is uniformly illuminated by a 325 nm beam of a HeCd laser (Brewer manual).

### 4.3.2 Retrieval algorithms

Beer's law expresses the attenuation of light by an absorbing or scattering medium. In application to the problem at hand it takes the form

$$I(\lambda) = I_0(\lambda)e^{-\alpha(\lambda)X\mu-\beta(\lambda)\frac{p_s}{p_0}m_R-\delta(\lambda)m_a} \quad (4.1)$$

where

$$\alpha(\lambda) = \frac{1}{X} \int_{z_0}^{\infty} \sigma(\lambda, T(z))\rho(z)dz \quad (4.2)$$

and

$$X = \frac{kT_0}{p_0} \int_{z_0}^{\infty} \rho(z)dz \quad (4.3)$$

at the selected wavelength  $\lambda$ ,  $I(\lambda)$  is the direct normal irradiance at the Earth surface;  $I_0(\lambda)$  is the intensity that would be measured outside the earth's atmosphere (ETC intensity) at  $\lambda$ ;  $\alpha(\lambda)$  is the monochromatic ozone absorption coefficient, where  $z_0$  is the station elevation,  $T$  is the temperature in Kelvin,  $\sigma(\lambda, T)$  is the ozone cross section,  $\rho(z)$  is the altitude-dependent ozone number density and  $X$  is the total ozone column [in Dobson Units (DU) equals to 2.69

$\times 10^{16}$  ozone molecules per square centimeter). In Eq.4.3,  $T_0$  is 273.15 kelvin and  $k$  is the Boltzmann constant ;  $\mu$  is the relative slant path through ozone (air mass value),  $\beta(\lambda)$  is the Rayleigh scattering coefficient;  $p_s$  is the station pressure;  $p_0$  is the mean sea level pressure at 1013.25 hPa;  $m_R$  is the relative optical air mass corresponding to Rayleigh scattering (extinction);  $\delta(\lambda)$  is the aerosol optical depth;  $m_a$  is the relative optical air mass corresponding to aerosol scattering (extinction).

The DOAS analysis requires a reference spectrum to which all measured spectra are compared. In this case the extra terrestrial solar radiation (ETC) of the primary standard instruments is determined by the zero air mass extrapolation (Langley plot method) performed at the Monua Loa observatory. The ETC for the station instruments operated in the Global Atmospheric Watch (GAW) are determined by comparison with standard instruments and their values are updated in regular intervals by inter-comparison with standard instruments.

Beer's law applies to monochromatic radiation. However, both the Dobson and Brewer instruments measure fluxes in finite band-width. The error involved in using the single wavelength assumption underlying Eq. 4.1 is greatly reduced if the rapidly changing cross-section of ozone is convolved with the appropriate slit function (the spectral sampling function) (*Vanier and Wardle, 1969; Bernhard et al., 2005*).

Dobson spectrophotometers measure the ratio between the irradiance at two wavelengths, one strongly absorbed and the other weakly affected by ozone. TOZ is retrieved using double wavelength pairs resulting from the combinations of AD, AC or CD wavelengths pairs, where A is the combination of wavelengths 305.5 and 325.4 nm, C of 311.5 and 332.4 and D of 317.6 and 339.8. The observation of double wavelength pairs is chosen in order to minimize the aerosol effects within the retrieval algorithm (*WMO, 2003; Basher, 1982*). For example TOZ derived by AD observations is calculated by the following equation



$$X_{A,D} = \frac{N_A - N_D - (\Delta\beta_{AD})\frac{p_s}{p_0}m_p - (\Delta\delta_{AD})m_a}{\mu(\Delta\alpha_{AD})} \quad (4.4)$$

$$N_A = \ln\left[\frac{I(305.5)_0}{I(325.4)'_0}\right] - \ln\left[\frac{I(305.5)}{I(325.4)'}\right] \quad (4.5)$$

$$N_D = \ln\left[\frac{I(317.6)_0}{I(339.8)'_0}\right] - \ln\left[\frac{I(317.6)}{I(339.8)'}\right]$$

$$\Delta\beta_{AD} = [\beta(305.5) - \beta(325.4)] - [\beta(317.6) - \beta(339.8)] \quad (4.6)$$

$$\Delta\delta_{AD} = [\delta(305.5) - \delta(325.4)] - [\delta(317.6) - \delta(339.8)]$$

$$\Delta\alpha_{AD} = [\alpha(305.5) - \alpha(325.4)] - [\alpha(317.6) - \alpha(339.8)]$$

where  $N$  is the R dial reading,  $\mu$  the ozone air mass,  $\alpha$  is the ozone absorption coefficient,  $\beta$  is the Rayleigh scattering coefficient and  $\delta$  is the particle scattering coefficient.

The Brewer TOZ retrieval algorithm is based on the following equation

$$MS11 = \frac{MS9 - B_1}{A_1\mu} \quad (4.7)$$

where  $A_1$  is the absorption coefficient for the ozone measurements determined by a linear combination of ozone absorption coefficients of different wavelengths selected by the slit mask;  $B_1$  includes the extraterrestrial constants for the wavelengths used in ozone measurements. They are obtained by comparisons with standard instruments and updated by inter-comparison with the

traveling standard instruments. In equation 4.7, MS11 is the TOZ amount and MS9 is the result of a linear combination of logarithmic intensities measured at different wavelengths multiplied by weighting coefficients

$$MS9 = MS5 - 0.5MS6 - 1.7MS7 \quad (4.8)$$

where

$$MS5 = F_5 - F_3 \quad (4.9)$$

$$MS6 = F_5 - F_4 \quad (4.10)$$

$$MS7 = F_6 - F_5 \quad (4.11)$$

where  $F_i$  ( $i = 3, \dots, 6$ ) indicate the logarithms of the intensities counts respectively at wavelengths 310.0, 313.5, 316.8, 320.0 nm.

The coefficients in Eq. 4.8 are determined by the multiplication for  $i = 3, \dots, 6$  of  $F_i$  with  $w_i = (+1, -0.5, -2.2, +1.7)$ . Those coefficients are adopted as operational coefficients in all the Brewer network and they have been selected to remove the effect of the extinction due to aerosol ( $\tau^{aod}$ ), assuming to vary slowly and linearly with the wavelengths (Angström formula), and the absorption of  $SO_2$ .

$$\sum_i w_i = 0 \quad (4.12)$$

$$\Delta\tau^{aod} = \sum_i w_i \tau_i^{aod} = \sum_i w_i (a\lambda_i) \approx 0 \quad (4.13)$$

$$\Delta\alpha^{SO_2} = \sum_i w_i \alpha_i^{SO_2} = 0 \quad (4.14)$$

The nominal wavelengths can differ slightly from the operational one used in the retrieval algorithm (see SC-test in Section 4.4.3) and, therefore the network coefficients can vary considerably from the instruments related weighting coefficients ( $w_{i,r_i}$ ) as reported in the summary files of calibration tests (ls file), see Table 4.1 for the Brewer instruments operated in Arosa.

The accuracy of TOZ measurements depends on the knowledge of ozone absorption coefficients used for total ozone determination. The ozone absorption coefficients (see equation 4.4 and 4.7) are the effective volume of material ( $O_3$ ) that can attenuate the radiation by absorption and result from the product of the ozone cross section and the number density of ozone molecules. The ozone cross section in the Huggins band (300 to 390 nm) decreases strongly with the increasing wavelength and shows a pronounced temperature dependence. The Huggins band is currently used for spectroscopic remote-sensing of ozone by many experimental techniques (Dobson spectrophotometers, Brewer spec-

**Table 4.1:** Comparison between the Brewer algorithm's weighting coefficients adopted in all the network ( $w_i$ ) and the instrument related ( $w_{i,r_i}$ ) operated at Arosa.

		F <sub>3</sub>	F <sub>4</sub>	F <sub>5</sub>	F <sub>6</sub>
$w_i$		1.00	-0.50	-2.20	1.70
$w_{i,r_i}$	B040	1.00	0.19	-3.55	2.36
$w_{i,r_i}$	B072	1.00	0.08	-3.32	2.24
$w_{i,r_i}$	B156	1.00	-0.06	-3.06	2.12

trophotometers, also for satellite instruments, such as TOMS- or DOAS-based instruments, etc). The ozone spectral data used in this study are described in Chapter 4.4.2.

## 4.4 Data and method

### 4.4.1 Used measurements

At Arosa (46°78'N, 9°68'E), two Dobson instruments (fabrication number D101 installed in 1968, and D062 in 1992), two single Brewer MKII (fabrication number B040 in 1988 and B072 in 1994) and one double Brewer MKIII (fabrication number 156 installed in 1998) instruments are co-located and operated simultaneously. These datasets allow a direct comparison for quality control and for studying the differences between the two types of spectrophotometers. In this study, the period between 1995-2004 has been selected due to more stable comparisons with the standard instruments [for more details see (*Scarnato et al.*, 200xb)]. Moreover, the present analysis is constrained to quasi simultaneous direct sun measurements performed within 10 minutes, in order to minimize changes in atmospheric conditions in the comparison. As Arosa is above the inversion layer of the Swiss plateau, direct sun observations are possible during approximately 70% of the days of the year. This site is far away from pollution sources and therefore SO<sub>2</sub> and AOD can be neglected.

Vertical ozone profile measurements are performed three times per week at Payerne (46°50'N, 6°58'E, 491 m a.s.l.), in the center of the Swiss Plateau, using a small sonde carried aloft by a meteorological balloon that bursts at an altitude of typically 30 to 33 km. The Brewer-Mast (BM) ozone sensor has been continuously used from November 1966 to August 2002 and after they were replaced by Electro Chemical Cell (ECC) ozonesondes (*Stübi et al.*, 2008). Several corrections were made in order to improve the homogeneity and the quality of the time series (*Jeannet et al.*, 2004). The ozone profiles at Payerne are linearly scaled by a correction factor to match the total ozone which is measured in Arosa with a Dobson spectrophotometer. Dobson data

have been used to normalize the data due to its longer time series. The ozone profile has been used to retrieve the temperature effect in the TOZ retrieved by Dobson and Brewer spectrophotometers.

#### 4.4.2 Spectral ozone measurements

We have investigated the influence in TOZ retrieved with different laboratory cross-sections using *Bass and Paur* (1985); *Malicet et al.* (1995); *Burrows et al.* (1999). Due to the drastic change of the cross-sections across the Huggins band of more than two orders of magnitude, laboratory measurements using a single system (with the same combination of absorption path and ozone pressure) at high accuracy are rendered difficult. Rather, the spectral resolution of the ozone cross section depends on the experimental set-up employed (*Orphal*, 2003). Spectral absorption cross-sections of ozone published by *Bass and Paur* (1985) have a high spectral resolution. This data set is the current remote-sensing standard for ozone. The measurement of *Malicet et al.* (1995) have fairly similar characteristics. Measurements by *Burrows et al.* (1999) have a lower resolution, representative for most remote-sensing experiments in the UV-visible, as it is used for the GOME instrument on the ERS-2 satellite. In the following table 4.2, we specify the measurements used here (including the instruments with which they were performed).

When using other cross section as standard it is recommended that these cross-sections are scaled to the standard set in the relevant spectral region, i.e. using a non linear least square fit, *Orphal* (2003).

#### 4.4.3 Temperature influence on total ozone measurements

Dobson and Brewer retrieval algorithms have different sensitivities to temperatures due to the wavelength selection and slightly different approximations (see equation 4.4 and 4.7). The variability in atmospheric temperature is ignored in both Dobson and Brewer retrieval algorithms (see section 4.3.2), and

**Table 4.2:** Spectral absorption cross-sections of ozone published by Bass and Paur (1985), Malicet et al. (1995) and Burrows et al. (1999).

	<i>Bass and Paur (1985)</i>	<i>Malicet et al. (1995)</i>	<i>Burrows et al. (1999)</i>
<b>Instrument</b>	1.8 m Ebert scanning monochromator	1.5 m Czerny-Turner spectrometer	GOME-FM (monochromator with 4 diode-array detectors)
<b>Spectral Resolution [nm]</b>	< 0.025	not stated	0.2 - 0.4
<b>Wavelength Range [nm]</b>	245 - 343	245 - 343	231 - 794
<b>Wavelength Uncertainty [nm]</b>	< 0.025	not stated	0.03
<b>Data format step [nm]</b>	0.05	0.01	0.12 - 0.21
<b>Temperatures [°C]</b>	-70, -55, -45, -30, 0, 25	-55, -45, -30, 0	-71, -52, -32, 0, 20
<b>Temperature uncertainty [°C]</b>	0.25	0.05	2
<b>Light source reference spectra recorded</b>	Simultaneously	Before and after	Before and after
<b>Absolute scaling</b>	Hearn value at 253.65 nm and 1% increase between 25/-70 °C ( <i>Orphal, 2003</i> )	Measurements of total pressure	Chemical titration at 20°C assuming temperature independent
<b>Stated cross-section uncertainty [%]</b>	1.0	1.8	2.6 - 4.6

therefore the use of different retrieval wavelengths with their specific sensitivities can lead to differences in calculated TOZ (*Komhyr et al., 1993; Burrows et al., 1999*) (see e.g. Figure 4.1 for *Bass and Paur (1985)* spectra). Since 1992, the *Bass and Paur (1985)* spectra have been used as reference for the calculation of TOZ at all Global Atmospheric Watch (GAW) stations (*Vanicek, 2006*).

The effective ozone cross section has been defined as

$$\sigma_{O_3,eff}(\lambda) = \frac{\int_{800hPa}^{10hPa} \sigma_{O_3}(\lambda, T(p)) \cdot O_3(p) dp}{\int_{800hPa}^{10hPa} O_3(p) dp} \quad (4.15)$$

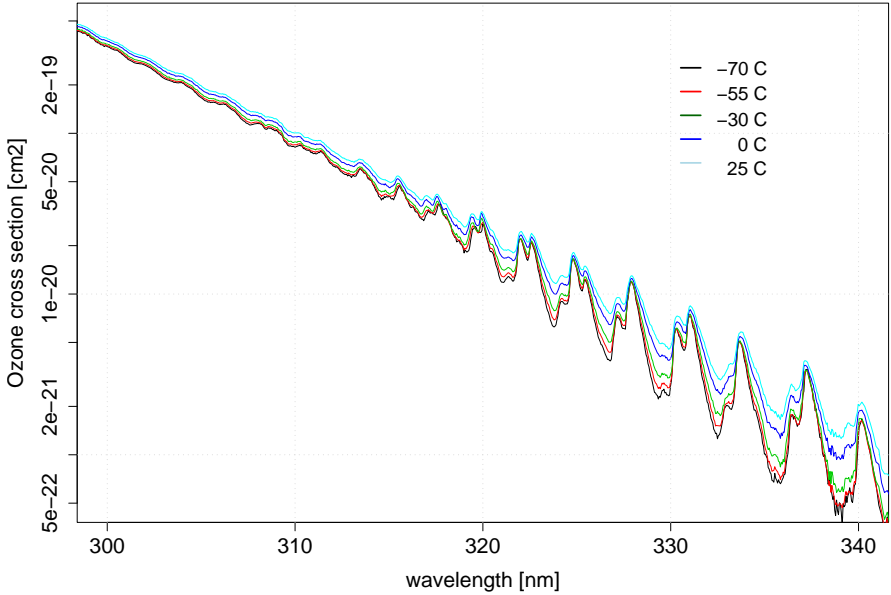


**Figure 4.1:** *Bass and Paur (1985) ozone cross section temperature dependence in the Huggins band.*

where the knowledge of the temperature and the ozone profile and the slit widths are required to convolve at each altitude ozone cross section and ozone. Different approaches have been also validated, in order to provide easier methods to correct the data and to know the introduced uncertainty in the correction. An alternative method is to consider the effective ozone temperature  $T_{eff}$  defined as

$$T_{eff} = \frac{\int_{800hPa}^{10hPa} T(p) \cdot O_3(p) dp}{\int_{800hPa}^{10hPa} O_3(p) dp} \quad (4.16)$$

where air temperature ( $T$ ) and ozone profile ( $O_3$ ) are multiplied at the dif-

ferent pressure levels from the tropospheric pressure at Arosa altitude to the burst level of the soundings. Eq. 4.16 allows to determine the uncertainty introduced if T and O<sub>3</sub> profiles are not available and correction for a temperature at a pressure level is necessary. The effective ozone temperature has been compared with the effective ozone stratospheric temperature ( $T_{eff}^{ST}$ ) defined as in Eq. 4.16, but where T and O<sub>3</sub> are multiplied at the different pressure levels from the stratospheric pressure level located at 200 hPa at Arosa.

Different models have been proposed in the past to reproduce the temperature dependence of the ozone cross section. Exponential models are very sensitive to baseline uncertainties, so experimental data are better reproduced by a quadratic polynomial function, agreeing within 1% to the measurements in a range of 245 and 330 nm (*Orphal, 2003*).

$$\sigma(\lambda, T) = c_0(\lambda) + c_1(\lambda)T + c_2(\lambda)T^2 \quad (4.17)$$

Equation 4.17 has been used to calculate the error in the TOZ retrieved using an ozone cross section  $\sigma(\lambda, T)$  at a fixed temperature. Equation 4.17 must be convolved with the slit function of the instrument. Brewer instruments have 6 very narrow slits (approximately of optical width around 1.2 nm), one for each wavelength used to retrieve TOZ and SO<sub>2</sub> and one for dark counting. Very narrow slits introduce diffraction broadening, Brewer optics are designed to reduce aberrations and the slit function is nearly triangular.

Dobson instruments have 2 slits, namely S2 and S3. Shorter wavelengths pass through the narrow slit (S2) characterized by a slit function of triangular shape and optical width around 1.8 nm, and the large slit (S3) is characterized by a slit function with a trapezoidal shape and optical width around 5.8 nm. The only available information of slit function shapes available from Dobson instruments originates from the World Primary Standard Dobson 83 (D083) (*Komhyr et al., 1993*).

The individual slit functions of the Brewer operational instruments have been characterized using the information stored in the dispersion test file in Brewer



pc. This test, performed during the calibration process which mostly every year took place, establishes the relationship between the step number of the micrometer that moves the grating and the wavelengths seen through each exit slit. The retrieval wavelength is selected in the sun scan test (SC-test), which provides the optimal position of the micrometer for most of the measurements, to minimize the sensitivity of  $O_3$  and  $SO_2$  calculations to small changes in the angle of the grating. The slit function which is measured with the Brewer by scanning through a laser line or discharge lamp with each of the slits, has to be mirrored to become a slit function. For single spectral lines, the shape of the scan represents the slit function of the instrument, which in general changes with wavelength.  $c_i(\lambda)$  with  $i=0,1,2$  (Eq. 4.17) have been adapted for the slit function weights  $S(\lambda', \lambda)$

$$c_i(\lambda) = \frac{\int S(\lambda', \lambda)c_i(\lambda')d\lambda'}{\int S(\lambda', \lambda)d\lambda'} \quad (i = 0, 1, 2) \quad (4.18)$$

$\lambda$  are the operational wavelengths and  $\lambda'$  are those wavelengths within the slit width. In this way the slit function of each slit is convolved with the ozone cross section spectra to determine the effective coefficients  $c_i(\lambda)$  ( $i=0,1,2$ ) and the  $\sigma(\lambda, T)$  is used as the effective (slit-averaged) ozone cross section.

#### 4.4.4 Stray light effect

The so called stray light effect includes any measured radiation which falsifies the ozone signal. It includes unwanted radiation scattered within the instrument due to deficiencies in the optics, a poor selection from the dispersive elements of the desired wavelengths and unwanted radiation scattered in the atmosphere by air molecules and aerosols entering in the field of view.

Radiation, at short wavelengths in Huggins band, is strongly attenuated by ozone and at large air mass values is further attenuated by Rayleigh scattering in the air path. These conditions give light scattered from optical components

more weight on a relative basis. Furthermore, the theory of Dobson instrument measurements was developed for monochromatic spectral bands and no account was made of the spectral variation of parameters, particularly of ozone absorption, across the instrument's finite bandwidths. The deficiency of this assumption of monochromaticity is its failure to account for the small monotonic decrease in the effective absorption coefficient of a finite band with increasing air mass and absorber amount (bandwidth effect) (*Vanier and Wardle*, 1969; *Komhyr et al.*, 1993). The bandwidth effect arises from the relative attenuation with the increasing air mass and absorber amount of those wavelength intervals within the band which are more strongly absorbed, and hence a relative increase in the energy weighting of the wavelength intervals within the band which are less absorbed, i.e. which have smaller absorption coefficients.

For direct sunlight AD measurements, errors of +1%, +3%, and +10% may be present at air masses 2.5, 3.2 and 3.8 respectively (*Basher*, 1982; *Varotsos et al.*, 1998). The error due to the scattering effect is important when aerosol is present (*Thomas and Holland*, 1977); this effect is neglected as first approximation at Arosa which is an alpine unpolluted site.

Concerning the Brewer spectrophotometers, Brewer MKIII (B156) instruments are more efficient in suppressing the effect of the stray light due to the double dispersive element than MKII instruments (B040 and B072).

Brewer and Dobson spectrophotometers have different field of view, respectively 3 and 8 degree (*WMO*, 2003). As consequence Dobson instruments see more light scattered into the field of view than Brewer. This can affect the retrieval of ozone values for Dobson measurements at high TOZ values and low angles.

A simple parameter suitable to describe the stray light effects is the air mass times total ozone, called ozone slant path (OSP).

## 4.5 Results and Discussion

### 4.5.1 Total ozone multi annual time series

The time series of Dobson and Brewer measurements at Arosa show very similar seasonal variability of TOZ [e.g. panels (a) and (b) in Figure 4.2 for B040 and D101 for AD observations]. However, despite being quasi-simultaneous measurements within 10 minutes they differ on average by 2% with a seasonal cycle of  $\pm 1$  % peak to peak and maximum difference in winter (panel (c) in Figure 4.2). Comparison with others instruments operated at Arosa show similar differences. A similar bias has also been documented for several mid-latitude stations, (*Kerr et al.*, 1988; *Staehelin et al.*, 1998b; *Köhler*, 1999; *WMO*, 2003; *Vanicek*, 2006).

Possible sources for the observed differences are the instrumental design, the calibrations of individual instruments with different standard traveling instruments and the retrieval algorithms that use a set of different wavelengths with different ozone cross section temperature- and OSP-dependencies.

### 4.5.2 Effective ozone temperature variation and its influence on total ozone measurements

The temperature cycle, shown in Figure 4.3 and Table 4.3, is ignored in both Dobson and Brewer retrieval algorithms, where the absorption cross sections values are at  $-46.3$  °C in Dobson and  $-44$  °C in Brewer spectrometry.

The error in TOZ retrieved can be estimated using Eq. 4.15. The temperature sensitivities of Dobson and Brewer effective absorption coefficients (see equation 4.4 and 4.7) has been calculated by Eqs. 4.17 and 4.18 based on temperature dependence of the *Bass and Paur* (1985) spectra (see Figure 4.4). The differences between the effective ozone cross section calculated convolving T and O<sub>3</sub> at each level as Eq. 4.15 or using ozone weighted temperature columns as in Eq. 4.16 and following Eq. 4.17 and 4.18 are negligible. The second order polynomial fit in Eq. 4.17 leads to significant difference in ozone

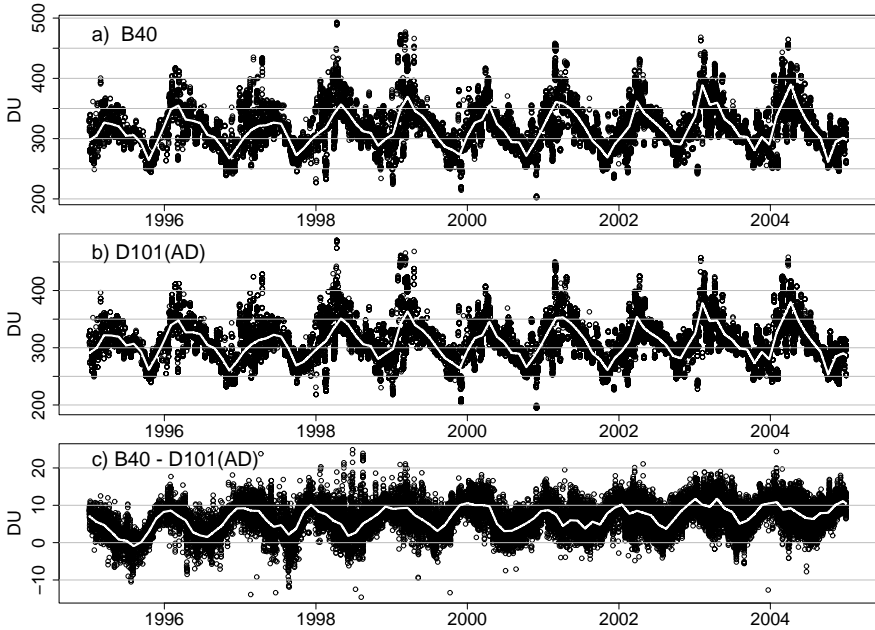


**Figure 4.2:** a) Brewer 040 ( $B040$ ) and b) Dobson 101 using AD wavelengths ( $D101(AD)$ ) total ozone time series at Arosa. c) Their differences for quasi-simultaneous observations within 10 minutes.

cross section temperature dependence, when using  $c_i$  derived from a fit of 6, 5, or 4 temperatures of *Bass and Paur* (1985) measurements. The ozone cross section gradient per Celsius calculated in this study, using different set of weighting coefficients are compared in Table 4.4 with the published values by *Kerr et al.* (1988) and *Kerr* (2002). The  $\sigma(\lambda, T)$  temperature gradient results very sensitive to the weighting coefficients applied. The retrieval wavelengths can slightly differ from nominal wavelength,  $w_{i,r_i}$  can better reduce  $SO_2$  and aerosols influence (wavelength dependent) see Eqs. 4.13 and 4.14. The use of not proper instrument related weighting coefficients ( $w_i$  instead of  $w_{i,r_i}$ ) can lead in average to less than 1% of error in TOZ retrieved by Brewer.

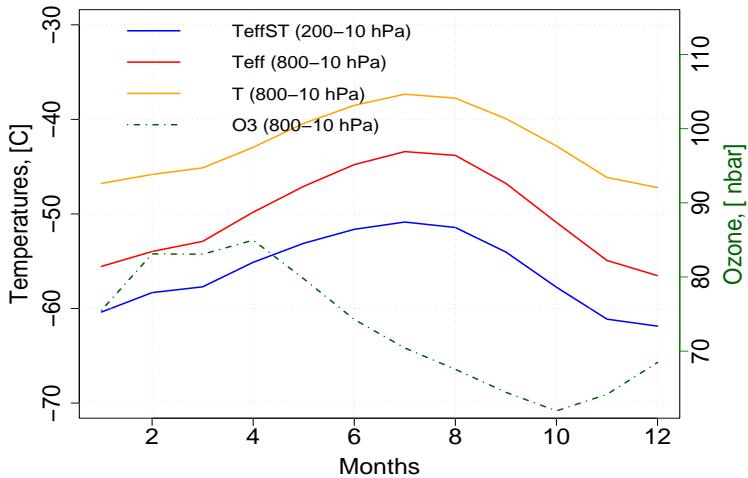


**Figure 4.3:** Seasonal variation (mean values over 1995-2004) of the key parameters used in this study: Averaged ozone concentration from ozone sondes ( $O_3$ ), averaged air temperature ( $T$ ) and effective ozone temperature ( $T_{eff}$ ) and  $T_{eff}^{ST}$ .

Brewer retrieval algorithm in general exhibits less temperature sensitivity than Dobson (see Figure 4.4 panel (a) for  $c_i$  calculated using all the 6 temperatures measurements and  $w_i$  in the Brewer algorithms). The differences in the ozone cross section sensitivities within three Brewer instruments operated at Arosa are due to small differences in the optics, cut off levels and in the operational retrieval wavelengths, which are used to minimize the sensitivity of TOZ and  $SO_2$  calculations to small changes in the angle of the grating (SC-test). The retrieval algorithm sensitivity on the  $\Delta\alpha/\Delta T$ , shown in Table 4.4, to wavelengths and slit function widths variation (of 0.01 nm and 0.1 nm respectively) can give uncertainty of approximately  $\pm 0.0226 \%$ /C.

**Table 4.3:** Ozone effective temperature ( $T_{eff}$  and  $T_{eff}^{ST}$ ) and air temperature ( $T$ ) mean and quantiles above Payerne.

	mean [°C]	first quantile [°C]	third quantile [°C]
$T_{eff}$	-49.46	-53.47	-45.08
$T_{eff}^{ST}$	-56.04	-59.22	-53.47
$T$	-42.56	-45.90	-39.57

**Table 4.4:** Ozone temperature dependence for operational wavelengths of Brewer 040 and 072 (MKII) and B156 (MKIII) compared with the values published by Kerr et al. (1988); Kerr (2002) for the ozone cross section published by Bass and Paur (1985). Different temperature sets ( $T$ ) of measurements has been used to calculate the ozone cross section temperature dependence, which results strongly dependent on weighting coefficient adopted in the retrieval and on the temperature range used for the determination of  $c_i$ .

		$\Delta\alpha/\Delta T, [\%/^{\circ}C]$			
		This study	Kerr et al. (1988)	Kerr (2002)	This study
		All T	All T	5 lowest T	4 lowest T
		$w_i, w_{i,r_i}, w_{i,D}$			$w_i, w_{i,r_i}$
MKII	(B040)	0.0810, 0.0013, 0.2560	(B014) 0.07	(B014) 0.094	0.2264, 0.1372
	(B072)	0.0998, 0.0322, 0.2385	-	-	0.2491, 0.1822
MKIII	(B156)	0.0880, 0.0339, 0.2456	-	-	0.1141, 0.1112

SO<sub>2</sub> and AOD influence can be neglected in Arosa in the studied period (1995 - 2004). Therefore, the Brewer retrieval algorithm could be reduced to a simple double-ratio method using the weighting coefficients as in the Dobson retrieval, i.e.  $w_{i,D}=(1, -1, 1, -1)$ . Brewer retrieval algorithm using  $w_{i,D}$  results 0.1167 %/°C more temperature sensitive than Dobson [ $\Delta\alpha_{D083}/\Delta T$  is 0.13 %/°C (Komhyr et al., 1993)]. Using  $w_{i,D}$  in the retrieval algorithm, its sensitivity to small variation of retrieval wavelengths and slit widths decrease the uncertainty of the Brewer  $\Delta\alpha_B/\Delta T$  to  $\pm 0.012$  %/°C.

The ozone cross section temperature effect in the difference of the observations, considering the first and third quantile of  $T_{eff}$  at Payerne, is shown in panel (b) of Figure 4.4, and in Table 4.5 it is also shown its dependency on the weighting coefficients applied in the retrieval algorithms.

Dobson and even more Brewer spectrophotometer have very narrow slit widths, but the  $O_3$  spectra have a complicated structure in function of  $\lambda$  on temperature. *Bass and Paur* (1985) experimental data of the ozone cross section covers only half of the range of Dobson slit at 320 nm. Bass and Paur extrapolated their data until 340 nm to cover the Dobson wavelengths. *Malicet et al.* (1995) measured the ozone spectra and its temperature dependence with an improved wavelength resolution and including the full range of Dobson slit widths. *Burrows et al.* (1999) spectra has a low resolution but wide range and it is used in the satellite retrieval. Therefore, the influence of the resolutions and uncertainties of different spectra in retrieving TOZ has been studied and summarized.

The Brewer absolute retrieval ozone cross sections result very sensitive to the instrument optics, to the weighting coefficients applied ( $w_i$ ,  $w_{i,r_i}$ ,  $w_{i,D}$ ) and reference spectra adopted (see Table 4.6). Brewer absolute ozone cross section can differ up to 15% applying different spectra, Dobson absolute ozone cross section just up to 2%. The ozone cross section temperature gradient changes in magnitude and sign (Table 4.7) in function of reference spectra applied. TOZ measurements by Brewer instruments show a more pronounced temperature sensitivity using *Malicet et al.* (1995) or *Burrows et al.* (1999) spectra instead of *Bass and Paur* (1985), the contribute in the seasonal bias results to be minimum (see panels (b) in Figure 4.5 and 4.6).

**Table 4.5:** Cross section effect in the seasonal bias of the difference of Brewer and Dobson TOZ measurements.

	$w_i$	$w_{i,r_i}$	$w_{i,D}$
1 <sup>st</sup> and 3 <sup>rd</sup> quantile [°]	0 - 0.6	0.2 - 1.3	0 - -1

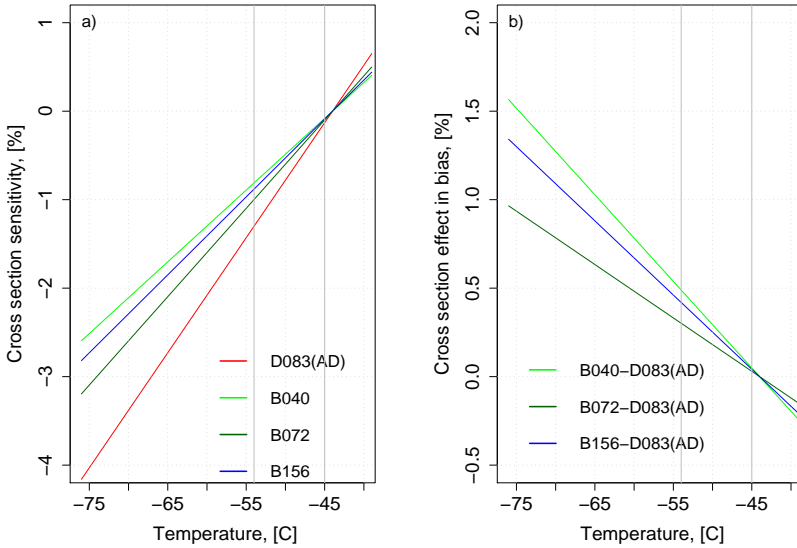


**Figure 4.4:** a) Effective ozone cross section temperature sensitivity per Celsius for Brewer 156, 072 and 040 (B156, B072, B040) and Dobson standard instrument 083 (D083). b) Cross section temperature effect in the difference of the observations by Brewer 156, 040 e 072 and Dobson 083(AD) spectrophotometers using Bass and Paur (1985) as spectra reference. The effective ozone cross section results from application of Eqs. 4.17 and 4.18 in the Brewer retrieval algorithm using  $w_i$ .

**Table 4.6:** Absolute ozone cross sections at the retrieval temperatures for Brewer 040 and 072 (MKII) and B156 (MKIII) and Dobson spectrophotometers using different spectra. Differences between  $\sigma_{B040}(MS9, -44)$  using  $w_{i,r_i}$ ,  $w_i$  or  $w_{i,D}$  are shown for Bass and Paur (1985), Malicet et al. (1995) and Burrows et al. (1999) reference spectra.

	$\sigma_{B040}(MS9, -44)$	$\sigma_{B072}(MS9, -44)$	$\sigma_{B156}(MS9, -44)$	D083(AD)
	$w_i, w_{i,r_i}, w_{i,D}$			
Bass and Paur (1985)	0.3365, 0.3422, 0.4146	0.3471, 0.4876, 0.4099	0.4737, 0.4479, 0.4068	1.4219
Malicet et al. (1995)	0.3584, 0.3739, 0.3940	0.3729, 0.5269, 0.3940	0.5119, 0.4759, 0.4090	1.4519
Burrows et al. (1999)	0.3097, 0.4517, 0.4212	0.3615, 0.4972, 0.4090	0.3440, 0.4422, 0.4072	1.4560



**Table 4.7:** *Effective temperature sensitivity for B040 and B072 (MKII), B156 (MKIII) and D083 using different spectra as reference (Malicet et al. (1995) and Burrows et al. (1999)). The temperature dependence for Burrows et al. (1999) spectra has been calculated using 4 temperatures to fit the second order polynomial function in Eq. 4.17.*

	$\Delta\alpha/\Delta T$ , [%/°C]	
	<i>Malicet et al. (1995)</i>	<i>Burrows et al. (1999)</i>
	$w_i, w_{i,r_i}, w_{i,D}$	$w_i, w_{i,r_i}, w_{i,D}$
MKII (B040)	-0.1314, -0.1624, 0.2129	0.0931, 0.0202, 0.3043
MKII (B072)	-0.1204, -0.1462, 0.2156	0.0850, 0.237, 0.3265
MKIII (B156)	-0.1280, -0.1525, 0.2245	0.0574, 0.0102, 0.3419
D083	-0.1101	-0.0186

The higher variability of the Brewer instruments for different cross section is due to its much higher resolution, in combination with measurement noise in the experimentally determined ozone cross sections. While for the Dobson instruments an average over many nanometers for each slit is relevant, in the case of the Brewer the resolution of the ozone cross section data is more coarse, and therefore more sensitive to measurement uncertainties in these cross section data. The retrieval algorithm sensitivity has been validated also for *Malicet et al. (1995)* and *Burrows et al. (1999)* concerning wavelength or slit function variation. The retrieval algorithm sensitivity to wavelength or slit function width variation can lead to uncertainties in the temperature gradient of approximately  $\pm 0.033$  % for *Malicet et al. (1995)* and of  $\pm 0.005$  % *Burrows et al. (1999)*.

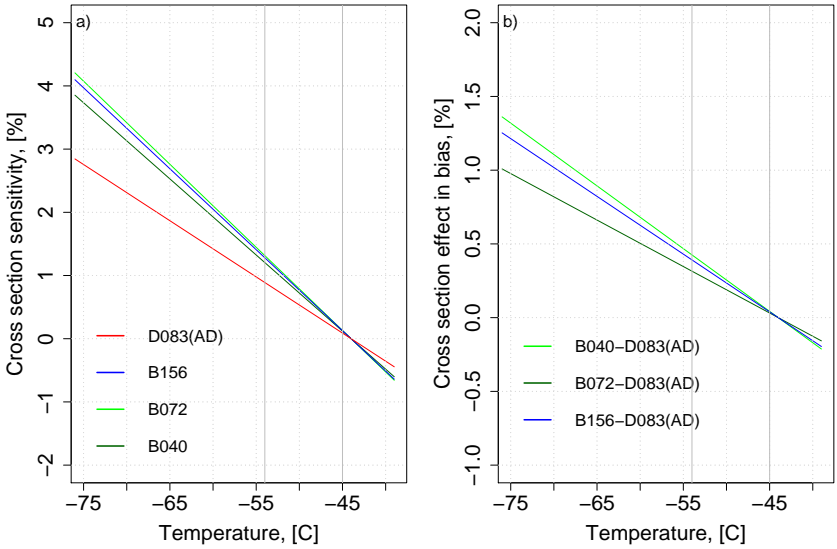


**Figure 4.5:** a) Effective ozone cross section temperature sensitivity per Celsius for Brewer 156, 072 and 040 (B156, B072, B040) and Dobson standard instrument 083 (D083) using *Malicet et al. (1995)* as spectra reference. b) Cross section temperature effect in the difference of the observations by Brewer 156, 040 and 072 and Dobson 083(AD) spectrophotometers.

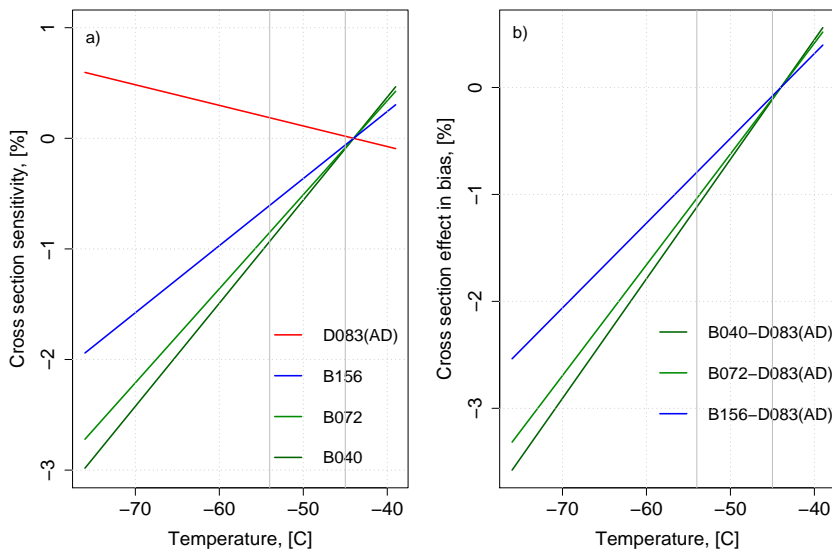


**Figure 4.6:** a) Effective ozone cross section temperature sensitivity per Celsius for Brewer 156, 072 and 040 (B156, B072, B040) and Dobson standard instrument 83 (D83) using *Burrows et al. (1999)* as spectra reference. b) Cross section temperature effect in the difference of the observations by Brewer 156, 040 and 072 and Dobson 083(AD) spectrophotometers.

### 4.5.3 Ozone slant path effect and its influence on observations

In this section we extract information on stray light effects by simple parameterization with ozone slant path (OSP) defined as air mass times ozone ( $\mu$ \*TOZ). The readings of quasi simultaneous measurements within the same types of instruments have been compared in function of the OSP in order to study the stray light effect due to optical components. 20469 direct sun observations have been compared for Dobson D101 and D062 with AD wavelengths.

The differences of quasi simultaneous TOZ measurements of the same type of spectrophotometers in function of the OSP do not show systematic differences, providing evidences, that no internal stray light problems of the instruments operated at Arosa exist or that such problems affect the Dobson and Brewer instruments in a very similar way. Brewer and Dobson TOZ observations have been corrected for the ozone cross section temperature dependence. The differences between Dobson and Brewer MKII (B040) instruments increase up to almost 4% with the increase of the OSP (see Figure 4.7). Even slightly higher values have been found in the differences between the observations of D101(AD) and B156 MKIII. Instrumental discrepancies at low OSP values (not explainable in terms of stray light effect) are around 2%. At higher OSP values than 800 DU the differences of the measurements show a OSP dependence between 1-2%.

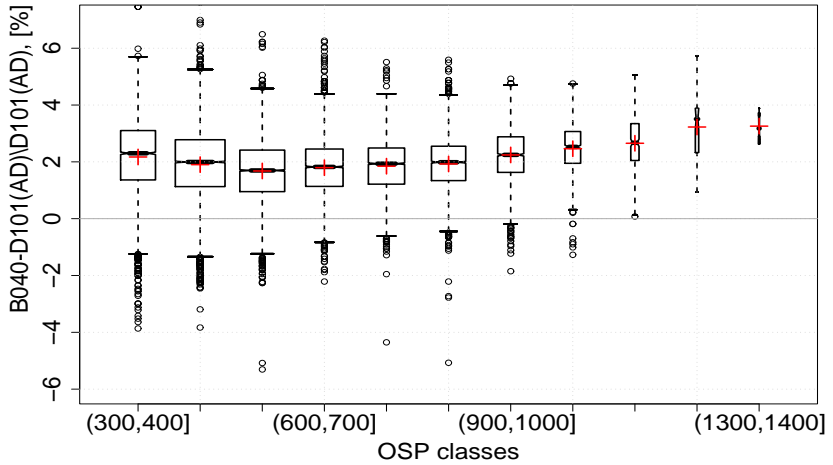


**Figure 4.7:** *Difference of direct sun TOZ observations (1995-2005) by Brewer 040 and Dobson 101(AD) vs Ozone Slant Path. Coincident data within 10 minutes are used. The observations have been corrected for the temperature effect using method provided in section 4.5.2. The box plots are drawn with widths proportional to the square-roots of the number of observations in the groups. The red cross indicates the mean value; minimum and maximum value, lower and upper hinge and median are also indicated with the shape of boxes. Number of observations per classes: 4606, 9361, 7610, 5289, 4975, 4441, 2579, 931, 258, 43, 4 for OSP classes (300,400) to (1300,1400) respectively.*

#### 4.5.4 Effect of temperature variability and stray light on seasonal cycle

Monthly means difference of the TOZ observations at Arosa by the Brewer triad and Dobson instruments show difference of 2.25% with a seasonal bias of  $\pm 1.15\%$  peak to peak. The contributions of the temperature sensitivity of the *Bass and Paur* (1985) ozone cross section and OSP have been stepwise eliminated from the observational data, using the methods described earlier. A polynomial second order function fits the difference of the observations already corrected for temperature effect. The residual between the instrumental offset and OSP dependency (evident for higher OSP classes than 800 DU) has been eliminated.

The temperature effect results to be comparable with the contribution of the stray light effect in the seasonal differences. Monthly means can be reduced to 2.05 % with a seasonal bias of  $\pm 0.6\%$  peak to peak using *Bass and Paur* (1985)'s ozone cross sections and the estimated OSP effect (significant after 800 DU). Instrumental seasonal discrepancies remain unexplained in the order of 1%, (see Figure 4.8). The use of  $w_{i,r_i}$  or  $w_{i,D}$  better minimize the seasonal bias in the monthly mean difference. If  $w_{i,r_i}$  or  $w_{i,D}$  are applied in the retrieval algorithm, ETC values should be calculate resulting from the new weighting of the extraterrestrial constants. By the way  $w_{i,r_i}$  differ from the  $w_i$  considerably, and using  $w_{i,r_i}$  the information on TOZ amount from wavelength 313 nm would be neglected. The use of  $T_{eff}^{ST}$  instead of  $T_{eff}$  leads to an overcorrection for temperature effect in TOZ. The TOZ datasets have also been reprocessed by using other spectra references (see Figure 4.9 and 4.10). Retrieving using *Malicet et al.* (1995), monthly means differences of the TOZ observations by the Brewer and Dobson instruments are -1.8% with a seasonal bias of  $\pm 1.05\%$  peak to peak. Correction for temperature and OSP effect lead to mean values around  $-1.9 \pm 0.6\%$ . Retrieving using *Burrows et al.* (1999), monthly means difference are  $-3.63 \pm 1.09\%$  peak to peak. The temperature gradient applied results too strong to reduce the bias probably because of the ozone cross section temperature dependence fit in Eq. 4.17, where only 3 of lowest temperatures have been used due to not easy to correct wavelengths shifts in the spectra at 0 and 20 Celsius.

Indeed, *Bass and Paur* (1985) and *Malicet et al.* (1995) spectra result to better minimize the differences between TOZ measurements, despite the use of  $w_i$  in Brewer retrieval algorithms explain just in part the seasonal bias.

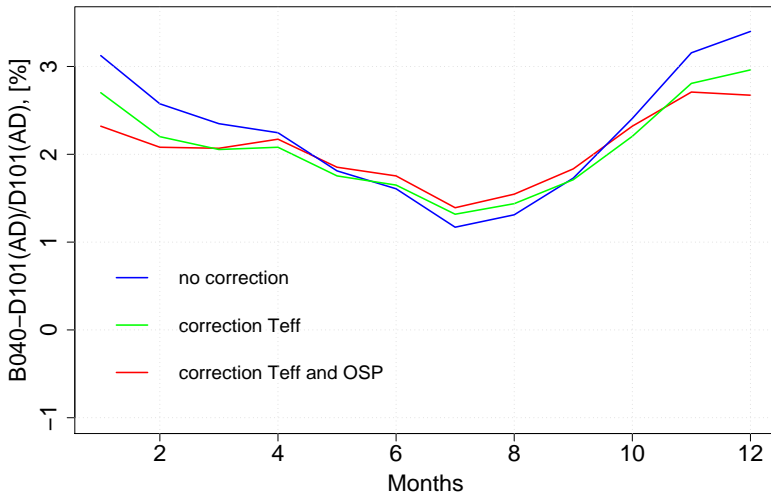


**Figure 4.8:** Monthly mean values of the difference of the  $B040$  and  $D101(AD)$  observations (in blue) retrieving with **Bass and Paur (1985)** spectra reference, eliminating first the temperature contribution (in green) and secondly also the ozone slant path effects (in red). Data: 1995-2003, coincident data within 10 min.

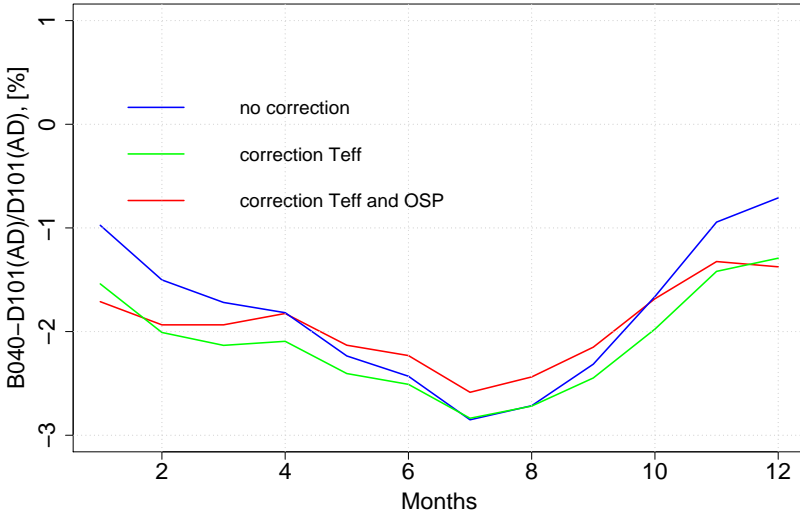


**Figure 4.9:** Monthly mean of the difference of the B040 and D101(AD) observations (in blue) retrieving with *Malicet et al. (1995)* spectra reference, eliminating first the temperature contribution (in green) and secondly the ozone slant path effects (in red). Data: 1995-2003, coincident data within 10 min.



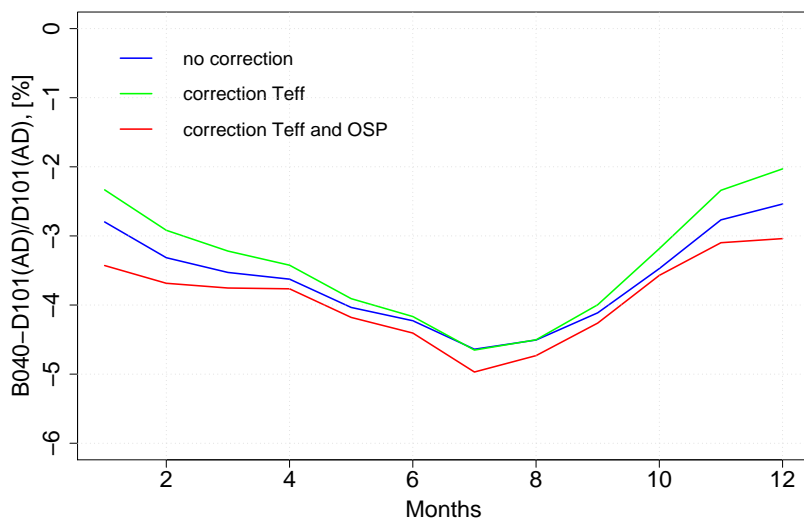


**Figure 4.10:** Monthly mean of the difference of the B040 and D101(AD) observations (in blue) retrieving with *Burrows et al. (1999)* spectra reference, eliminating stepwise the temperature contribution (in green) and also the ozone slant path effects (in red). Data: 1995-2003, coincident data within 10 min.

## 4.6 Conclusions

A systematic seasonal cycle in the difference of TOZ measurements of Brewer and Dobson instruments has been documented at many sites at mid-latitudes. The differences can be attributed to differences in the optics, in the retrieval wavelengths and in the sensitivities of the retrieval algorithms. The stratospheric ozone mean temperature has a substantial variability over the year but the presently used Dobson and Brewer retrieval algorithms ignore this influence. The temperature sensitivity for each instrument can be calculated, knowing accurately the operational retrieval wavelengths and the slit width functions. The Brewer absolute ozone cross section and temperature dependencies can strongly vary from one instrument to another. The retrieval algorithm sensitivity to wavelengths and slit function widths variation (of 0.01 nm and 0.1 nm respectively) can lead to uncertainties in the temperature gradient of approximately  $\pm 0.0226$  %/C. Brewer retrieval algorithm results, furthermore, very sensitive to the weighting coefficients applied. An optimization of the weighting coefficients for back ground pollution conditions and for the instrumental operational wavelengths is also recommended to better minimize the seasonal bias in TOZ observations. In this case Brewer TOZ observations should be reprocessed using proper ETC values. The application of this coefficients would not enhance uncertainties on small slit widths and wavelength variation. The ozone cross sections uncertainties between Dobson spectrophotometers are difficult to verify, because it is missing a slit function characterization for the operational instruments and, it is unknown the relation between the Dobson 083 slit functions provided in (*Komhyr et al.*, 1993) and the Dobson 101 and 062 instruments at Arosa. However, a sensitivity test to small slit widths and retrieval wavelengths variation confirms a higher stability than Brewer spectrophotometers. In order to better estimate differences applying different spectra from the actual reference, new weighting coefficients must be calculate to maximize the intensity of any ozone cross section spectra reference. We show that the derived retrieval sensitivity on stratospheric temperature strongly depends on the ozone cross section spectra used and on the weighting coefficients applied. Brewer absolute ozone cross section can differ up to 15% applying different spectra, Dobson absolute ozone cross section

only up to 2%. Moreover, the TOZ observations at large OSP values can be influenced by stray light problems, caused by different field of views, optics and suboptimal wavelength selection. We have tried to attribute the observed seasonal differences of the TOZ measurements at Arosa to temperature dependence of the ozone cross sections of the used wavelengths and to OSP. This requires a parameterization of the stray light effect, and it has been used a OSP polynomial second order fit. When we account for the effects of the ozone effective temperature based on the spectra by *Bass and Paur* (1985) and of the OSP, the seasonal amplitude in the difference of the measurements reduces from 2% to 1%. Conversely, the use of the spectral data of *Burrows et al.* (1999) instead of *Bass and Paur* (1985) or *Malicet et al.* (1995) increases the differences between Dobson and Brewer TOZ observations at Arosa. This finding illustrates, that the accuracy of ground based spectrophotometric TOZ measurements is presently most strongly limited by the temperature dependence of the ozone cross section measured by difficult laboratory experiments. These data are also critical for comparison of ground based and satellite TOZ measurements. The more complex Brewer retrieval algorithm shows stronger sensitivity with respect to uncertainties within the published cross sections in the Huggins bands. This probably reflects the optimization of the weighting of the wavelengths in the Brewer retrieval algorithm, which were selected to minimize the effect of sulfur dioxide and AOD interferences.

## 4.7 Acknowledgments

We wish to thank for very valuable discussions Tom Peter, Susan Solomon, Irina Petropavlovskikh, Bob Evans, Peter Kriedron, Elizabeth Weatherhead and Joerg Maeder for R-program language hints. The work of B.S. was supported by a research grant of MeteoSwiss as part of the Meteo Swiss Global Atmospheric Watch (GAW) program.



## Chapter 5

# Long Term Total Ozone Observations at Arosa (Switzerland) with Dobson and Brewer Instruments (1988-2007)

Scarnato B.<sup>1</sup>, Staehelin J.<sup>1</sup>, Stuebi R.<sup>2</sup>, Schill H.<sup>2</sup>

<sup>1</sup>ETH, Zurich; Switzerland, <sup>2</sup>MeteoSwiss, Aerological Station; Payerne  
Switzerland

Planned to be submitted to Journal of Geophysical Research

### 5.1 Abstract

Dobson and Brewer spectrophotometers are the standard instruments for ground based total ozone monitoring in the World Meteorological Organization's Global Atmospheric Watch (GAW) program (WMO, 2003). Both types of instruments have been simultaneously operated at Arosa (Switzerland) since 1988, presently two Dobson and three Brewer instruments (one of which is type Mark III) are used. The large data set of quasi simultaneous measurements (here defined as observations performed within maximally 10 minutes) allows for the determination of both inter and intra instrumental

precision. The results for one standard deviation are  $\pm 0.5$  % for Dobson AD observations and  $\pm 0.15$  % for Brewer total ozone measurements. In order to transform Brewer into Dobson total ozone observations, empirical transfer functions are used to describe the well known difference in seasonal variations of the two types of instruments (on the order of 2% with a seasonal cycle of  $\pm 1$  % peak to peak with a maximum in winter). The statistical model includes as explanatory variables, for quasi-simultaneous ozone measurements, ozone effective temperature and air mass multiplied with total ozone. However, even when applying these transfer functions a drift between Arosa's Dobson and Brewer observations of approximately of 3% (reported earlier) in the earlier 1990s remains unexplained.

## 5.2 Introduction

The stratospheric ozone shield has been affected by anthropogenic emissions of ozone depleting substances (ODS), the most pronounced effect of anthropogenic ozone depletion occurred over Antarctic and was termed Antarctic ozone hole (e.g., *Solomon*, 1999). Anthropogenic ozone depletion over mid-latitudes is much smaller [decrease on the order of a few percent per decade were observed during the 1980s (e.g., *Staehelin et al.*, 2001; *WMO*, 2003). In order to be able to document small long term changes, a world wide network of ground based spectrophotometers is operated since the middle of the 1979s under the auspices of the World Meteorological Organization (WMO). The data quality of total ozone measurements of Dobson spectrophotometers (*Komhyr*, 1980a) is ensured by a network based on a Primary Dobson instrument, which is regularly calibrated by the Langley plot method at Mauna Loa observatory and maintained by ESRL-NOAA (*Komhyr et al.*, 1989). The calibration scale is subsequently transferred to a traveling standard instrument, used to compare with regional standard Dobson instruments. The station instruments are calibrated by side-by-side comparisons against the regional standard instruments during Dobson inter-comparisons, which are planned to take place every four years. A similar network has been organized for Brewer instruments. The network is based on a Triad of Brewer instruments operated

at Toronto and a WMO traveling instrument is used to transfer and to update the instrument constants of operational Brewer instruments (*Fioletov et al.*, 2005). The Brewer instruments have been commercially available since the mid 1980s using more advanced technology than their Dobson counterparts (*Kerr et al.*, 1981; *Kerr*, 1985).

Total ozone (TOZ) measurements of Dobson and Brewer instruments are known to exhibit systematic differences in their seasonal variation, (e.g., *Köhler*, 1999; *Kerr et al.*, 1988; *Stahelin et al.*, 1998a). Because of these differences, it has been recommended by WMO not to replace Dobson by Brewer instruments but rather to operate them simultaneously in order to obtain better understanding of the instrumental stability of collocated instruments (*WMO*, 2003). However, in order to make best use of the redundancy of collocated Dobson and Brewer spectrophotometers, transfer functions need to be established. This is a primary goal of this study.

Since 1979 the global ozone shield has been almost continuously monitored from space. The calibration of satellite ozone instruments is difficult to control and satellites lifetimes are limited and therefore, a well maintained network of ground based stations is required for both satellite validation and the reconstruction of a combined satellite ozone time series suitable for ozone trend analysis.

At Arosa TOZ measurements began at 1926. Several Dobson instruments have been employed over the years and the data has been homogenized (*Stahelin et al.*, 1998a) to create the longest TOZ time series in the world.

In 1988 the first Brewer instrument was installed at Arosa. Presently 3 Brewer spectrophotometers are simultaneously operated together with two Dobson instruments. It has been previously shown that the seasonal bias between the two instruments is, at least in part, due to the seasonal variation of ozone slant path and ozone effective temperature which affects the ozone cross section used in Dobson and Brewer instruments (*Scarnato et al.*, 200xa). The goal of the present paper is to convert Brewer measurements to the Dobson scale, via the construction of an empirical transfer function. The instrumental precision of the standard total ozone instruments is presented in Section 5.4.1 and the

empirical transfer function in Section 5.4.2. In addition a drift of Dobson and Brewer TOZ measurements which occurred in the first part of the 1990s and reported earlier by *Staehein et al.* (1998a) is discussed in Chapter 5.4.3. Finally, the result and conclusion are presented in the subsequent section.

## 5.3 Measurements and Methods

### 5.3.1 Total ozone measurements at Arosa since 1988-2007 and inter-comparison results

The instruments used for TOZ at Arosa observations are listed in Table 5.1.

Direct sun Dobson measurements at Arosa are regularly performed during the working days (Monday to Friday) approximately every 1-2 hours permitting meteorological conditions using a semi-automated procedure (*Hoegger et al.*, 1992). This results in more than ten single measurements during fair summer days. More numerous observations are available from the automated Brewer

**Table 5.1:** *Instruments used in the relative period. The number indicate the fabrication number.*

Dobson instruments	used in the period
D015	1950 - 1992
D101	1967 - up to now
D062	1992 - up to now
Brewer instruments	
B040	1988 - up to now
B072	1992 - up to now
B156	1998 - up to now



instruments. Lamp test are regularly performed at Arosa to ensure the data quality of the Dobson spectrophotometers (*Komhyr*, 1980b). Standard lamp test readings are also used to correct possible instrumental drifts.

**Dobson inter-comparison results:** Dobson inter-comparisons with the standard traveling instrument have taken place since 1986 more or less every four years (see table 5.2 and 5.3) following the standard practice for Dobson spectrophotometers. In 1986, instrument D101 was recalibrated against D083, and the instrumental constants were confirmed by the Dobson inter-comparison held in 1990 at Arosa. D062 was installed in 1992 at Arosa and the instrumental constants were determined by comparison with D101. Tables 5.2 and 5.3 contain the differences in percent of the stations Dobson instrument against the standard instrument used in the inter-comparisons before any instrument change.

In 2003 and 2006 Arosa Dobson instruments were compared with the regional standard instruments Dobson 064 and 074 (D064 and D074). Prior to this they were compared with D065. TOZ AD observations were high compared to the reference Dobson instrument, except in 2003. In the data presented here no direct use was made of the inter-comparison (IC) 1995 corrections.

The data has been scaled using the inter-comparison results of 1990 and 1999, and the temporal evolution was scaled according to the knowledge of the lamp test history. (Note that in *Staehelin et al.* (1998b) the Dobson data were scaled

**Table 5.2:** *Percentage of difference of Dobson 101 AD wavelengths observations (D101) from the reference standard at the initial inter-comparison in 1995, 1999, 2003, 2006. Those percentage are averages for AD observations and air mass values between 1.15 and 3.2. The results of 1996 refer to the intercomparison of 1990.*

Inter-comparison	1995	1999	2003	2006
Reference-Instr	D065	D065	D064	D074
D101 (AD) [%]	1.95	0.90	0.55	-0.15

**Table 5.3:** Percentage of difference Dobson 062 AD wavelengths observations ( $D062(AD)$ ) from the reference standard at the initial inter-comparison in 1995, 1999, 2003, 2006. Those percentage are averages for AD observations and air mass values between 1.15 and 3.2.

Inter-comparison	1995	1999	2003	2006
Reference-Instr	D065	D065	D064	D074
D062 (AD) [%]	1.52	0.52	-0.28	0.49

using the results of IC 1990 and 1995, but only half of the correction has been applied. However, the difference in TOZ data is small when comparing the corrected data used in *Stachelin et al.* (1998b) and the correction used in this paper).

**Brewer inter-comparison results:** In the recent years Brewer inter-comparisons with the traveling reference instrument have taken place nearly every summer, whereas they were performed sometimes in larger intervals prior to 1998 (1989-1991-1992-1993-1996-1998). Most Brewers in the GAW network have been calibrated with Brewer 017 [the traveling standard instrument used by the International Ozone Service Inc. (IOS)]. Regular maintenance, constant monitoring of the 017 instrument's parameters and periodic comparisons with the Brewer Triad provides high quality calibrations. Its frequent inter-comparisons with the Primary Brewer Reference have shown the agreement in ozone calculations within 0.8%, (*Mc Elroy et al.*, 2004). The results of the initial comparisons of B040 with the traveling instrument are shown in Table 5.4. At Arosa, Brewer 040 data has been corrected, making use of the different Brewer calibrations with the traveling standard instrument Brewer 017 and of the standard lamp (SL) history of the instrument. During the calibrations prior to 1996 *not only* the extraterrestrial constants (ETC) were adapted, *but also* the absorption coefficients of  $O_3$  and  $SO_2$  were adjusted. Since 1996, these values have remained constant, as it was recognized that only changes in the optics of the instrument would justify such an adaption. For the Brewer 040 homogenization, the absorption coefficients

are kept constant on the 1996 values  $\alpha_{O_3}=0.34$  and  $\alpha_{O_3/SO_2}=1.1415$ . ETC values are based on the inter-comparisons with the traveling standard instrument Brewer 017, whereas for the periods between the inter-comparisons the results of the standard lamp tests are used. ETCs remained essentially stable with the exception of the period between September 1988 to July 1990 (see Table 5.4). During this period high-frequent oscillations occurred (most probably caused by the fluctuations of humidity within the instrument) and a 5-day running means of lamp test (SL) test were used to apply the corrected ETC.

**Table 5.4:** *Percentage of difference of Brewer 040 (B040) from the reference traveling standard instrument (B017) at the initial inter-comparison in 1989, 1993, 1996, 1999, 2005, 2006, 2007. The percent of difference are the effects on the total ozone values at different air masses with respect the different changes in ETC's and Absorption. Coefficients of B040 since 1988. Between 1999 and 2004 there were no changes in ETC in respect to reference instrument B017.*

Inter-comparison	1989	1993	1996	1999	2005	2006	2007
Reference-Instr	017	017	017	017	017	017	017
B040 [%] $\mu = 1.0$	0.2	-1.8	1.5	2.6	-1.0	2.0	-1.0
B040 [%] $\mu = 2.0$	0.1	-1.1	0.2	1.3	-0.5	1.0	-0.5
B040 [%] $\mu = 3.0$	0.0	-0.8	-0.2	0.9	-0.3	0.7	-0.3

### 5.3.2 Multi-linear regression model used for transfer function

Quasi simultaneous observations are used in the comparison of the spectrophotometers in order to exclude the influence of changes in air mass in the comparison.

In a multiple regression model, a set of independent variables  $x_i$  explain a portion of the variance of a dependent variable  $y$  at a certain significance level (through a significance test of  $R^2$ ), allowing one to establish the relative predictive importance of the independent variables

$$y = \sum_{i=1}^n (a_i x_i) + \epsilon \quad (5.1)$$

Where  $y$  is the target variable,  $x_i$  are independent variables,  $a_i$  with  $i = 1, \dots, n$  the regression coefficients and  $\epsilon$  the residual.

Via this approach, the coherence of measurements, also within the same type of instruments, has been studied looking at the residual of the model. Furthermore, a Brewer TOZ time series has been reconstructed from Dobson data.

$$TOZ_B = a_1 TOZ_D + a_2 (\mu \cdot TOZ_D) + a_3 (\mu \cdot TOZ_D^2) + a_4 (x_T \cdot TOZ_D) + \epsilon \quad (5.2)$$

Where  $TOZ_B$  and  $TOZ_D$  are Brewer and Dobson total ozone measurements. In accordance to *Scarnato et al.* (200xa), the following explanatory variables are used: the air mass factor  $\mu$  is a geometrical coefficient that takes into account the direct beam slant path through the atmosphere, which may be viewed as a parameter to describe stray light effects;  $x_T$  is the influence of the atmospheric temperature. Two approaches have been considered to represent

$x_T$ : ozone weight effective temperature ( $T_{eff}$  integrated from 800-10 hPa and  $T_{eff}^{ST}$  integrated from 200-10 hPa) and local temperature at a pressure level ( $T_p$ ).  $T_{eff}$  and  $T_{eff}^{ST}$  were calculated using temperature and ozone profile measurements of the regular ozone sonde station of Payerne (located in the Swiss plateau, see *Jeannet et al.* (2004)). For more details see *Scarnato et al.* (200xa).

## 5.4 Results and Discussion

### 5.4.1 Comparison of measurements of the same type of instrument

For comparison of quasi-simultaneous observations of Dobson instruments a time window of 10 minutes is selected. Table 5.5 summarizes the results for different wavelengths pairs.

CD wavelength pair observations are recommended for high air mass values (*WMO*, 2003). Dobson observations at Arosa are made with an air mass value between 1.088 and 4.125. Therefore, large air mass values are not contained in our study. Between 1988 and 2007, less than 7% over 22893 observations are available at air mass values between 3 and 4.

**Table 5.5:** Mean difference in percentage between simultaneous measurements with AD, CD and AC wavelengths pair by Dobson 062 and 101.

wavelengths pairs	mean [%]	stand. dev. [%]
AD	0.064	$\pm 0.401$
AC	-0.206	$\pm 0.638$
CD	0.333	$\pm 0.973$

AD wavelength pair observations show a monotonic decrease of TOZ in function of the increase of air mass relative to CD observations and they suggested instead of AD measurements at air mass values higher than 4, when TOZ observations are higher than with the AD pair. This condition is very rare in Arosa: only 4 observations during the period 1988-2007, due to the low sensitivity of primarily Dobson 062 (caused by a more dense wedge at higher R values compared with D101; this reduces the sensitivity at high air masses), and the total ozone measurement reading method of the two Arosa instruments.

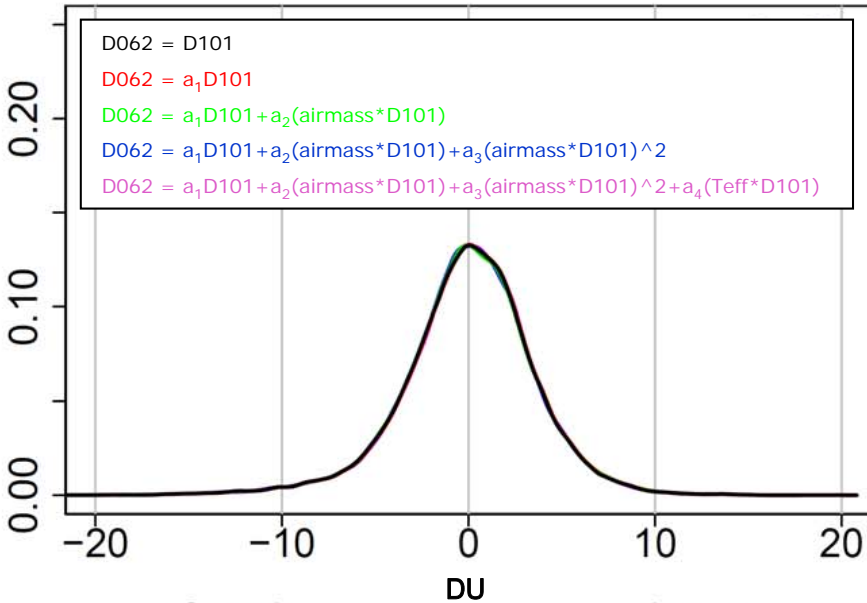


**Figure 5.1:** Density distribution of the residual of the model for total ozone measurements by Dobson 101 and 062 using AD wavelengths pair (D101 and D062) performed within maximally 10 minutes, in 1988 - 2007 period. X-axis shows the residual of the model in DU and y-axis the frequency.

Therefore the use of CD observations for high air mass values is expected to improve the TOZ time series at Arosa only to a very small extent.

The regression model introduced in Section 5.3.2 (Eq. 5.1), has been used as diagnostic tool to verify the coherence of the observations. It can provide information on the atmospheric temperature effect on the observations (missing any further characterization of operational slit widths) and on the internal stray light that can affect the instruments in different ways. In Figure 5.1, the density distribution of the residuals of the regression model for D101 and D062 with AD wavelength observations in 1992-2007 period is presented. The influence of  $T_{eff}$  and OSP are added stepwise. The measurements, in general, do not seem to be affected by variation of atmospheric temperature and OSP. The residual indicates a larger Full Width Half Intensity (FWHI) in summer than in winter. In summer observations are taken for a wide range of air mass values. The uncertainty in the extraterrestrial constant in the TOZ retrieval algorithm has an enhanced effect on measurements at small air mass values, which are more frequent in summer. The standard deviation is about  $\pm 0.5\%$  for AD observations, which can be viewed as the instrumental precision of well maintained Dobson instruments. The respective values are higher for CD and AC wavelength pair observations, which are not used in the standard series of the Arosa measurements.

Brewer measurements have a high sampling frequency. Observations within 1 minute are on average within 0.1% (1 standard deviation) and observations within 10 minutes differ on average by  $0.15\% \pm 0.2\%$ . This result confirms a higher instrumental precision of the more modern Brewer instrument compared with the older Dobson spectrophotometers. The residual of the regression model for Brewer 040 and 156 TOZ observations (see Figure 5.2) exhibits no temperature dependence and a small OSP effect.

The agreement of the observations is somewhat reduced in summer compared with winter due to the range in which observations are taken (i.e. larger range of air mass). Moreover, the error due to the uncertainty in the ETC can be enhanced at small air mass values.

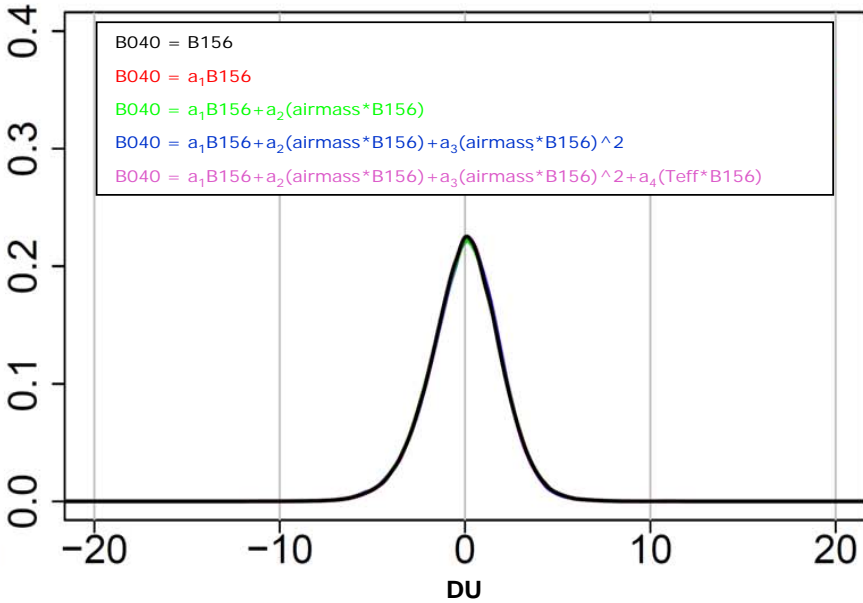


**Figure 5.2:** Density distribution of the residual of the model for total ozone measurements by Brewer 040 and 156 (B040 and B156) performed within maximally 10 minutes, in 1998 - 2007 period. X-axis shows the residual of the model in DU and y-axis the frequency.



### 5.4.2 Comparison of Dobson and Brewer observations

The residuals of the transfer function (multi-regression model) applying stepwise the different proxies introduced in Eq. 5.2 are presented in Figure 5.3. The density distribution for both the residual over the 1988 - 2007 period and for the same period the individual months are included.

The residual distribution of Equation 5.1 has been reduced from a FWHM value of about 10 DU to 6.6 DU applying  $T_{eff}$  and OSP (with a polynomial second order). The residual distribution is asymmetric and not centered on

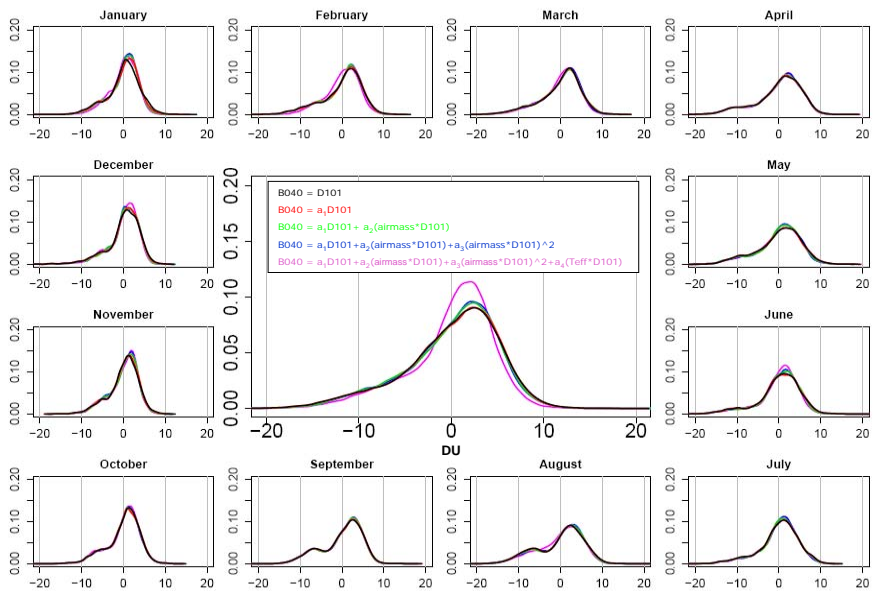


**Figure 5.3:** Density distribution of the residual of the model for total ozone measurements by Brewer 040 and Dobson 101 with AD observations ( $B040$  and  $D101$ ) performed within maximally 10 minutes, in 1998 - 2007 period. X-axis the residual of the model in DU and in y-axis the frequency.

0 ( $\approx 3$  DU). A second, smaller peak centered at - 7 DU is present mainly in August and September. This results from August and September observations in the 1988-1990 period with no correlation found with stray-light problems. Eliminating 1988-1990 period from the data, the residual distribution becomes symmetric with the mean value around 0 and FWHI about 6.4 DU. Further analysis are necessary to explain the existence of these systematic differences. The main results of the regression models are shown in Table 5.6 and 5.7.

The standard errors for the coefficients of the explanatory variables are small compared to the coefficients themselves. The OSP term exhibits greater variability, most likely because it is more connected to the instrumental geometry and optics.

The regression coefficient calculated for the  $T_{eff}$  is comparable with the result determined theoretically using the temperature dependence of the ozone cross sections in *Scarnato et al.* (200xa). In the difference (in percentage) of B40 and D101 with AD observations, it has been calculated a  $T_{eff}$  effect of - 0.05% / °C and by the statistical method it is found  $-0.1571 \pm 0.0013\%$  / °C. The regression coefficient here presented could give indication not only the temperature dependence of the ozone cross section but also the influence of the temperature fluctuation on the ground which could affect the optics of the two instruments. Comparing the weighted regression coefficients, OSP contribution is similar to  $T_{eff}$ , in agreement with *Scarnato et al.* (200xa).

If the ozone balloon measurements required to determine  $T_{eff}$  are not available, it is suggested to use as a proxy the temperature close at 20 hPa. This level is above the ozone maximum, usually around 50 hPa at mid-latitudes. If 50 hPa is used an overcorrection for temperature effect may occur. A comparison between temperatures at different pressure levels,  $T_{eff}$  and  $T_{eff}^{ST}$  (table 5.8) indicates a higher  $T_{eff}$  than  $T_{eff}^{ST}$  because of the high ozone effective temperature in the troposphere.

**Table 5.6:** Brewer transfer function scaled by Dobson 101 AD observations. The regression coefficients  $a_i = i, \dots, n$  are here presented for all proxies and the significances ( $a_1$  for TOZ by D101 with AD wavelenghts pair,  $a_2$  for OSP,  $a_3$  for  $OSP^2$  and  $a_4$  for  $T_{eff}$ ). All the regression coefficients are highly significant (with code 0: ‘\*\*\*’).

	Regression Coefficients	Estimate	Std. Error
B040vsD101(AD) 1988-2007	TOZ by D101(AD)	9.468e-01	6.710e-04
	$OSP$	-7.301e-03	3.640e-04
	$OSP^2$	5.058e-06	2.730e-07
	$T_{eff}$	-1.547e-03	1.352e-05
	Median residuals	0.9078	
	Multiple R-Squared	0.999	
	P-value	< 2.2e-16 ***	
B072vsD101(AD) 1994-2007	TOZ by D101(AD)	9.468e-01	6.710e-04
	$OSP$	-7.301e-03	3.640e-04
	$OSP^2$	5.058e-06	2.730e-07
	$T_{eff}$	-1.547e-03	1.352e-05
	Median residuals	0.1256	
	Multiple R-Squared	0.999	
	P-value	< 2.2e-16 ***	
B156vsD101(AD) 1998-2007	TOZ by D101(AD)	9.620e-01	6.061e-04
	$OSP$	-3.884e-03	3.377e-04
	$OSP^2$	2.373e-06	2.523e-07
	$T_{eff}$	-1.261e-03	1.178e-05
	Median residuals	0.1172	
	Multiple R-Squared	0.9999	
	P-value	< 2.2e-16 ***	

**Table 5.7:** Brewer transfer function scaled by Dobson 062 AD observations. The regression coefficients  $a_i = i, \dots, n$  are here presented for all proxies and the significances ( $a_1$  for TOZ by D062 with AD wavelenghts pair,  $a_2$  for  $OSP$ ,  $a_3$  for  $OSP^2$  and  $a_4$  for  $T_{eff}$ ). All the regression coefficients are highly significant (with code 0: '\*\*\*').

	Regression Coefficients	Estimate	Std. Error
B040vsD062(AD) 1992-2007	TOZ by D062(AD)	9.555e-01	7.231e-04
	$OSP$	-6.063e-03	3.876e-04
	$OSP^2$	5.151e-06	2.933e-07
	$T_{eff}$	-1.380e-03	1.469e-05
	Median residuals	0.7176	
	Multiple R-Squared	0.9998	
	P-value	< 2.2e-16 ***	
B072vsD062(AD) 1994-2007	TOZ by D062(AD)	9.630e-01	5.079e-04
	$OSP$	6.244e-03	2.781e-04
	$OSP^2$	-4.664e-06	2.083e-07
	$T_{eff}$	-1.069e-03	9.909e-06
	Median residuals	0.0863	
	Multiple R-Squared	0.9999	
	P-value	< 2.2e-16 ***	
B156vsD062(AD) 1998-2007	TOZ by D062(AD)	9.693e-01	6.272e-04
	$OSP$	-3.906e-03	3.497e-04
	$OSP^2$	3.805e-06	2.641e-07
	$T_{eff}$	-1.120e-03	1.225e-05
	Median residuals	-0.01415	
	Multiple R-Squared	0.999	
	P-value	< 2.2e-16***	

**Table 5.8:** *Temperature at the pressure level of 300, 200, 100, 50, 30 and 10 hPa compared with the effective temperature in the stratosphere and over the entire profile (1988-2007).*

	P300	P200	P100	P050	P030	P010	$T_{eff}^{ST}$	$T_{eff}$
Min. :	-60.89	-94.89	-74.14	-78.10	-80.67	-82.87	-75.65	-67.79
1 <sup>st</sup> Qu.:	-48.77	-61.87	-61.19	-60.53	-59.48	-52.00	-59.22	-53.47
Median :	-44.43	-58.14	-58.36	-56.97	-54.49	-44.04	-55.19	-48.95
Mean :	-44.71	-58.06	-58.63	-57.80	-55.62	-45.92	-56.04	-49.45
3 <sup>rd</sup> Qu.:	-40.46	-53.85	-56.06	-54.44	-50.81	-38.49	-52.38	-45
Max. :	-32.53	-40.25	-44.61	-47.13	-38.78	-18.35	-45.85	-39.9

### 5.4.3 Relative Long term stability of Dobson and Brewer series at Arosa

The time series for Dobson 101 with AD observations and Brewer 040 are discussed here. These two instruments were chosen due to their operation over the entire period. Figure 5.4 presents TOZ time series for Brewer 040 and Dobson 101 with AD wavelength observations. The instruments reproduce the TOZ seasonal cycle and day-to-day variability in a very similar way. However the differences of TOZ of Brewer instruments with Dobson AD, AC and CD wavelength pair observations, exhibit a seasonal cycle of amplitude about 2% (see third plot in Figure 5.4). Similar differences between Brewer and Dobson observations have been documented at other sites (*Köhler, 1999; Kerr et al., 1988; Vanicek, 2006*). In order to make the Dobson measurements comparable with Brewer observations, the transfer function introduced in Eq. 5.2 (Section 5.3.2) is applied (see fourth plot in Figure 5.4).

The importance of the elimination of instrumental discrepancies needs be stressed. The replacement of measurements of Dobson by Brewer instruments without constructing a transfer function can lead to unrealistic TOZ trends.

The transfer function in Eq. 5.2, allows one to reconstruct a Brewer TOZ time series with Dobson data. It significantly reduces the differences in the seasonal cycle and the scatter of the differences, introducing as explanatory variables at a significant level (Table 5.6) the effective temperature ( $T_{eff}$ ) and the ozone slant path (OSP) at the second order. However, the long term drift of 3% between the Dobson and Brewer series at Arosa, documented earlier (*Stahelin et al., 1998a*), cannot be removed via this procedure and remains unexplained. A drift of similar magnitude has been found in the observations of Hradec Kralove (Czech Republic), also after correction for temperature effect suggested by *Kerr (2002)*, (*Vanicek, 2006*). Arosa optical depth (AOD) was strongly enhanced after the eruption of volcano Pinatubo in June 1991. However, the temporal evolution of the volcanic stratospheric aerosol explain from 1992 some of the shift between TOZ of the two types of instruments.

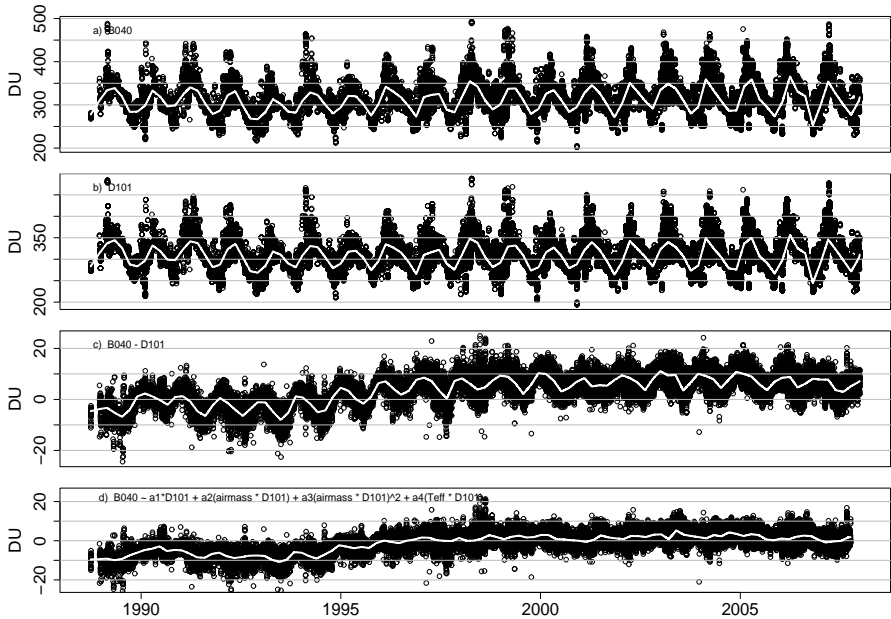


**Figure 5.4:** TOZ time series for B040 and D101 with AD wavelengths in panel a) and b) and their difference in panel c). Below Brewer 040 data are converted to Dobson 101 AD observations considering the  $T_{eff}$  and OSP (see eq. 5.2).

#### 5.4.4 Comparison of Arosa data with NIWA satellite measurements

Satellite column ozone measurements can be used to detect instrumental problems in ground based measurements, particularly if they appear as sudden changes. It has also been tried to find evidence from comparison with satellite measurements, whether the temporal behavior of the Dobson or Brewer series of Arosa is more reliable. However, no single reliable working satellite instrument covers the period 1990 to 1995, which is the most critical period in the Arosa record. It has been decided to use the NIWA data (Bodeker *et al.*, 2005) for this comparison. The data combines satellite-based ozone measure-

ments from 4 Total Ozone Mapping Spectrometer (TOMS) instruments, 3 different retrievals from the Global Ozone Monitoring Experiment (GOME), and data from 4 Solar Backscatter Ultra-Violet (SBUV) instruments. Comparisons with the global ground based Dobson spectrophotometer network are used to remove offsets and drifts between the different satellite measurements to produce a global homogeneous data set that combines the advantages of the superior spatial coverage of satellite data with the long-term stability of ground based measurements. Figure 5.5 shows the averaged monthly mean of the difference between NIWA data versus ground based measurements. NIWA and Dobson data exhibit a good agreement of 1.5% in average  $\pm 0.5\%$  peak-to-peak with a maximum in spring when TOZ reaches its maximum. A significant seasonal bias (see Figure 5.5), and drift (see Figure 5.6), is found when comparing NIWA data with Brewer measurements.



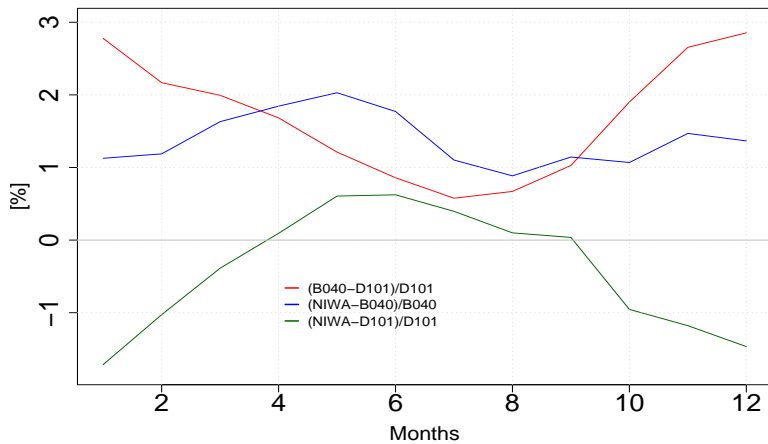


**Figure 5.5:** Monthly mean difference of TOZ by ground based and satellite measurements (NIWA) with bandpass over Arosa.

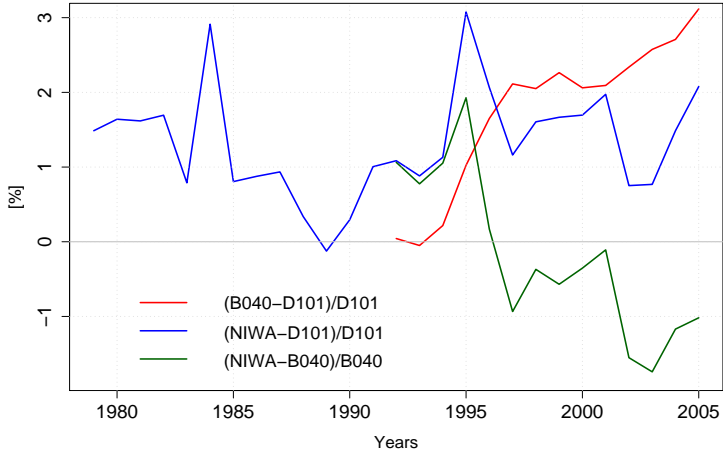


**Figure 5.6:** Yearly mean difference of TOZ by ground based and satellite measurements (NIWA) with bandpass over Arosa.

## 5.5 Discussion and Conclusions

Total ozone time series of high data quality are important to document the effect of the anthropogenic release of ozone depleting substances on the global ozone layer and the expected recovery of stratospheric ozone from the implementation of the Montreal Protocol. Since ozone trends are small at mid-latitudes, the long term stability of ozone measurements is an outstanding problem. The long term series of Arosa started in 1926, is entirely based on Dobson spectrophotometers until 1988 (Figure 5.7). The long term stability of the early Dobson time series was assessed using the statistical Langley plot method (applied every year in order to update the instrumental constant (Dütsch, 1984). The Arosa series up to 1990 was homogenized using only information of the Arosa records (Stahelin *et al.*, 1998a).

During the 1970s a network of ground based total ozone measurements was developed in which the data quality of the measurements is ensured by the comparison with the World Primary Dobson instruments which is absolutely calibrated by the Langley plot method regularly performed at the Manua Loa observatory at Hawaii. This methodology strongly has improved the data quality of the world wide Dobson network. At Arosa, Dobson instrument D101 was first calibrated against a WMO standard instrument in 1986 and the calibrations of the Dobson instruments were subsequently updated by regular comparisons with standard instruments. The long total ozone time series at Arosa was adjusted to the WMO scale using an overlap of 4 years of measurements *Stahelin et al.* (1998a).

Since 1988, completely automated Brewer spectrophotometers have been operated at Arosa in order to increase the reliability of the ozone measurements. The data quality of the global Brewer network is based on a similar concept: using Langley plot calibration at the Mouna Loa Observatory for the absolute calibration. The Dobson and Brewer observations at Arosa allow one to deduce information about the instrumental precision of both types of instruments and to determine an instrumental transfer function between Dobson and Brewer measurements which describe systematic differences of the seasonal variation of the ozone readings. Such a transfer function must

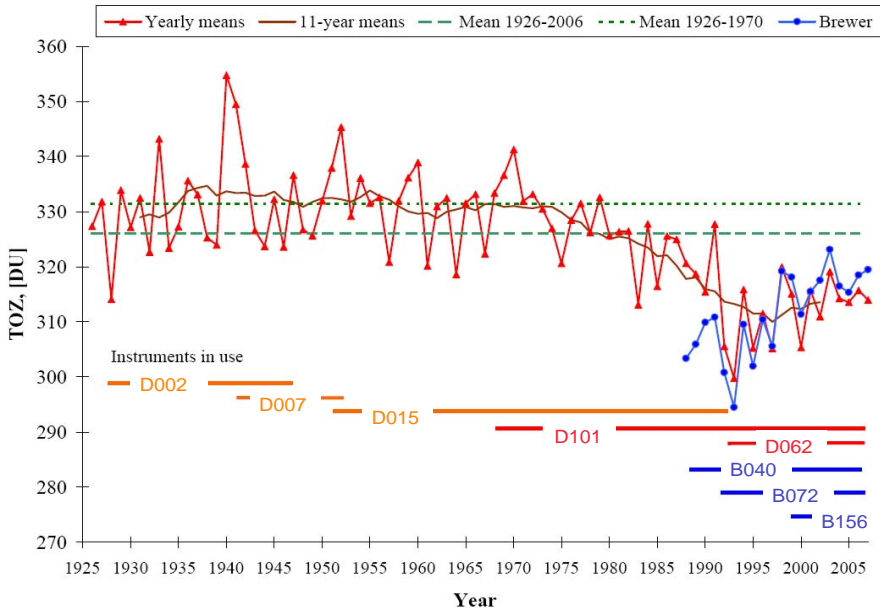


**Figure 5.7:** Total Ozone time series at Arosa from 1926 to 2006. The data has been homogenized for Dobson 101 with AD wavelengths (D101). The instruments used in the relative time period are listed. Measurements are shown as annual (red) and 11- years (brown) means in Dobson unites (DU) ( $DU = 0.01$  mm of thickness of the ozone layer at standard condition ( $p = 1013$  hPa,  $273$  K)). In dashed green line, TOZ mean values from 1926 to 2006. In green dotted line, TOZ mean value, before ozone depletions occurred from 1926-1970. In blue Brewer 040 (B040) yearly mean to enfatize the need of a transfer function to determine reliable trends.

be constructed before the replacement of a Dobson with a Brewer instrument, otherwise the instrumental change would introduce a strong discontinuity in the data, preventing the use of time series in long term trend analysis. The Dobson and Brewer total ozone time series at Arosa show a remarkable relative drift in the first part of the 1990s when the measurements are processed by using the results of the regular inter-comparisons. It is difficult to evaluate

which of the instrumental series is more reliable (Figure 5.7). Unfortunately only one Dobson (D101) and one Brewer (B040) instrument were continuously operated at Arosa between 1990 and 1995 (D015 was taken out of service in 1992 and replaced by D062 and only one Brewer instrument was installed at Arosa prior 1992). In the later period, the total ozone measurements of individual instruments are much more consistent. The results of the measurements performed at the beginning of the inter-comparisons provide information about the relative stability of the Arosa instruments against the standard instrument during the period after the last inter-comparison, when the instrumental constants were updated. The largest shift between D101 and the standard instrument D065 was recorded in the 1995 inter-comparison which was ignored in our analysis. The comparison between the ground based measurements at Arosa and the combined NIWA satellite time series shows substantial inter annual differences and a much better consistency with the Dobson than Brewer measurements. However, this cannot be viewed as clear evidence for a better stability of the Dobson time series over the Brewer time series, because the combined NIWA satellite time series was tight to the Dobson ground based network when homogenizing the instrumental records of the individual instruments. Finally, the procedure of comparisons of Brewer station with the Brewer traveling instrument was changed in the middle of the 1990s and the effect of this change need to be quantitatively assessed before the potential reasons of relative drift can be clarified. Further aspects might include the stability of the reference instruments and the possibility of a significant relative drift of the world primary instruments cannot be round out by this analysis.

## 5.6 Acknowledgments

The work of B.S. was supported by research grant of MeteoSwiss as part of the meteo Swiss Global Atmospheric Watch (GAW) program. We thank Joerg Maeder for valuable advice in applying statistical modeling and data handling and the Dobson operators at Arosa to have carefully operated measurements thought all this years. Moreover we wish to thank for very valuable discus-

sions Tom Peter, Susan Solomon, Bob Evans, Irina Petropavlovskikh, Peter Kriedron and Elizabeth Weatherhead.

## 5.7 Appendix

We included in a further run of the model the aerosol surface density (sad) as indicator of stratospheric aerosol. This provides some preliminary evidence that the large shift between Dobson and Brewer data of Arosa between (1988-1995) could be caused by aerosol load after Pinatubo eruption. However, the difference between the two types of instruments, considering the period 1988-1992, remains unexplained Figure 5.8.

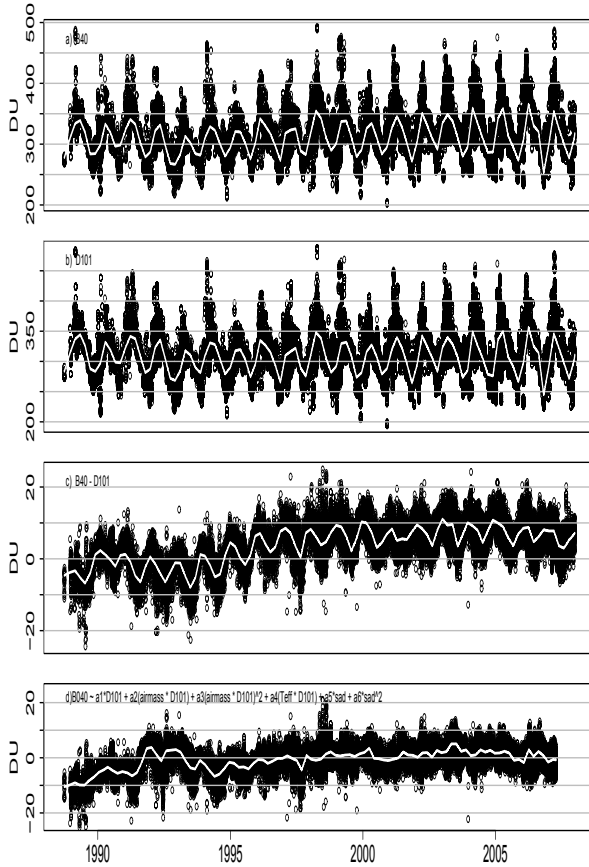


**Figure 5.8:** *Density distribution of the residual of the model including also sad for TOZ measurements by B040 and D101 with AD wavelengths performed within maximally 10 minutes, in 1988 - 2007 period. X-axis shows the residual of the model in DU and y-axis the frequency.*

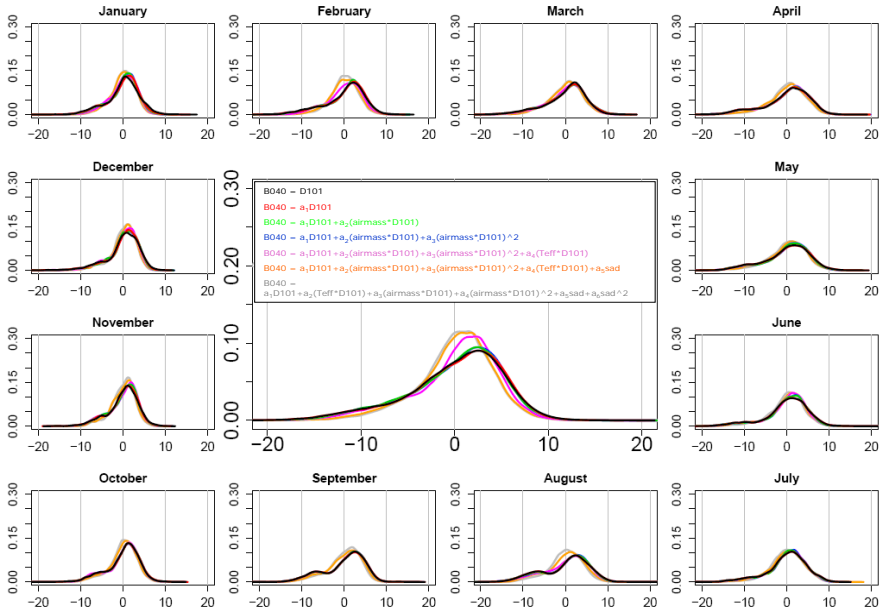


**Figure 5.9:** Density distribution of the residual of the model for total ozone measurements by B040 and D101 with AD wavelengths performed within maximally 10 minutes, in 1988 - 2007 period. X-axis shows the residual of the model in DU and y-axis the frequency.



## Chapter 6

# Final Remarks

Since ozone trends are small at mid-latitudes the long term stability of ozone measurements is an inherently important problem. Total ozone can be measured by ground based instruments as well as from satellite instruments. Data quality can be better handled by ground based spectrophotometers than satellite instruments. However, satellite instruments can provide global coverage and therefore high quality ground based measurements are also very relevant for validation of satellite ozone measurements. The purpose of this thesis is to study instrumental differences of Dobson and Brewer spectrophotometers and improve the data quality. It makes use of the unique situation in Arosa (Switzerland) where data is available from 5 co-located spectrophotometers and of the long term meteorological and ozone sounding data in Payerne.

The instrument characteristics and retrieval algorithms have been examined in detail. A method to correct TOZ observations for the ozone cross section temperature sensitivity has been provided, based on the optical proprieties of the instruments.

It has been found that the TOZ retrieved has a temperature sensitivity strongly dependent on the ozone cross section spectra used in the retrieval algorithms. After an inspection of different ozone cross sections reported in literature (*Bass and Paur, 1985; Malicet et al., 1995; Burrows et al., 1999*), the more sophisticated Brewer retrieval algorithm results more sensitive to the uncertainty of the spectra in use because of the narrow slit widths and the retrieval weighting coefficients, which were selected in order to minimize

SO<sub>2</sub> and AOD interference with TOZ measurements. The use of *Bass and Paur* (1985) or *Malicet et al.* (1995) spectra gives the optimal cross sections for Dobson and Brewer ground based instruments: the differences of the TOZ retrieved by the two instruments result to be minimized. The systematic bias in the differences of the observations, with a maximum amplitude in winter, has been explained in terms of temperature sensitivity of the ozone cross section and ozone slant path effect (OSP) (i.e. possible leading stray light problems): the seasonal amplitude in the difference of the observations has been decreased from 2% to less than 1%, using *Bass and Paur* (1985) or *Malicet et al.* (1995) cross sections.

The redundant TOZ data by Dobson and Brewer has been used to derive information of instrument precision of simultaneous measurements. A multiple linear regression model, based on the assumptions of Chapter 4, has been proposed as an innovative method to identify instrumental differences and changes also within the same type of instruments (i.e. temperature sensitivity within Dobson instruments, possible stray light problems not detected with lamp test). Using the same approach an empirical transfer function can be provided to adjust Brewer data based on Dobson measurements (or vice versa). The knowledge of an accurate transfer function is highly necessary before the replacement of Dobson with Brewer instrument, to prevent discontinuity in long term dataset.

Dobson and Brewer long term TOZ time series of Arosa show a drift of 3% in the first part of the 1990s when the measurements are processed by using the results of regular intercomparisons. The magnitude of this drift is not reconcilable to atmospheric temperature changes. It is difficult to evaluate which of the instrument time series is more reliable, due to the lack of sufficient independent measurements over the considered period. Unfortunately only one Dobson (D101) and one Brewer (B040) instrument were continuously in operation at Arosa between 1990 and 1995 and no single reliable working satellite instrument covers the period 1990 to 1995. The comparison between the ground based measurements of Arosa and the combined NIWA satellite time series shows, in addition to substantial inter annual differences, a much better agreement with the Dobson than Brewer time series. However, this

cannot be taken as clear evidence for a better stability of the Dobson time series over the Brewer series, because the combined NIWA satellite time series uses Dobson ground based network when homogenizing the instrumental records of the individual instruments.

Changes in the procedure of comparisons of Brewer station with the Brewer traveling instrument were adopted in the middle of the 1990s and the effect of this change remains to be quantitatively assessed. Further aspects might include the stability of the reference instruments and possibly the effect of the aerosol of the volcanic eruption of Mt. Pinatubo.



# List of Figures

2.1	Earth's atmosphere layers and temperature profile. . . . .	6
2.2	Ozone profile . . . . .	9
2.3	Radiative forcing of climate change from atmospheric gas changes	11
2.4	Chapman ozone life cycle reactions . . . . .	12
2.5	Total column ozone estimated using Chapman chemistry vs TOMS measurements . . . . .	15
2.6	Conversion of halogen source gases . . . . .	16
2.7	Polar vortex and ozone hole . . . . .	21
2.8	Stratospheric air temperatures in both polar regions . . . . .	25
2.9	Arctic and Antarctic ozone distribution . . . . .	26
2.10	Mixing ratio of anthropogenic Halocarbons . . . . .	31
2.11	Temporal evolution of global ozone amounts . . . . .	33
2.12	Ozone variations for 60 °S-60 °N from ground based data . . . . .	35
3.1	Dobson design and optics . . . . .	39
3.2	Brewer MKII design and optics . . . . .	40
3.3	Brewer MKIII design and optics . . . . .	41

4.1	<i>Bass and Paur</i> (1985) ozone cross section temperature dependence in the Huggins band. . . . .	57
4.2	Brewer 040 (B040) and Dobson 101 using AD wavelengths (D101 AD) total ozone time series at Arosa and their difference . . . . .	62
4.3	Seasonal variation (mean values over 1995-2004) of the key parameters used in this study: Averaged ozone concentration from ozone sondes ( $O_3$ ), averaged air temperature (T) and effective ozone temperature ( $T_{eff}$ ) and $T_{eff}^{ST}$ . . . . .	63
4.4	Brewer and Dobson effective ozone cross section temperature sensitivity per Celsius. Reference spectra <i>Bass and Paur</i> (1985)	66
4.5	<i>Malicet et al.</i> (1995) effective ozone cross section temperature effect . . . . .	68
4.6	<i>Burrows et al.</i> (1999) effective ozone cross section temperature effect . . . . .	69
4.7	Difference of direct sun TOZ observations (1995-2005) by Brewer 040 and Dobson 101(AD) vs Ozone Slant Path. . . . .	71
4.8	Reference spectra ( <i>Bass and Paur</i> , 1985), difference of B040 and D101(AD) observations eliminating stepwise different contributes . . . . .	73
4.9	Reference spectra ( <i>Malicet et al.</i> , 1995), difference of B040 and D101(AD) observations eliminating stepwise different contributes	74
4.10	Reference spectra ( <i>Burrows et al.</i> , 1999), difference of B040 and D101(AD) observations eliminating stepwise different contributes	75
5.1	Density distribution of the residual of the regression model for total ozone observations by Dobson 101 and 062 for the period 1992 - 2007 . . . . .	88

---

5.2	Density distribution of the residual of the regression model for total ozone observations by Brewer 040 and 156 for the period 1998 - 2007 . . . . .	90
5.3	Density distribution of the transfer function for Brewer 040 scaled by Dobson 101 for AD observations . . . . .	91
5.4	TOZ time series for B040 and D101(AD), their difference and Brewer 040 homogenized data for Dobson 101(AD) . . . . .	97
5.5	Monthly mean difference of TOZ by ground based and satellite measurements (NIWA) with bandpass over Arosa. . . . .	99
5.6	Yearly mean difference of TOZ by ground based and satellite measurements (NIWA) with bandpass over Arosa. . . . .	100
5.7	Total Ozone time series at Arosa from 1926 to 2006 . . . . .	102
5.8	Density distribution of the residual of the regression model including sad for TOZ observations by Dobson 101 and 062 for the period 1992 - 2007 . . . . .	105
5.9	Density distribution of the residual of the regression model for total ozone observations by Dobson 101 and 062 for the period 1992 - 2007 . . . . .	106





# List of Tables

4.1	Brewer algorithm's weighting coefficients . . . . .	53
4.2	Spectral absorption cross-sections of ozone published by <i>Bass and Paur</i> (1985), <i>Malicet et al.</i> (1995) and <i>Burrows et al.</i> (1999). . . . .	56
4.3	Ozone effective temperature ( $T_{eff}$ and $T_{eff}^{ST}$ ) and air temperature (T) mean and quantiles above Payerne. . . . .	64
4.4	Ozone temperature dependence for operational wavelengths of Brewer 040 and 072 (MKII) and B156 (MKIII) compared with the values published by <i>Kerr et al.</i> (1988); <i>Kerr</i> (2002) . . . . .	64
4.5	Cross section effect in the seasonal bias of the difference of Brewer and Dobson TOZ measurements. . . . .	65
4.6	Absolute ozone cross sections at the retrieval temperatures for Brewer 040 and 072 (MKII) and B156 (MKIII) and Dobson spectrophotometers using different spectra. . . . .	66
4.7	Effective temperature sensitivity for Brewer 040 and 072 (MKII), B156 (MKIII) and Dobson (D083) using different spectra . . . . .	67
5.1	Instruments used in the relative period . . . . .	82
5.2	Dobson 101 (D101) stability . . . . .	83
5.3	Dobson 062 (D062) stability . . . . .	84
5.4	Brewer 040 (B040) stability . . . . .	85

5.5	Difference in percentage between simultaneous Dobson measurements . . . . .	87
5.6	Brewer transfer function scaled by Dobson 101 AD observations	93
5.7	Brewer transfer function scaled by Dobson 062 AD observations	94
5.8	Temperature . . . . .	95

# Bibliography

- Basher, R. E., Review of the dobson spectrophotometer and its accuracy, *Global Ozone Research and Monitoring Projects, Report 13*(World Meteorological Organization, WMO, Geneva.), 1982.
- Bass, A. M., and R. J. Paur, The ultraviolet cross-sections of ozone. i. the measurements. ii - results and temperature dependence, *Atmospheric ozone; Proceedings of the Quadrennial*, pp. 606–616, 1985.
- Bernhard, G., R. D. Evans, G. J. Labow, and S. J. Oltmans, Bias in dobson total ozone measurements at high latitudes due to approximations in calculations of ozone absorption coefficients and air mass, *Journal of Geophysical Research*, 110, D10,305, doi:10.1029/2004JD005,559, 2005.
- Bertaux, J., G. Megie, T. Widemann, E. Chassefiere, R. Pellinen, E. Kyrola, S. Korpela, and P. Simon, Monitoring of ozone trend by stellar occultations: The gomos instrument, *Advances in Space Research*, 11(3), 237–3242, 1991.
- Bodeker, G., H. Shiona, and H. Struthers, The niwa assimilated total column ozone data base and assimilated trace gas profile data base for validation of ccms, *paper presented at CCMVal 2005 Workshop, October 2005, Boulder, Colo.*, 2005.
- Brönnimann, S., J. Staehelin, J. Cain, and S. Farmer, Total ozone observations prior to the igy. ii: Data and quality, *Quart. J. Roy. Meteorol. Soc.*, 129(593), 2819–2843, 2003a.
- Brönnimann, S., J. Staehelin, S. Farmer, J. Cain, T. Svendby, and T. Svene, Total ozone observations prior to the igy. i: A history, *Quart. J. Roy. Meteorol. Soc.*, 129(593), 2797–2817, 2003b.

- Burkholder, J. B., J. J. Orlando, , and C. J. Howard, Ultraviolet-absorption cross-sections of  $\text{Cl}_2\text{O}_2$  between 210 and 410 nm, *J. Phys. Chem.*, *94*(2), 687–695, 1990.
- Burrows, J. P., A. Richter, A. Dehn, B. Deters, S. Himmelmann, and J. Orphal, Atmospheric remote-sensing reference data from gome - 2. temperature-dependent absorption cross sections of  $\text{O}_3$  in the 231-794 nm range, *Journal of Quantitative Spectroscopy and Radiative Transfer*, *61*(4), 509–517, 1999.
- Chapman, S., A theory of upper atmospheric ozone, *Mem. Roy. Met. Soc.*, *3*(10), 103–125, 1930.
- Chu, W. P., M. P. McCormick, J. Lenoble, C. Brogniez, and P. Pruvost, Sage ii inversion algorithm, *Journal Geophysical Research*, *94*(6), 8339–8351, 1989.
- Crutzen, P. J., Influence of nitrogen oxides on atmospheric ozone content, *Quarterly Journal of the Royal Meteorological Society*, *96*(408), 320–, 1970.
- Dobson, G. M. B., A photoelectric spectrophotometer for measuring the amount of atmospheric ozone, *Proceedings of the Physical Society*, *43*, 324–339, 1931.
- Dobson, G. M. B., Atmospheric ozone and movement of air in stratosphere, *Pure and applied geophysics*, *106*, 1520–1530, 1973.
- Dütsch, H. U., An update of the arosa ozone series to the present using a statistical instrument calibration, *Quart. J. R. Met. Soc.*, *110*, 1079–1096, 1984.
- Farman, J. C., R. J. Murgatroyd, A. M. Silnickas, and B. A. Thrush, Ozone photochemistry in the antarctic stratosphere in summer, *Quarterly Journal of the Royal Meteorological Society*, *111*(470), 1013–1025, 1985.
- Fioletov, V. E., J. B. Kerr, C. T. McElroy, D. I. Wardle, V. Savastiouk, and T. S. Grajnar, The brewer reference triad, *Geophysical Research Letters*, *32*(20), 2005.

- Götz, F. W. P., A. R. Meetham, D. Phil, and D. G.M.B, The vertical distribution of ozone in the atmosphere., *Proceedings of the Royal Society of London*, 145(855), 416–446, 1934.
- Gunson, M. R., and et al., The atmospheric trace molecule spectroscopy (atmos) experiment: Deployment on the atlas space shuttle missions, *Journal Geophysical Research Letters*, 23, 2333–2336, 1996.
- Hoegger, B., D. Levrat, J. Staehelin, H. Schill, and P. Ribordy, Recent developments of the light climatic observatory - ozone measuring station of the swiss meteorological institute (lko) at arosa, *Journal of Atmospheric and Terrestrial Physics*, 54 (5), 497–498, 1992.
- Hofmann, D. J., and S. Solomon, Ozone destruction through heterogeneous chemistry following the eruption of el chichon, *Journal Geophysical Research*, 94, 5029–5041, 1989.
- James, N. I., Introduction to circulating atmospheres, *Cambridge University Press. Cambridge, U.K.*, 1994.
- Jeannet, P., R. Stübi, G. Levrat, P. Viatte, and J. Staehelin, Ozone balloon soundings at payerne (switzerland): Trend analysis over the period 1967–2002, *Proceed. of stratospheric ozone workshop*, pp. 19–21, 2004.
- Johnston, H., Catalytic reduction of stratospheric ozone by nitrogen oxides, *Proceedings of the National Academy of Sciences of the United States of America*, 68(11), 2898–, 1971a.
- Johnston, H., Reduction of stratospheric ozone by nitrogen oxide catalysts from supersonic transport exhaust, *Science*, 173(3996), 517–600, 1971b.
- Kerr, J. B., Automated brewer spectrophotometer, *Proceedings of the 4th Ozone Symposium on Atmospheric Ozone, D. Reidel, Norwell, Mass.*, 396–401, 1985.
- Kerr, J. B., New methodology for deriving total ozone and other atmospheric variables from brewer spectrophotometer direct sun spectra, *Journal of Geophysical Research-Atmospheres*, 107(D23), 2002.

- Kerr, J. B., C. T. McElroy, and R. Olafson, Measurements of ozone with the brewer spectrophotometer, *Proc. of Quadrennial International Ozone Symposium, J. London*, 74–79, 1981.
- Kerr, J. B., I. A. Asbridge, and W. F. J. Evans, Intercomparison of total ozone measured by the brewer and dobson spectrophotometers at toronto, *Journal of Geophysical Research-Atmospheres*, 93(D9), 11,129–11,140, 1988.
- Köhler, U., A comparison of the new filter ozonometer microtops ii with dobson and brewer spectrometers at hohenpeissenberg, *Geophysical Research Letter*, 26(10), 1385–1388, 1999.
- Komhyr, W., Operations handbook - ozone observations with a dobson spectrophotometer, *World Meteorological organization Global Ozone Research an Monitoring Project*, 1980a.
- Komhyr, W. D., Dobson spectrophotometer systematic total ozone measurement error, *Geophysical Research Letters*, 7(2), 161–163, 1980b.
- Komhyr, W. D., and R. D. Evans, Dobson spectrophotometer total ozone measurement errors caused by interfering absorbing species such as so<sub>2</sub>, no<sub>2</sub>, and photochemically produced o<sub>3</sub> in polluted air, *Geophysical Research Letters*, 7(2), 157–160, 1980.
- Komhyr, W. D., R. D. Grass, and R. K. Leonard, Dobson spectrophotometer 83: A standard for total ozone measurements, *Geophysical Research Journal*, 94, 9847–9861, 1989.
- Komhyr, W. D., C. L. Mateer, and R. D. Hudson, Effective bass-pair 1985 ozone absorption-coefficients for use with dobson ozone spectrophotometers, *Journal of Geophysical Research-Atmospheres*, 98(D11), 20,451–20,465, 1993.
- Lucke, R., and et al., The polar ozone and aerosol measurement (poam) iii instrument and early validation results, *Journal Geophysical Research*, 104(18), 785–799, 1999.

- Malicet, J., D. Daumont, C. Charbonnier, A. Parisse, A. Chakir, and J. Brion, Ozone uv spectroscopy. ii. absorption cross-sections and temperature dependence, *Journal of Atmospheric Chemistry*, *21*, 263–273, 1995.
- Mc Elroy, C. T., V. Savastiouk, and L. Ken, Calibrating the brewer spectrophotometers with the traveling standard brewer 017, *Proc. of XX Quadr. Ozone Symp.*, edited by Zeferos, C.S., University of Athens, 2004.
- McElroy, M. B., S. R. J., and M. K, The changing stratosphere, *Planetary and Space Science*, *40*(2-3), 373–401, 1992.
- Molina, L. T., and M. J. Molina, Production of  $\text{Cl}_2\text{O}_2$  from the self-reaction of the ClO radical, *J. Phys. Chem.*, *91*(2), 433–436, 1987.
- Molina, M. J., and F. S. Rowland, Stratospheric sink for chlorofluoromethanes - chlorine atom catalyzed destruction of ozone, *Bulletin of the American Meteorological Society*, *55*(5), 491–491, 1974.
- Molina, M. J., and F. S. Rowland, Some unmeasured chlorine atom reaction-rates important for stratospheric modeling of chlorine atom catalyzed removal of ozone, *Journal of Physical Chemistry*, *79*(6), 667–669, 1975.
- Mordecai, B. R., The history of ozone. the schönbein period, 1839-1868, *Division of History of Chemistry of the American Chemical Society*, *26*(1), 2001.
- Mozurkewich, M., and J. Calvert, Reaction probability of  $\text{N}_2\text{O}_5$  on aqueous aerosols, *J. Geophys. Res.*, *93*(15), 889–896, 1988.
- Newman, P. A., et al., *Stratospheric Ozone, An Electronic Textbook*, todaro, m ed., 2008.
- Orphal, J., A critical review of the absorption cross-section of  $\text{O}_3$  and  $\text{NO}_2$  in the ultraviolet and visible., *J. Photoch. and Photobio.*, pp. 185–209, 2003.
- Pope, F. D., B. K. D. Hansen, J., R. R.F., and S. S. P., Ultraviolet absorption spectrum of chlorine peroxide,  $\text{ClOOCl}$ , *Journal Phys. Chem. A.*, *111*, 4322–4332, 2007.

- Rodriguez, S., et al., A study on the relationship between mass concentrations, chemistry and number size distribution of urban fine aerosols in milan, barcelona and london, *Atmospheric Chemistry and Physics*, 7, 2217–2232, 2007.
- Scarnato, B., J. Staehelin, J. Gröbner, R. Stübi, and H. Schill, Total ozone observations at arosa (switzerland) by dobson and brewer: Temperature and ozone slant path effect. (in preparation), *Journal of Geophysical Research-Atmospheres*, 200xa.
- Scarnato, B., J. Staehelin, R. Stübi, and H. Schill, Long term total ozone observations at arosa (switzerland): A transfer function. (in preparation), *Journal of Geophysical Research-Atmospheres*, 200xb.
- Solomon, S., The mystery of the antarctic ozone hole, *Review of Geophysics*, 26(2), 131–148, 1988.
- Solomon, S., Increased chlorine dioxide over antarctica caused by volcanic aerosols from mount pinatubo, *Nature*, pp. 245–248, 1993.
- Solomon, S., Stratospheric ozone depletion: A review of concepts and history, *Review of Geophysics*, 37(3), 275–316, 1999.
- Staehelin, J., R. Kegel, and N. R. P. Harris, Trend analysis of the homogenized total ozone series of arosa (switzerland), 1926–1996, *Journal of Geophysical Research-Atmospheres*, 103(D7), 8389–8399, 1998a.
- Staehelin, J., A. Renaud, J. Bader, R. McPeters, P. Viatte, B. Hoegger, V. Bugnion, M. Giroud, and H. Schill, Total ozone series at arosa (switzerland): Homogenization and data comparison, *Journal of Geophysical Research-Atmospheres*, 103(D5), 5827–5841, 1998b.
- Staehelin, J., N. Harris, C. Appenzeler, and J. Eberhard, Ozone trend: A review, *Review of Geophysics*, 39(2), 231–290, 2001.
- Strutt, C. R., The optics research of robert john strutt, fourth baron rayleigh, *Applied optics*, 3(10), 1964.



- Stübi, R., G. Levrat, B. Hoegger, P. Viatte, J. Staehelin, and F. J. Schmidlin, In-flight comparison of brewer-mast and electrochemical concentration cell ozonesondes, *J. Geophys. Res.*, 113(D13302), 2008.
- Thomas, R. W. L., and A. C. Holland, Ozone estimates derived from dobson direct sun measurements: effect of atmospheric temperature variations and scattering, *Applied optics*, 16(3), 1977.
- Tolbert, M. A., M. J. Rossi, and G. D. M, Heterogeneous interactions of chlorine nitrate hydrogen chloride and nitric acid with sulfuric acid surfaces at stratospheric temperatures, *Geophysical Research Letter*, 15, 847–850, 1988.
- Vanicek, K., Differences between ground dobson, brewer and satellite toms-8, gome-wfdoas total ozone observations at hradec kralove, czech, *Atmos. Chem. Phys. Discuss.* [www.atmos-chem-phys-discuss/6/5839/2006/](http://www.atmos-chem-phys-discuss/6/5839/2006/), 6, 5839–5865, 2006.
- Vanier, J., and I. Wardle, The effects of spectral resolution on total ozone measurements, pp. 395–399, 1969.
- Varotsos, C. A., G. J. Chronopoulos, A. P. Cracknell, B. E. Johnson, A. Katsambas, and A. Philippou, Total ozone and solar ultraviolet radiation, as derived from satellite and ground-based instrumentation at dundee, scotland, *International Journal of Remote Sensing*, 19(17), 3301–3305, 1998.
- WMO, G., Report of the international ozone trends panel 1989, *Global Ozone Res. and Monit. Proj.*, Geneva, 18, 1989.
- WMO, G., Comparison of total ozone measurements of dobson and brewer spectrophotometers and recommended transfer function, *Global Ozone Res. and Monit. Proj.*, Geneva, 149, 2003.
- WMO, U., Scientific assessment of ozone depletion: 2006, 2007.

# Acknowledgements

Guess, at the end you start to think about the beginning.

First of all I want to thank those have given me a chance: Johannes Staehelin, Tom Peter and Rene Stübi. I clearly remember the day of the longest interview of my life and the other valuable candidates. Although, what made them chose me is still a mystery for me, I am really grateful for this opportunity! I really enjoyed these years in Zuerich and at the ETH.

Going ahead thanking...

My dear Rich, the column of my life, for being always present and supportive. Not to mention for having fed me during these long months of hard work. :)

Alessandro Zardini, the best men on the chat. Moved in Copenhagen, but still present in my life as he would be one floor upstairs. It has been nice to start the day with the message “RITHM, RITHM”. :)

Jörg Maeder, the king of R-language, to have showed me many times the way from the stone age to the space world of R.

Andi Zünd, the Karma man, to have inspired me to ‘calm and relax’ concepts unknown to most of the Italians. Grateful to have shared tricks on latex.

Ulrich Krieger, Beiping Luo and Frank Wienhold because short discussions can make also the difference.

Peter Kriedron for the continuous valuable scientific AND NON discussions.

Susan Solomon, Irina Petropavlovskikh, Bob Evans, Elizabeth Weatherhead to have enthusiastically supported me in these years.

All my friends who made my life full

Daniel and Kristen Cziczo, Elena Alessandri, Junbo Cui, Parick Koch, Berko Sierau, the magnificent Uwe Weers, Olivia Martius, Thomas Spengler, my GREAT rowing team (Ursula, Sylvi, Isabel).....

Last but not least,

my family and my dad, who was proud coming at the train station in Monza to pick me up. He would have enjoyed also to listen the final results.

THANKS,  
Barbara



# Curriculum Vitae

Barbara Scarnato

Date of birth 09.06.1977  
Place of birth Milan, Italy

## Education

- April 2008 PhD student at the Swiss Federal Institute of Technology Zurich (ETH Zurich), Institute for Atmospheric and Climate Science (IACETH), Atmospheric Chemistry group. Thesis title: Total Ozone Measurements at Arosa (Switzerland): Seasonal Variation and Precision of Dobson and Brewer Observations.
- 2004 MSc Physics. Thesis title: Atmospheric particle size distribution by Differential Mobility Particle Sizer and Optical Particle Counter.

## Professional positions

- 2005 - 2008 Teaching assistance at the Institute for Atmospheric and Climate Science, ETH Zurich.
- 2004 - 2005 Product manager for aerosol particle instruments, Luchsinger srl, Via Bergamo 25, Curno
- 2000 - 2005 Mathematics and Physics help lectures for high school students
- 2000 - 2005 Analysis Mathematic 1 and 2 and Technical Physics help-lectures at University of Architecture, Milan

## Publications

- 2007 (*Rodriguez et al.*, 2007), A study on the relationship between mass concentrations, chemistry and number size distribution of urban aerosols in Milan, Barcelona and London.
- in preparation (*Scarnato et al.*, 200xa), Total Ozone Observations at Arosa (Switzerland) by Dobson and Brewer: Temperature and Ozone Slant Path Effect.
- in preparation (*Scarnato et al.*, 200xb), Long Term Total Ozone Observations at Arosa (Switzerland): A transfer function.

## Recent Presentations

- December 2007 Direct sun total ozone measurements by Dobson and Brewer: Temperature and ozone slant path effect. Invited seminar at NOAA (Boulder) and NASA Goddard (Greenbelt). Poster presentation at AGU San Francisco.
- November 2006 Intercomparison of Dobson and Brewer Total Ozone measurements from Arosa (Switzerland) - Tenerife, November 2006. Invited talk at SAUNA workshop.
- October 2006 Intercomparison of Dobson and Brewer Total Ozone measurements from Arosa (Switzerland), using a statistical model” - Boulder. Invited seminar at NOAA.
- April 2006 Comparison of Stratospheric ozone measurements by Dobson and Brewer spectrophotometers.- Vienna, EGU. Poster presentation
- June 2005 Comparison of Brewer and Dobson total ozone measurements, Time of coincidence” - Delft, The 9th Brewer Users Group Meeting. Poster presentation.
- 2005 A Study on Particle Size Distributions (micro and nanoparticles) in the Urban Atmosphere of Milan ” - EAC 2005. Poster presentation.

Zürich, March 2008

